INCOMPRESSIBLE VISCOUS FLOW IN A CURVED PIPE

by

GORDON FRANCIS PICKETT

A thesis submitted to the University of London
for the degree of Doctor of Philosophy
in the Faculty of Science

Department of Mathematics,
Imperial College of Science
and Technology.

May 1968

ABSTRACT

When a fluid flows through a curved pipe, a secondary flow is set up, the fluid in the middle of the pipe moving outwards and that near the walls moving inwards. Near the entrance to the bend, the secondary flow changes a great deal and in some cases appears oscillatory. If the bend is of sufficient length, the changes in secondary flow are damped by viscosity and a region where the flow is fully developed is reached. It has been shown theoretically and experimentally, that the dynamical similarity of fully developed laminar flow depends on a non-dimensional parameter

$$K_w = \frac{2aW_o}{\nu}\left(\frac{a}{R}\right)^{1/2} ,$$

where W_o is the mean axial velocity, ν is the coefficient of viscosity and 'a' is the radius of the pipe which is bent into a circle of radius R .

The first part of the present work investigates the particular case of entry flow where the viscous forces are not dominated by the centrifugal forces. The second part investigates the fully developed laminar flow region for small and large values of the parameter K_w . The

effects of torsion in a coiled pipe are discussed and theoretical results for the increase in resistance due to curvature are obtained for pipes of small and large curvature ratio κ defined as $\kappa = a/R$. These results are used to determine the point at which the flow separates and it is found that the theoretical results agree reasonably well with the available experimental observations.

ACKNOWLEDGMENTS

I would like to express my sincere thanks to my supervisor, Mr. L. Sowerby, M.A., for his constant encouragement and assistance through numerous discussions.

I would also like to acknowledge the financial assistance of the Science Research Council.

CONTENTS

CHAPTER 1

Introduction to the physical problem

When a fluid flows through a curved pipe, a pressure gradient is required across the pipe to balance the centrifugal force arising from the curvature. The pressure at the outer wall (i.e. that part of the wall furthest from the centre of curvature of the pipe) must be greater than that at the inner wall. The fluid near the wall of the pipe is moving more slowly than the fluid some way from the walls and hence the pressure gradient is reduced. As a result of these different pressure gradients, the faster flowing fluid moves outwards, whilst the slower flowing fluid moves inwards. This flow is known as the secondary flow and it is superposed on the main stream. In the case of a circular curved pipe lying in a horizontal plane, the fluid in the middle of the pipe moves outwards and that above and below it, moves inwards; thus the resultant flow is helical in the top and bottom halves of the pipe.

The secondary flow has the effect of shifting the high velocity region towards the outer wall and creating a much thicker layer of slowly moving fluid at the inner

wall. The total frictional loss of energy near the walls of the pipe is, however, increased and the flow experiences more resistance in passing through the pipe.

The flow in a curved pipe can be divided into three regions. At the entrance to the bend, the upstream velocity distribution is modified in the 'inlet region'. The velocity distribution at the point where the bend begins will be called the injection velocity; it may be formed by a preceeding section of pipe or by the flow of a fluid directly into the pipe. If the bend is of sufficient length, 'fully developed curved flow' will be established. In this region, the velocity profile is invariant with axial distance down the pipe. Towards the end of the bend, this velocity profile is again modified in an 'outlet region'. If the bend leads into a straight pipe, the effect of the bend may extend to an order of 50 diameters downstream.

In the majority of engineering situations, bends are generally restricted to right angled or 180^{o} bends and there is no fully developed region. There are, however, some situations, such as in heat exchangers, where a pipe is wound into a coil; the flow in such a coil does become fully developed if the coil is not wound too tightly. Also, the flow in these pipes is nearly always turbulent.

Because of this, the theoretical work carried out to date - most of which concerns itself with laminar flow in the fully developed region - does not have many applications to engineering problems. As a consequence, the study of laminar secondary flows has been neglected.

Renewed interest in these flows has emerged, however, due to the fact that the flow in the cardiovascular system is usually laminar. In contrast to the requirements of engineering, where the increase in resistance due to curvature is mostly sought, a knowledge of the velocity distribution is required in the study of cardiovascular systems so that the distribution of injected substances may be better understood.

Historical Survey

The first theoretical study of flow in a curved pipe was carried out by Dean (1,2), who pointed out that in laminar flow, the dynamical similarity in the fully developed region depends on the non-dimensional parameter - the Dean number -

$$K_D = \frac{2W_c^2 a^3}{\nu^2 R}$$

where W_c is the axial velocity at the centre of the pipe, ν is the kinematic coefficient of viscosity and a is the radius of the pipe which is bent into a circle of radius R . He derived a solution of the equations of motion by considering the secondary flow as a small perturbation upon the Poiseuille flow. Extending his solution so as to include the dominant fourth order terms, he calculated the flux as a function of K_D . This expression was found later to be accurate for values of K_D up to 162.

The experimental results of White (3) in 1929 confirmed that in the laminar region, the parameter K_D adequately defines the flow. He introduced a more convenient parameter

$$K_W = \frac{2aW_o}{\nu}\left(\frac{a}{R}\right)^{1/2}$$

where W_o is the mean axial velocity and showed that the critical Reynolds number at which the flow becomes turbulent, increases with the curvature ratio. It can be shown that for sufficiently small K_W , it is related to K_D by

$$K_W = \sqrt{1/2\ K_D} \ .$$

He also obtained an empirical formula for the increase in resistance in a pipe due to curvature

$$\frac{\gamma_c}{\gamma_s} = \left[1 - \left\{1 - \left(\frac{11.6}{K_w}\right)^{0.45}\right\}^{2.22}\right]^{-1} , \quad (1.1)$$

valid for $11.6 < K_w < 2000$, and showed that the flow can remain laminar for values of K_w up to 5000 (Goldstein (4), 1938).

In 1937, Keulegan and Beij (5) summarised the experimental results of White, Taylor (6) and Adler (7) for the critical Reynolds number, in the curve shown in fig (1.1). Curve I gives the minimum critical Reynolds number with disturbed inlet conditions and is based on the work of Taylor, White and Adler. Curve II was derived by Keulegan and Beij with a special inlet design to minimise disturbances. It is interesting to note that with a sufficiently long bend, it is possible to have turbulent flow at the inlet leading to laminar flow in the bend.

Adler, in 1934, deduced that for large K_w , the viscous effects tend to be restricted to a boundary layer on the walls of the pipe. He assumed that outside the boundary layer, the surfaces of equal total pressure

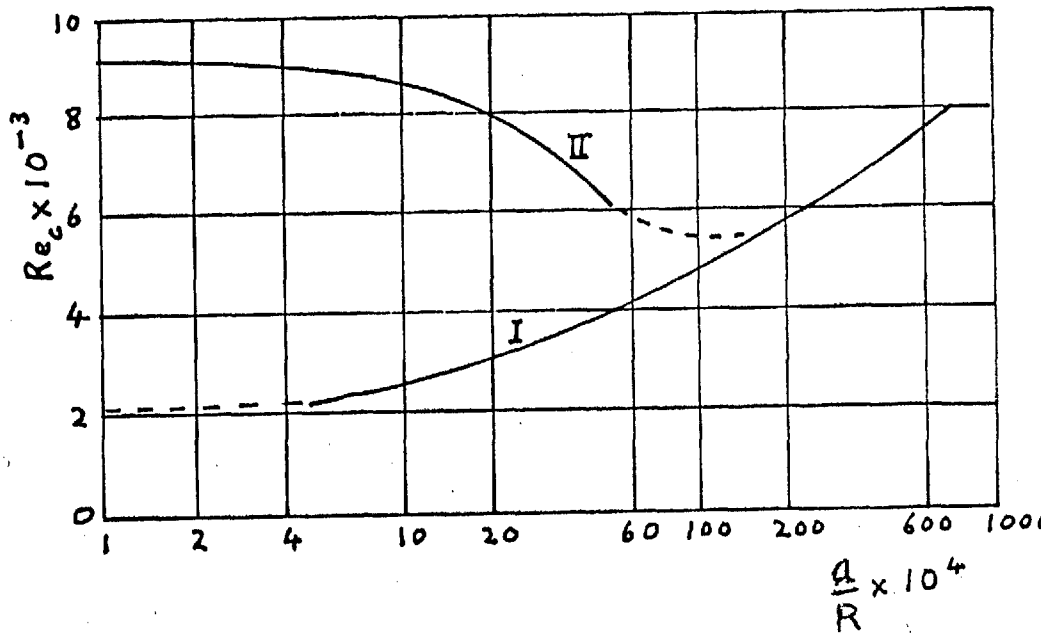

Fig. (1.1). Critical Reynolds number for fully developed flow in curved pipes. Curve I after Taylor, White and Adler. Curve II after Keulegan and Beij with special inlet designed to minimise disturbances.

were perpendicular to the plane of the pipe and obtained a simple velocity distribution for this region. Applying a Polhausen (8) method to the momentum equations in the boundary layer he obtained an expression for the increase in resistance due to curvature. Barua (9) and Mori and Nakayama (10) made similar assumptions and obtained more accurate values of the resistance. These theories will

be considered in detail in Chapter 6.

The work so far carried out in the inlet region is by no means straightforward; there are large discrepancies found in the results reported in the literature for losses in the flow of a fluid through right angled and 180^{o} bends. The reason for these discrepancies is that the upstream conditions have a large effect on the downstream flow.

Most of the theoretical work carried out to date assumes that the inlet velocity profile has been formed by viscous forces acting in a preceeding length of straight pipe. It is then assumed that in the inlet region, the centrifugal forces dominate the viscous forces and that the viscous forces can be neglected. Thus, in the initial stages of a bend, secondary flow is generated by the centrifugal force. A physical explanation for this phenomenon was offered by Squire and Winter (11) as follows: if a small elemental cylinder of fluid is considered such that its axis is normal to the flow and in the plane of the bend, and if it has a rotation about its axis, the axis will be turned about an axis perpendicular to the plane of the pipe as it proceeds down the bend and it will set up a rotation about an axis perpendicular to the other two, by analogy with the gyroscope. They

obtained a simple formula for the generation of vorticity, namely

$$d\omega_s = 2\omega_n d\theta \quad ,$$

where ω_s is a measure of vorticity in the direction of the flow, ω_n is the component of vorticity along the radius vector generating the streamline and θ measures the axial distance along the streamline. This result applied only to a streamline, but was found to be approximately representative of flow in the inlet region of a pipe of very small curvature ratio.

In the same year Hawthorn (12) extended the understanding of the generation of vorticity by considering the effect of centrifugal forces on the Bernoulli surfaces. He deduced that no secondary vorticity would be produced if the Bernoulli surfaces were perpendicular to the radius vector generating the bend.

The flow in the outlet transition region is even more complicated and the results have been restricted almost entirely to experimental results.

A detailed review of the experimental work on losses due to bends can be found in a paper by Hawthorn (13); much of the work is restricted, however, to turbulent

flow, whereas this thesis will be concerned with laminar flow.

Description of present research.

The object of this thesis is to investigate in detail a type of entry flow not as yet considered and to analyse and extend the theories of previous workers in the study of fully developed laminar flow. The basis of this study will be the Navier-Stokes equation of motion and the equation of continuity for an incompressible, viscous fluid. These equations are written out in a convenient coordinate system.

Although previous theories of flow in the inlet region neglected the effects of viscosity, there are certain cases where this effect is not negligible and others where it is dominant. Such cases are those where the fluid is injected into a bend so that, in the initial stages, secondary vorticity is generated by the viscous effects at the wall and not by the centrifugal forces. Clearly, as the injection profile is distorted, centrifugal forces act in the regions effected by viscosity and as this region grows eventually occupying the complete cross section of the pipe, the centrifugal forces can, for large

Reynolds number flow, dominate the viscous forces over most of the cross section. In the first part of the thesis, the type and subsequent development of such injection velocities is considered.

In the second part, the fully developed flow region is investigated for the two cases of low and high Dean number flows. The flow in pipes of large curvature ratio is considered and torsional effects, which are a practical consequence of large curvature ratio pipes, are discussed. A more accurate solution for flow at low Dean numbers is derived so that the increase in resistance due to curvature can be found. The investigation into the flow at high Dean numbers follows a similar line of approach as previous theories. It is, however, extended to include curvature effects and to satisfy more boundary conditions. Finally, it is hoped that a better understanding is obtained of the assumptions made and the results derived from such an approach.

CHAPTER 2

The Coordinate System and General Equations of Motion.

The two coordinate systems used throughout this thesis are illustrated in fig. (2.1). The surface of a pipe of circular section, coiled in a circle, is a torus; the figure shows O_z , the axis of the torus and a section of it by an axial plane that makes an angle θ with a fixed axial plane. The radius of any cross section is 'a', and R is the radius of the circle in which the pipe is coiled; the distance along the pipe axis from the fixed plane is thus $R\theta = s$. The position of any point P is specified by the orthogonal coordinates (r, ψ, s) and the corresponding components of velocity at this point are (u,v,w).

The alternative coordinate system (r_1, θ, z) that will be found useful is also shown and the corresponding velocity components (u_1, w_1, v_1) . It is also useful to exhibit the corresponding vorticity components for this particular system as $(\omega_n, \omega_t, \omega_b)$.

If ν is the coefficient of kinematic viscosity and ρ and p are the density and pressure respectively, the Navier-Stokes and the continuity equations for a

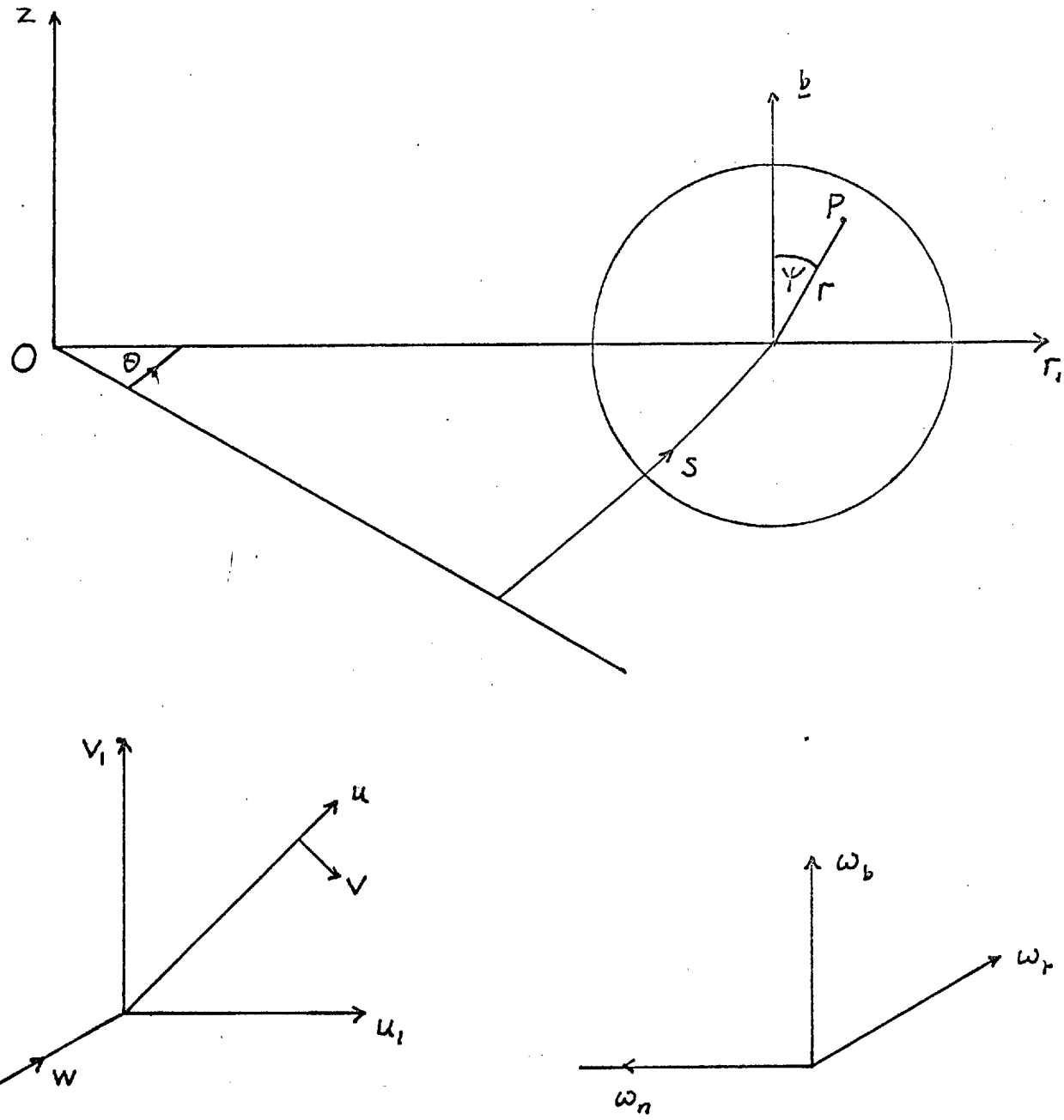

Fig. (2.1). The (r,Ψ,s) and (r_1,θ,z) coordinate systems.

steady incompressible fluid are

$$\underline{v} \wedge \underline{\text{curl}}\ \underline{v} = \underline{\text{grad}}\ \left(\frac{p}{\rho} + \frac{1}{2}v^2\right) + \nu\ \underline{\text{curl}}\ \underline{\text{curl}}\ \underline{v}\ , \qquad (2.1)$$

$$\text{div}\ \underline{v} = 0\ , \qquad (2.2)$$

where $\underline{v} = (u,v,w)$,

$$\left.\begin{aligned} \text{div}\ \underline{v} &= \frac{1}{rh}\left\{\frac{\partial}{\partial r}(rhu) + \frac{\partial}{\partial \psi}(hv) + \frac{\partial}{\partial s}(rw)\right\}\ , \\ \underline{\text{curl}}\ \underline{v} &= \frac{1}{rh}\begin{vmatrix} \hat{\underline{r}} & r\hat{\underline{\psi}} & h\hat{\underline{s}} \\ \partial/\partial r & \partial/\partial\psi & \partial/\partial s \\ u & rv & hw \end{vmatrix} \end{aligned}\right\} \qquad (2.3)$$

$$h = 1 + \frac{r \sin\psi}{R}\ , \qquad (2.4)$$

and R is the radius of the pipe bend.

The full equations of motion depicting flow in curved pipes can then be written as

$$u\frac{\partial u}{\partial r} + \frac{v}{r}\frac{\partial u}{\partial \psi} + \frac{w}{h}\frac{\partial u}{\partial s} - \frac{v^2}{r} - \alpha w^2 = -\frac{1}{\rho}\frac{\partial p}{\partial r}$$

$$- \frac{\nu}{rh}\left[\frac{\partial}{\partial \psi}\left\{\frac{h}{r}\left(\frac{\partial}{\partial r}(rv) - \frac{\partial u}{\partial \psi}\right)\right\} + \frac{\partial}{\partial s}\left\{\frac{r}{h}\left(\frac{\partial}{\partial r}(hw) - \frac{\partial u}{\partial s}\right)\right\}\right] , \tag{2.5}$$

$$u\frac{\partial v}{\partial r} + \frac{v}{r}\frac{\partial v}{\partial \psi} + \frac{w}{h}\frac{\partial v}{\partial s} - \frac{\beta w^2}{r} + \frac{uv}{r} = -\frac{1}{\rho r}\frac{\partial p}{\partial \psi}$$

$$- \frac{\nu}{h}\left[\frac{\partial}{\partial s}\left\{\frac{1}{rh}\left(\frac{\partial}{\partial \psi}(hw) - \frac{\partial}{\partial s}(rv)\right)\right\} - \frac{\partial}{\partial r}\left\{\frac{h}{r}\left(\frac{\partial}{\partial r}(rv) - \frac{\partial u}{\partial \psi}\right)\right\}\right] \tag{2.6}$$

$$u\frac{\partial w}{\partial r} + \frac{v}{r}\frac{\partial w}{\partial \psi} + \frac{w}{h}\frac{\partial w}{\partial s} + \alpha uw + \frac{\beta vw}{r} = -\frac{1}{\rho h}\frac{\partial p}{\partial s}$$

$$+ \frac{\nu}{r}\left[\frac{\partial}{\partial r}\left\{\frac{r}{h}\left(-\frac{\partial u}{\partial s} + \frac{\partial}{\partial r}(hw)\right)\right\} + \frac{\partial}{\partial \psi}\left\{\frac{1}{rh}\left(\frac{\partial}{\partial \psi}(hw) - \frac{\partial}{\partial r}(rv)\right)\right\}\right] \tag{2.7}$$

$$\frac{\partial}{\partial r}(rhu) + \frac{\partial}{\partial \psi}(hv) + \frac{\partial}{\partial s}(rw) = 0 , \tag{2.8}$$

where

$$\alpha = \frac{1}{h}\frac{\partial h}{\partial r} \qquad \text{and} \qquad \beta = \frac{1}{h}\frac{\partial h}{\partial \psi} \tag{2.9}$$

The problem is now to find solutions of these equations subject to the boundary conditions; these require that

the velocity (u,v,w) should be zero at the surface of the pipe,

$$\text{i.e.} \qquad u = v = w = 0 \quad \text{at} \quad r = a \ , \tag{2.10}$$

and that the flux through any cross section of the pipe is constant.

PART I

THE FLOW IN THE INLET REGION OF A CURVED CIRCULAR PIPE

CHAPTER 3

Introduction

If fluid is injected into a curved, circular pipe so that the axial velocity is initially non zero at the wall edge, an infinitely thin boundary layer is subsequently formed round the walls of the pipe since the velocity at the wall must be zero. The thickness of the boundary layer will increase with distance downstream eventually filling the whole cross section of the pipe. Until this happens, there is a core of fluid effectively uninfluenced by viscosity. Since the flux across any cross section is constant and the boundary layer thickness is increasing, this core is accelerated and there is a corresponding fall in pressure.

The pressure is also altered if secondary flow is generated in the core, the condition for which - as will be seen later - is that there is a component of vorticity along the radius vector generating the pipe.

The fully developed flow is theoretically attained asymptotically; because of the complicated nature of the flow, however, a solution is obtained which is valid only for a short distance down the pipe. In this region, the

effect of curvature on the developing velocity distribution is investigated.

The method used here is similar to that due to Goldstein and Atkinson (14) for the corresponding problem in a straight circular pipe. They derived a series expansion solution in ξ, where ξ is a non-dimensional parameter defining distance down the pipe. The series obtained is found to give reasonable results when compared with the experimental observations of Nikuradse (15), for values of ξ up to 0.05; there is, however, some discrepancy very near the entry probably caused by the singularity in the solution at $\xi = 0$.

The solution obtained from the present analysis includes that of Goldstein and Atkinson as a special case (i.e. when the curvature ratio is zero and with constant velocity injection) and for small curvature ratios, the solution probably has a similar region of validity as that for a straight pipe. For large curvature ratios, however, it will be seen that the region of validity is necessarily reduced.

Boundary Layer Equations

The problem is considered for large values of the Reynolds number defined as $Re = \frac{2aW_o}{\nu}$ and the approximations usual in boundary layer theory can be applied to equations (2.5)-(2.8). Thus, if the boundary layer thickness is taken to be of order $Re^{-1/2}$ and terms of order one and $Re^{-1/2}$ are considered to allow for a growing boundary layer, the equations representing the motion in the boundary layer are

$$u\frac{\partial w}{\partial r} + \frac{v}{r}\frac{\partial w}{\partial \psi} + \frac{w}{h}\frac{\partial w}{\partial s} + \alpha uw + \beta\frac{vw}{r} = -\frac{1}{\rho h}\frac{\partial p}{\partial s} + \nu\left[\frac{\partial^2 w}{\partial r^2} + \left(\frac{1}{a}+\alpha\right)\frac{\partial w}{\partial r}\right], \tag{3.1}$$

$$\frac{v^2}{r} + \alpha w^2 = \frac{1}{\rho}\frac{\partial p}{\partial r}, \tag{3.2}$$

$$u\frac{\partial v}{\partial r} + \frac{v}{r}\frac{\partial v}{\partial \psi} + \frac{w}{h}\frac{\partial w}{\partial s} + \frac{uv}{r} - \beta\frac{w^2}{r} = -\frac{1}{\rho r}\frac{\partial p}{\partial \psi} + \nu\left[\frac{\partial^2 v}{\partial r^2} + \left(\frac{1}{a}+\alpha\right)\frac{\partial v}{\partial r}\right], \tag{3.3}$$

together with the equation of continuity

$$\frac{\partial}{\partial s}(rw) + \frac{\partial}{\partial r}(rhu) + \frac{\partial}{\partial \psi}(hv) = 0 \,. \qquad (3.4)$$

Continuing a conventional boundary layer analysis, it is clear from equation (3.2) that the pressure variation can be neglected across the boundary layer. Since this approximation yields only third order differential equations, nothing can be said of the behaviour of the radial component of velocity u some way from the wall of the pipe. Consequently, the analysis will break down if terms containing u, which do not tend to zero away from the wall, are retained.

One such term is αuw in equation (3.1), but this may be rejected if the curvature ratio is such that terms of order $Re^{-1/2}(\frac{a}{R})$ can be ignored relative to terms of order $Re^{-1/2}$ and one. Terms of order $Re^{-1/2}$ were retained in equations (3.1)-(3.4) so that the analysis would incorporate the theory of Goldstein and Atkinson as a special case, obtained by letting $\frac{R}{a} \longrightarrow \infty$. Thus, for small curvature ratio, the terms of order $Re^{-1/2}(\frac{a}{R})$ can be rejected whilst retaining comparable accuracy to that for a straight pipe. If, however, $\frac{a}{R}$ is of order one, the analysis can be continued without terms of order $Re^{-1/2}(\frac{a}{R})$, but the results obtained will be valid for a smaller region because of the reduced accuracy of the

equations; a consequence of retaining some terms of order $Re^{-1/2}$ and rejecting others.

The only other term that will create difficulties in this respect, supposing there to be no initial secondary flow, is $u\frac{\partial w}{\partial r}$. This is because the axial velocity in the core is, in general, a function of r. The nature of the complications that arise will be considered as and when they occur.

Rejecting terms of order $Re^{-1/2}(\frac{a}{R})$, equations (3.1), (3.3) and (3.4) reduce to

$$u\frac{\partial w}{\partial r} + \frac{v}{r}\frac{\partial w}{\partial \psi} + \frac{w}{h_o}\frac{\partial w}{\partial s} + \frac{\beta_o vw}{a} = -\frac{1}{\rho h_o}\frac{\partial p}{\partial s} + \nu\left[\frac{\partial^2 w}{\partial r^2} + \frac{1}{a}\frac{\partial w}{\partial r}\right], \quad (3.5)$$

$$u\frac{\partial v}{\partial r} + \frac{v}{r}\frac{\partial v}{\partial \psi} + \frac{w}{h_o}\frac{\partial v}{\partial s} - \frac{\beta_o w^2}{a} + \frac{uv}{a} = -\frac{1}{\rho r}\frac{\partial p}{\partial \psi} + \nu\left[\frac{\partial^2 v}{\partial r^2} + \frac{1}{a}\frac{\partial v}{\partial r}\right], \quad (3.6)$$

$$\frac{\partial}{\partial s}(rw) + \frac{\partial}{\partial r}(rh_o u) + \frac{\partial}{\partial \psi}(h_o v) = 0, \quad (3.7)$$

where $h_o = 1 + \kappa \sin \psi$ and $\beta_o = \frac{1}{h_o} \frac{\partial h_o}{\partial \psi}$.

Since the variation of pressure is being neglected across the boundary layer, the pressure is determined from the inviscid flow in the main stream which is the core. If w_1 is the axial component of velocity in the core and there is no secondary flow in the core, the pressure in the core can be obtained from

$$\left.\begin{aligned} \frac{1}{\rho} \frac{\partial p}{\partial s} &= -w_1 \frac{\partial w_1}{\partial s} \\ \frac{1}{\rho} \frac{\partial p}{\partial r} &= \alpha w_1^2 \\ \frac{1}{\rho} \frac{\partial p}{\partial \psi} &= \beta w_1^2 \end{aligned}\right\} \quad (3.8)$$

The condition that there is no secondary flow in the core imposes restrictions on the type of injection velocity. The class of such injection velocities is considered next.

Clearly there must be no initial secondary flow and the initial axial component of velocity must be such as to generate no secondary vorticity.

Scorer and Wilson (16) obtained an equation for the

generation of vorticity in a curved streamline and for an inviscid, incompressible, constant density fluid, it takes the form

$$\frac{D}{Dt}\left(\frac{\omega_s}{q}\right) = \kappa\,\omega_n \,, \tag{3.9}$$

where q is the fluid velocity along a streamline, ω_s is the vorticity component along the streamline, ω_n is the vorticity component along the radius of curvature of the streamline and κ is the curvature ratio of the streamline. For pipes of small curvature ratio, the streamlines are approximately parallel to the walls of the pipe and equation (3.9) can be applied to the fluid in the core of the pipe. It is seen from this equation that no secondary vorticity is generated if ω_n is zero. Thus, using the (r_1,θ,z) coordinate system of fig. (2.1), no secondary vorticity is generated if

$$\omega_n = \frac{1}{r_1}\frac{\partial v_1}{\partial \theta} - \frac{\partial w_1}{\partial z} = 0 \,. \tag{3.10}$$

In the same coordinates

$$\omega_s = \frac{\partial u_1}{\partial z} - \frac{\partial v_1}{\partial r_1} = 0 \,, \tag{3.11}$$

since initially ω_s is zero by definition and by (3.9) and (3.10) no secondary vorticity is generated. It is therefore possible to see that a necessary condition for u_1 and v_1 and thus u and v to be zero in the core, throughout the region under consideration, is that $w_1 = w_1(r_1,\theta)$. The reason for this is that if w was a function of z , then v_1 would have to be a function of θ , which is not permissible.

For pipes of large curvature ratio, the streamlines are not approximately parallel to the pipe wall and the full vorticity equation has to be considered; namely

$$\frac{D}{Dt}\underline{\omega} = (\underline{\omega}.\underline{\text{grad}})\underline{v} \ . \qquad (3.12)$$

Since no secondary vorticity is to be generated in the core

$$\omega_n \frac{\partial w_1}{\partial r_1} + \omega_s \frac{\partial w_1}{\partial \theta} + \omega_b \frac{\partial w_1}{\partial z} = 0 \ , \qquad (3.13)$$

where $(\omega_n,\omega_s,\omega_b)$ are the components of vorticity corresponding to the (r_1,θ,z) coordinate system. Then, because ω_s is zero initially, ω_s must be zero in equation (3.13). Thus, since

$$\omega_b = \frac{1}{r_1}\frac{\partial}{\partial r_1}(r_1 w) - \frac{\partial u_1}{\partial \theta} \quad , \tag{3.14}$$

equation (3.13) can be written as

$$\left(\frac{1}{r_1}\frac{\partial v_1}{\partial \theta} - \frac{\partial w_1}{\partial z}\right)\frac{\partial w_1}{\partial r_1} + \left(\frac{\partial w_1}{\partial r_1} + \frac{w_1}{r_1} - \frac{\partial u_1}{\partial \theta}\right)\frac{\partial w_1}{\partial z} = 0 \quad ,$$

or

$$\frac{1}{r_1}\frac{\partial v_1}{\partial \theta}\frac{\partial w_1}{\partial r_1} + \frac{w_1}{r_1}\frac{\partial w_1}{\partial z} - \frac{\partial u_1}{\partial \theta}\frac{\partial w_1}{\partial z} = 0 \quad . \tag{3.15}$$

Again it can be seen that a necessary condition for u_1 and v_1 and thus u and v to remain zero in the core as the fluid flows into the bend is that $w_1 = w_1(r_1, \theta)$.

This condition, however, is not sufficient as can be seen by considering the continuity equation in the (r_1, θ, z) coordinate system

$$\frac{\partial}{\partial r_1}(r_1 u_1) + \frac{\partial w_1}{\partial \theta} + r_1\frac{\partial v_1}{\partial z} = 0 \quad . \tag{3.16}$$

For, if $w_1 = w_1(r_1, \theta)$, equation (3.15) yields the fact that v_1 is independent of θ . But v_1 is zero over the whole cross section initially and thus is identically zero throughout the core region. It can be seen therefore,

from equation (3.16), that if $\frac{\partial w_1}{\partial \theta}$ is non zero, there must be a contribution from u_1. It is assumed, however, in what follows, that this contribution is negligible relative to the terms retained in equation (3.8).

Transformation of Coordinates

So long as a core uninfluenced by viscosity exists, the following non dimensional variables may be formed:

$$\xi = \left(\frac{2s}{aRe}\right)^{1/2} , \quad \eta = \frac{a^2 - r^2}{4\varepsilon\, a^2 \xi} \tag{3.17}$$

where Re is the Reynolds number defined as

$$Re = \frac{2a\, W_o}{\nu} , \tag{3.18}$$

W_o is the initial mean axial velocity and ε is a function of ψ to be determined later.

Equation (3.7) using the above transformation can be satisfied by introducing two non-dimensional stream functions f and g and putting

$$w = \frac{W_o}{2\xi} \frac{\partial f}{\partial \eta}$$

$$v = \frac{r\, W_o}{2a\, h_o \xi \mathrm{Re}} \frac{\partial g}{\partial \eta} \qquad (3.19)$$

$$u = \frac{aW_o\, \varepsilon}{r h_o\, \mathrm{Re}} \left[\frac{1}{\xi} \frac{\partial f}{\partial \xi} - \frac{\eta}{\xi^2} \frac{\partial f}{\partial \eta} + \frac{1}{\varepsilon} \frac{\partial}{\partial \psi}(\varepsilon g) - \frac{\eta}{\varepsilon} \frac{d\varepsilon}{d\psi} \frac{\partial g}{\partial \eta} \right]$$

Transforming equation (3.5) and (3.6) and applying the results of (3.8), (3.9) and (3.19),

$$(1-4\varepsilon\eta\xi)\frac{h_o}{\varepsilon^2} f_{\eta\eta\eta} + f_\xi f_{\eta\eta} - f_\eta \left(f_{\eta\xi} - \frac{f_\eta}{\xi} \right) = -4\xi^2 w_c \frac{\partial w_c}{\partial \xi}$$

$$+ \frac{4h_o \xi}{\varepsilon} f_{\eta\eta} + \beta_o \xi g_\eta f_\eta + \xi g_\eta f_{\eta\psi} - \frac{f_{\eta\eta} \cdot \xi}{\varepsilon} \frac{\partial}{\partial \psi}(\varepsilon g) , \qquad (3.20)$$

$$(1-4\varepsilon\eta\xi)^2 \frac{h_o}{\varepsilon^2} g_{\eta\eta\eta} + (1-4\varepsilon\eta\xi) \left[f_\xi g_{\eta\eta} - f_\eta \left(g_{\eta\xi} - \frac{g_\eta}{\xi} \right) \right]$$

$$= \mathrm{Re}^2 \beta_o h_o^2 \xi (4\xi^2 w_c^2 - f_\eta^2) + (1-4\varepsilon\eta\xi) \left[4\varepsilon\xi(1-\alpha_o)(1-4\varepsilon\eta\xi)^{1/2} \right.$$

$$\left. + \frac{4h_o \xi}{\varepsilon} - \frac{1}{\varepsilon} \frac{\partial}{\partial \psi}(\varepsilon g) + \frac{\eta}{\varepsilon} \frac{d\varepsilon}{d\psi} \cdot g_\eta \right] + (1-4\varepsilon\eta\xi)^{1/2} \times$$

$$\left[4\varepsilon^2 \alpha_o \xi^2 (2-\alpha_o)(1-4\varepsilon\eta\xi) + 2\varepsilon\xi(1-\alpha_o) f_\xi - 2\varepsilon\xi(1-\alpha_o) \times \right.$$

$$\left\{\frac{2h_o}{\varepsilon}\xi(2+\alpha_o) - \frac{1}{\varepsilon}\frac{\partial}{\partial\psi}(\varepsilon g) + \frac{\eta}{\varepsilon}\frac{d\varepsilon}{d\psi}\cdot g_\eta\right\}$$

$$- \frac{2\varepsilon}{h_o}\xi\left\{f_\xi - \frac{\eta}{\xi}f_\eta + \frac{1}{\varepsilon}\frac{\partial}{\partial\psi}(\varepsilon g) - \frac{\eta}{\varepsilon}\frac{d\varepsilon}{d\psi}\cdot g_\eta\right\}\Bigg]\cdot g_\eta$$

$$+ (1-4\varepsilon\eta\xi)(g_{\eta\psi} - \beta_o g_\eta)g_\eta\,, \qquad (3.21)$$

in which a literal suffix denotes, as usual, differentiation with respect to the appropriate variables and where $w_1 = W_o\, w_c$ and $\alpha_o = \frac{\varkappa \sin\psi}{h_o}$.

The boundary conditions on f and g must be such as to allow $u = v = w = 0$ on the pipe wall and $w = w_1$, $v = 0$ at the interface of core and boundary layer. These are satisfied as follows:

$$\begin{aligned} &f_\eta = g_\eta = f_\xi = g_\psi = 0 \quad \text{at} \quad \eta = 0\,, \\ &f_\eta \to 2\xi w_c\,, \quad g_\eta \to 0 \quad \text{as} \quad \eta \to \infty. \end{aligned} \qquad (3.22)$$

Expansion in Series

Equations (3.20) and (3.21), subject to the boundary conditions of (3.22) may be solved by expansions in series of powers of ξ. It is assumed that f, g and w_c are

analytic functions of ξ , so that

$$f = \sum_{n=1}^{\infty} f_n \xi^n \ , \quad g = \sum_{n=1}^{\infty} g_n \xi^n \ , \quad w_c = \sum_{n=0}^{\infty} K_n \xi^n$$

where f_n , g_n and K_n are functions of η and ψ (the latter being obtained from expansions of r from $r = (1-4\varepsilon\eta\xi)^{1/2}$). The boundary conditions of (3.22) then become

$$f_n = \frac{\partial f_n}{\partial \eta} = g_n = \frac{\partial g_n}{\partial \eta} = 0 \quad \text{at} \quad \eta = 0 \ ,$$

$$\frac{\partial f_n}{\partial \eta} \longrightarrow 2K_{n-1} \ , \quad \frac{\partial g_n}{\partial \eta} \longrightarrow 0 \quad \text{as} \quad \eta \longrightarrow \infty \ \text{for} \ \ n \geq 1 \ . \tag{3.23}$$

Substituting the above expansions in (3.20) and (3.21) and equating coefficients of like powers of ξ , the terms independent of ξ yield

$$\frac{h_o}{\varepsilon^2} \frac{\partial^3 f_1}{\partial \eta^3} + f_1 \frac{\partial^2 f_1}{\partial \eta^2} = 0 \ , \tag{3.24}$$

$$\frac{h_o}{\varepsilon^2} \frac{\partial^3 g_1}{\partial \eta^3} + f_1 \frac{\partial^2 g_1}{\partial \eta^2} = 0 \ . \tag{3.25}$$

Before continuing, a more detailed investigation of the

expansion of the core velocity is required.

The core velocity is a function of r, ψ and s and it can be expanded as a power series in ξ as follows:

$$w_c = K_0(\psi) + [K_{10}(\psi) + \eta K_{11}(\psi)]\xi + [K_{20}(\psi) + K_{21}(\psi)\eta + K_{22}(\psi)\eta^2]\xi^2 + \ldots\ldots \quad (3.26)$$

The coefficients of ξ are of the type shown in view of the form of the expansion for r. Also, $K_0(\psi)$ is non zero for all $0 \leq \psi < 2\pi$, since it was assumed earlier that the injected flow is non zero at the wall edge.

Returning to equation (3.24), it is seen that since, at $\xi = 0$, the flow must approximate to the Blassius flow, and since f_1 must tend to $2K_0(\psi)$ as $\eta \longrightarrow \infty$,

$$f_1 = K_0(\psi)\, f_{10}(\eta) , \quad (3.27)$$

$$\varepsilon = \sqrt{\frac{h_0}{K_0(\psi)}} , \quad (3.28)$$

and

$$f'''_{10} + f_{10} f''_{10} = 0 , \quad (3.29)$$

where $f_{10}(0) = f'_{10}(0) = 0$, $f'_{10}(\eta) \longrightarrow 2$ as $\eta \longrightarrow \infty$,

and a prime is now used to denote differentiation of a function of one variable with respect to that variable.

Using (3.28), equation (3.25) can be solved in terms of f_{10} as

$$g_1(\eta) = Af_{10} + B\eta + C \ . \tag{3.30}$$

The boundary conditions of (3.23) are such that $A = B = C = 0$ and so

$$g_1(\eta) = 0 \ . \tag{3.31}$$

Equating the coefficients of the ξ terms from (3.20) and (3.21) and using the results of (3.31) and (3.28),

$$K_o\left[\frac{\partial^3 f_2}{\partial\eta^3} + f_{10}\frac{\partial^2 f_2}{\partial\eta^2} - f'_{10}\frac{\partial f_2}{\partial\eta} + 2f''_{10}\, f_2\right] = -4K_1K_o + 4\varepsilon K_o(\eta\, f'''_{10} + f''_{10}) \tag{3.32}$$

$$\frac{\partial^3 g_2}{\partial\eta^2} + f_{10}\frac{\partial^2 g_2}{\partial\eta^2} - f'_{10}\frac{\partial g_2}{\partial\eta} = 0 \ . \tag{3.33}$$

The solution of (3.33) with the boundary conditions of (3.23) is $g_2 = 0$ (see Appendix to this chapter).

Equating coefficients of like powers of ξ up to ξ^4 using $g_1 = g_2 = 0$ and 3.28,

$$K_o\left[\frac{\partial^3 f_3}{\partial\eta^3} + f_{10}\frac{\partial^2 f_3}{\partial\eta^2} - 2f'_{10}\frac{\partial f_3}{\partial\eta} + 3f''_{10}\, f_3\right] = -4(K_1^2+2K_oK_2)$$

$$- 2f_2\frac{\partial^2 f_2}{\partial\eta^2} + \left(\frac{\partial f_2}{\partial\eta}\right)^2 + 4\varepsilon\left[\eta\frac{\partial^3 f_2}{\partial\eta^3} + \frac{\partial^2 f_2}{\partial\eta^2}\right], \qquad (3.34)$$

$$K_o\left[\frac{\partial^3 g_3}{\partial\eta^3} + f_{10}\frac{\partial^2 g_3}{\partial\eta^2} - 2f'_{10}\frac{\partial g_3}{\partial\eta}\right] = Re^2\beta_o h_o^2\left[4K_o^2 - \left(\frac{\partial f_1}{\partial\eta}\right)^2\right], \qquad (3.35)$$

$$K_o\left[\frac{\partial^3 f_4}{\partial\eta^3} + f_{10}\frac{\partial^2 f_4}{\partial\eta^2} - 3f'_{10}\frac{\partial f_4}{\partial\eta} + 4f''_{10}\, f_4\right] = -12(K_3K_o+K_1K_2)$$

$$-2f_2\frac{\partial^2 f_3}{\partial\eta^2} - 3f_3\frac{\partial^2 f_2}{\partial\eta^2} + 3\frac{\partial f_2}{\partial\eta}\frac{\partial f_3}{\partial\eta} + 4\varepsilon\left[\eta\frac{\partial^3 f_3}{\partial\eta^3} + \frac{\partial^2 f_3}{\partial\eta^2}\right], \qquad (3.36)$$

$$K_o\left[\frac{\partial^3 g_4}{\partial\eta^3} + f_{10}\frac{\partial^2 g_4}{\partial\eta^2} - 3f'_{10}\frac{\partial g_4}{\partial\eta}\right] = Re^2\beta_o h_o^2\left[8K_oK_1 - 2\frac{\partial f_1}{\partial\eta}\frac{\partial f_2}{\partial\eta} - \right.$$

$$\left. -4\varepsilon\eta\left\{4K_o^2-\left(\frac{\partial f_1}{\partial\eta}\right)^2\right\}\right] - 2f_2\frac{\partial^2 g_3}{\partial\eta^2} + 2\frac{\partial f_2}{\partial\eta}\frac{\partial g_3}{\partial\eta} + \varepsilon\frac{\partial^2 g_3}{\partial\eta^2}(8-2\alpha_o)$$

$$+ 2\frac{\partial g_3}{\partial\eta}\left[\varepsilon f_1(1-\alpha_o) - \frac{1}{\varepsilon}\left(f_1 - \eta\frac{\partial f_1}{\partial\eta}\right)\right]. \qquad (3.37)$$

From the form of the expansion of w_c from (3.26), solutions for f_n of the form $f_n^{\infty} + F_n$ are required, where

$$\frac{\partial f_n^{\infty}}{\partial \eta} \longrightarrow 2K_{n-1,0}(\Psi) ,$$

$$\frac{\partial F_n}{\partial \eta} \longrightarrow 2[\eta K_{n-1,1}(\Psi) + \eta^2 K_{n-1,2}(\Psi) + \ldots + \eta^{n-1} K_{n-1,n-1}],$$

for $n \geq 2$. If the f_n^{∞} and F_n can be found, the boundary layer flow will match exactly on to the core flow.

Unfortunately, the F_n cannot be determined from an analysis of this type due to the fact that inconsistencies arise in the equations for large η . This can be illustrated by considering equation (3.32). For large η ,

$$(2\eta + B_1)2K_{11} - 4(K_{10} + \eta K_{11}) = -4(K_{10} + \eta K_{11}) ,$$

where B_1 is the constant of integration obtained by integrating the boundary condition $f'_{10} = 2$. This equation is satisfied only if K_{11} is negligible. The term $(2\eta + B_1)2K_{11}$ arises from $u\frac{\partial w}{\partial r}$ in equation (3.5) and it can be seen that equation (3.32) could be made

consistent if the axial momentum equation in the core was taken to be

$$u\frac{\partial w}{\partial r} + \frac{w}{h}\frac{\partial w}{\partial s} = -\frac{1}{\rho h}\frac{\partial p}{\partial s} .$$

The complications that arise by considering the more exact equations in the core are, however, manifold and deemed impractical because of the nature of a boundary layer analysis.

Since the g_n are functions of the f_n, it follows that any inconsistency in the determination of the f_n will effect the g_n. It will be seen later that the F_n need not be determined if only the behaviour of the core flow is required. In the calculation of the skin friction and the limiting streamlines, however, there is a contribution from the F_n, but it will be assumed negligible. The errors involved in this assumption will vary depending on the form of the velocity distribution in the core. It is probable that an accurate estimation of the error will be obtained only by comparing the theoretical results with possible future experiments.

From the form of the equations (3.32) - (3.37), the functions f_1, ε and f_{10}, and the boundary conditions on $f_n^{\ast}$, it is clear that $f_2^{\ast}$, $f_3^{\ast}$, $f_4^{\ast}$, g_3

and g_4 can be expressed as linear combinations of functions of η with coefficients in functions of ψ. They are:-

$$f_2^{*} = K_{10}f_{20} + \varepsilon f_{21} ,$$

$$f_3^{*} = (K_{20}K_o f_{30} + K_{10}^2 f_{31} + \varepsilon K_{10} f_{32} + \varepsilon^2 f_{33})/K_o ,$$

$$f_4^{*} = \Big[K_{30}K_o f_{40} + K_{10}K_{20} f_{41} + (K_{10}^3/K_o) f_{42} + (\varepsilon K_{10}^2/K_o) f_{43} + (\varepsilon^2 K_{10}/K_o) f_{44} + \varepsilon K_{20} f_{45} + (\varepsilon^3/K_o) f_{46} \Big] /K_o ,$$

$$g_3 = Re^2 \beta_o h_o^2 K_o g_{30} ,$$

$$g_4 = Re^2 \beta_o h_o^2 \Big[K_{10} g_{40} + \varepsilon g_{41} + \varepsilon K_o g_{42} + \alpha_o \varepsilon g_{43} + (K_o/\varepsilon) g_{44} + K_o \alpha_o \varepsilon g_{45} \Big] .$$

(3.38)

If the differential operators D_n and L_n are defined as

$$L_n = \frac{d^3}{d\eta^3} + f_{10} \frac{d^2}{d\eta^2} - (n-1) f'_{10} \frac{d}{d\eta} + n f''_{10} ,$$

$$D_n = \frac{d^3}{d\eta^3} + f_{10} \frac{d^2}{d\eta^2} - (n-1) f'_{10} \frac{d}{d\eta}$$

(3.39)

the $f_{ij}(\eta)$ and $g_{ij}(\eta)$ satisfy the following ordinary

differential equations which can be solved numerically:

$$\left.\begin{aligned} L_2\, f_{20} &= -4 \quad , \\ L_2\, f_{21} &= 4f''_{10}(1-\eta f_{10}) \quad , \end{aligned}\right\} \qquad (3.40)$$

$$\left.\begin{aligned} L_3\, f_{30} &= -8 \\ L_3\, f_{31} &= -4 + f'^{2}_{20} - 2f_{20}f''_{20} \, , \\ L_3\, f_{32} &= -2f_{20}f''_{21} - 2f_{21}f''_{20} + 2f'_{20}f'_{21} + 4(\eta f'''_{20}+f''_{20}) \, , \\ L_3\, f_{33} &= -2f_{21}f''_{21} + f'^{2}_{21} + 4(\eta f'''_{21} + f''_{21}) \, , \end{aligned}\right\} \qquad (3.41)$$

$$\left.\begin{aligned} L_4\, f_{40} &= -12 \, , \\ L_4\, f_{41} &= 12 - 2f_{20}f''_{30} - 3f_{30}f''_{20} + 3f'_{20}f'_{30} \, , \\ L_4\, f_{42} &= -2f_{20}f''_{31} - 3f_{31}f''_{20} + 3f'_{20}f'_{31} \, , \\ L_4\, f_{43} &= -2f_{20}f''_{32} - 3f_{32}f''_{20} + 3f'_{20}f'_{32} - 2f_{21}f''_{31} \\ &\quad -3f_{31}f''_{21} + 3f'_{21}f'_{31} + 4(\eta f'''_{31}+f''_{31}) \, , \\ L_4\, f_{44} &= -2f_{20}f''_{33} - 3f_{33}f''_{20} + 3f'_{20}f'_{33} - 2f_{21}f''_{32} \\ &\quad -3f_{32}f''_{21} + 3f'_{21}f'_{32} + 4(\eta f'''_{32} + f''_{32}) \, , \end{aligned}\right\} \qquad (3.42)$$

$$\left.\begin{aligned} L_4\, f_{45} &= -2f_{21}f''_{30} - 3f_{30}f''_{21} + 3f'_{21}f'_{30} + 4(\eta\, f'''_{30} + f''_{30}), \\ L_4\, f_{46} &= -2f_{21}f''_{33} - 3f_{33}f''_{21} + 3f'_{21}f'_{33} + 4(\eta\, f'''_{33} + f''_{33}), \end{aligned}\right\} \quad (3.42)$$

$$D_3\, g_{30} = 4 - f'^{2}_{10} \quad , \qquad (3.43)$$

$$\left.\begin{aligned} D_4\, g_{40} &= 8 - 2f'_{10}f'_{20} - 2f_{20}g''_{30} + 2f'_{20}g'_{30} \quad , \\ D_4\, g_{41} &= -2f'_{10}f'_{21} - 2f_{21}g''_{30} + 2f'_{21}g'_{30} + 8g''_{30} + 2f_{10}g'_{30} \quad , \\ D_4\, g_{42} &= 4\eta(4 - f'^{2}_{10}) \quad , \\ D_4\, g_{43} &= -2g''_{30} \quad , \\ D_4\, g_{44} &= -2g'_{30}(f_{10} - \eta\, f'_{10}) \quad , \\ D_4\, g_{45} &= -2g'_{30}f_{10} \quad . \end{aligned}\right\} \quad (3.44)$$

The boundary conditions on f_{ij} and g_{ij} are, from (3.19),

$$\left.\begin{aligned} & g_{ij}(0) = g'_{ij}(0) = 0 \ , \quad g'_{ij}(\infty) = 0 \ , \quad \begin{cases} i = 3,4 \\ j \geq 0 \end{cases} \\ & f_{ij}(0) = f'_{ij}(0) = 0 \ , \quad f'_{ij}(\infty) = 0 \ , \quad \begin{cases} i = 1,2,3,4 \\ j \geq 1 \end{cases} \\ & \qquad\qquad f_{io}(\infty) = 2 \ , \quad i = 1,2,3,4. \end{aligned}\right\} \quad (3.45)$$

Determination of the K_n

Since w_c is assumed to be an analytic function of ξ, it is possible to consider w_c in the forms

$$w_c = \sum_{n=0}^{\infty} K_n(\eta, \psi)\, \xi^n \ , \qquad (3.46)$$

$$w_c = \sum_{n=0}^{\infty} K_n^{*}(r, \psi)\, \xi^n \ , \qquad (3.47)$$

where the K_n are determined from the K_n^{*} by expanding $r = (1-4\varepsilon\eta\xi)^{1/2}$ as a power series in ξ.

From the equations of (3.8) determining the pressure in the core, it is essential, in order that they be compatible, that

$$\frac{\partial}{\partial \psi}\left(\frac{\partial w_c^2}{\partial s}\right) + 2\beta \frac{\partial w_c^2}{\partial s} = 0 , \tag{3.48}$$

$$\frac{\partial}{\partial r}\left(\frac{\partial w_c^2}{\partial s}\right) + 2\alpha \frac{\partial w_c^2}{\partial s} = 0 , \tag{3.49}$$

$$\frac{\partial}{\partial r}\left(\beta\, w_c^2\right) - \frac{\partial}{\partial \psi}\left(\alpha\, w_c^2\right) = 0 . \tag{3.50}$$

Equations (3.48) and (3.49) integrate readily yielding

$$\frac{\partial w_c^2}{\partial s} = \frac{A(s,\psi)}{h^2} \quad \text{and} \quad \frac{\partial w_c^2}{\partial s} = \frac{B(s,r)}{h^2} ,$$

and so

$$\frac{\partial w_c^2}{\partial s} = \frac{A(s)}{h^2} . \tag{3.51}$$

Equation (3.50) reduces to

$$\frac{\partial h}{\partial \psi}\frac{\partial w_c^2}{\partial r} - \frac{\partial h}{\partial r}\frac{\partial w_c^2}{\partial \psi} = 0 ,$$

which means that the Jacobian of h and w_c^2 with respect to r and ψ is identically zero. There is thus a functional relationship between h and w_c^2 and since

w_c is also a function of s

$$w_c = w_c(h,s) \tag{3.52}$$

Inserting the value of w_c from (3.47) in (3.51) and assuming that A is an analytic function of ξ, the $K_n^{\ast}$ can be derived from

$$[K_o^{\ast}+K_1^{\ast}\xi+K_2^{\ast}\xi^2+\ldots][K_1^{\ast}+2K_2^{\ast}\xi+3K_3^{\ast}\xi^2+\ldots] = \frac{A_1}{h^2} + \frac{A_2\xi}{h^2} + \frac{A_3\xi^2}{h^2} + \ldots \tag{3.53}$$

where the A_n are constants and, from (3.52), $K_o^{\ast}$ must be a function of h alone.

Equating coefficients of like powers of ξ, it is seen that the $K_n^{\ast}$ take the forms

$$\begin{aligned}
K_1^{\ast} &= \frac{A_1}{K_o^{\ast}h^2} \quad , \\
K_2^{\ast} &= \left[\frac{A_2}{h^2} - K_1^{\ast 2}\right]\cdot\frac{1}{2K_o^{\ast}} \quad , \\
K_3^{\ast} &= \left[\frac{A_3}{h^2} - 3K_1^{\ast}K_2^{\ast}\right]\cdot\frac{1}{3K_o^{\ast}} \quad , \\
K_4^{\ast} &= \left[\frac{A_4}{h^2} - 4K_1^{\ast}K_3^{\ast} - 2K_2^{\ast 2}\right]\cdot\frac{1}{4K_o^{\ast}} \quad , \text{etc.}
\end{aligned} \tag{3.54}$$

The K_{io} can be determined in terms of the A_n directly from these relations by expanding h as a power series in ξ . Thus

$$K_{oo} = K_o^{\ast}(h_o) \ ,$$

$$K_{1o} = \frac{A_1}{K_{oo}h_o^2} = K_1^{\ast}(h_o) \ , \tag{3.55}$$

and in general $K_{io} = K_i^{\ast}\ (h=h_o)$.

To determine the $K_i^{\ast}$ completely, the A_n's have to be evaluated. This is achieved by considering the fact that the flux through the pipe must be constant. Thus

$$\int_0^{2\pi}\int_0^{a} w_c(s=0)r\ dr\ d\psi = \int_0^{2\pi}\int_0^{a} w_c\ r\ dr\ d\psi$$

$$- \int_0^{2\pi}\int_0^{a} (w_c-w)r\ dr\ d\psi \ , \tag{3.56}$$

where w represents the axial velocity in the boundary layer which matches on exactly to the axial core velocity w_c . Substituting for w_c from (3.46) and (3.47);

substituting for w from (3.19) and transforming the last integral from r to η,

$$0 = \int_0^{2\pi}\int_0^a \sum_{n=1}^{\infty} K_n^{**}(r,\psi) r \xi^n dr\, d\psi - a^2 \int_0^{2\pi}\int_0^{1/4\varepsilon\xi} 2\varepsilon\xi \times$$

$$\left\{ \sum_{n=0}^{\infty} K_n(\eta,\psi)\xi^n - \frac{1}{2\xi}\frac{\partial f}{\partial \eta} \right\} d\eta\, d\psi .$$

From (3.26) $K_n(\eta,\psi) = \sum_{j=0}^{n-1} K_{nj}\eta^j \quad n \geq 1$, and so for large η,

$$f_{n+1} = \sum_{j=0}^{n-1} \frac{2K_{nj}\eta^{j+1}}{j+1} + B_{n+1} , \qquad (3.57)$$

where B_{n+1} is a function of ψ obtained up to $n = 3$ by numerically integrating equations (3.24), (3.32), (3.34) and (3.36).

Since $f_n(\eta) = 0$ at $\eta = 0$, the flux condition yields

$$\sum_{n=1}^{\infty} \int_0^{2\pi} \int_0^1 K_n^{*} \xi^n \, r \, dr \, d\psi = a^2 \sum_{n=0}^{\infty} \int_0^{2\pi} \varepsilon \, \xi^{n+1} \times$$

$$\left[\sum_{j=0}^{n-1} \frac{2K_{n,j} \eta^{j+1}}{j+1} - \left(\sum_{j=0}^{n-1} \frac{2K_{n,j} \eta^{j+1}}{j+1} + B_{n+1} \right) \right]_{\eta = \frac{1}{4\varepsilon\xi}} d\psi \, ,$$

whereupon, equating like coefficients of ξ ,

$$\int_0^{2\pi} \int_0^a K_n^{*}(r,\psi) r \, dr \, d\psi = -a^2 \int_0^{2\pi} \varepsilon \, B_n \, d\psi \quad , \quad n \geq 1 \, . \qquad (3.58)$$

This equation together with those of (3.54) are sufficient to determine the A_n and thus the axial core velocity. Since it was not necessary to approximate to the boundary layer velocity in determining (3.57), the development of the axial core velocity can be determined for any injected velocity profile which is a function of h and which does **not** in itself generate a large amount of vorticity.

APPENDIX

To prove that $g_2(\eta,\Psi) = 0$ for any Ψ and all η in $[0,\infty)$

From equation (3.33), g_2 satisfies the equation

$$\frac{\partial^3 g_2}{\partial \eta^3} + f_{10}\frac{\partial^2 g}{\partial \eta^2} - f'_{10}\frac{\partial g_2}{\partial \eta} = 0 , \qquad (A.1)$$

subject to the boundary conditions

$$g_2 = \frac{\partial g_2}{\partial \eta} = 0 \quad \text{at} \quad \eta = 0 , \quad \frac{\partial g_2}{\partial \eta} \to 0 \text{ as } \eta \to \infty. \qquad (A.2)$$

g_2 is proved identically zero by supposing that for any Ψ, there exists an η in $[0,\infty)$ such that $\frac{\partial g_2}{\partial \eta}(\eta,\Psi) > 0$ and obtaining a contradiction. If $\frac{\partial g_2}{\partial \eta} > 0$ for some η in $[0,\infty)$ then, in view of the boundary conditions, there will be at least one maximum point in this range. If this point is η_1, $\frac{\partial g_2}{\partial \eta}(\eta_1,\Psi) > 0$, $\frac{\partial^2 g_2}{\partial \eta^2}(\eta_1,\Psi) = 0$ and $\frac{\partial^3 g_2}{\partial \eta^3}(\eta_1,\Psi) < 0$. It is assumed that the injection velocity is nowhere negative and so $f'_{10}(\eta_1) \geq 0$. Therefore at $\eta = \eta_1$, the left hand side

of (A.1) must be less than zero. This is a contradiction which is repeated if $\frac{\partial g_2}{\partial \eta}$ is assumed negative for some η in $[0,\infty)$. Thus $\frac{\partial g_2}{\partial \eta}$ is zero throughout this range and for all ψ. Since g_2 must be zero at $\eta = 0$, it follows that g_2 must be identically zero.

CHAPTER 4

The Numerical Solution

Equations (3.29) and (3.39) - (3.44) together with the boundary conditions of (3.45) are entirely independent of external parameters such as $\varkappa$ or Re and can be calculated without reference to them. The coefficients of f_{ij} and g_{ij} are, however, dependent on these parameters and in particular, $K_1^{\ast} - K_4^{\ast}$ are dependent on $\varkappa$. These equations were solved numerically using Gill's process for the fourth order Runge-Kutta method, on the I.B.M. 7090 computer at Imperial College. As usual in computations of this type where succeeding functions depend on previously calculated functions, accuracy decreases owing to build up error. The first few functions were calculated to six decimal places, however, and it is reasonable to assume that the functions f_{4j}, that is the functions more prone to build up error, are accurate at least to three places of decimals. The results, together with the program for solving a set of successively dependent, simultaneous differential equations, can be found at the end of the thesis.

Comparing the behaviour of $f_{ij}(\eta)$ for large η with that of f_n^{∞} from (3.38), the functions B_n were found to be

$$B_1 = -1.7208\ K_{oo} \quad ,$$

$$B_2 = 1.3008\ K_{10} + 0.0717\ \varepsilon \quad ,$$

$$B_3 = [2.7561\ K_{20} - 4.6072\ K_{10}^2 + 3.0351\ \varepsilon\ K_{10} - 1.7196\ \varepsilon^2]/K_{oo} \quad , \tag{4.1}$$

$$B_4 = [3.8732\ K_{30}K_{oo} - 14.931\ K_{10}K_{20} + 14.655\ K_{10}^3/K_{oo} - 18.689\ \varepsilon K_{10}^2/K_{oo} + 16.335\ \varepsilon^2 K_{10}/K_{oo} + 5.569\ \varepsilon\ K_{20} - 7.185\ \varepsilon^3/K_{oo}]/K_{oo} \quad .$$

These functions were substituted into equation (3.58) together with the functions for the K_n^{∞} as given by (3.54) for the special case of constant injection velocity (i.e. $K_o = 1$) . The various integrals were evaluated numerically yielding values of A_1 , A_2 , A_3 and A_4 for various curvature ratios [see table (4.1)].

It is seen from table (4.1) that if the values for

A_1 - A_4 when $\varkappa = 0$ are inserted in (3.54),

$K_1^{\pi\pi} = 3.442$, $K_2^{\pi\pi} = -9.099$, $K_3^{\pi\pi} = 141.9$ and $K_4^{\pi\pi} = -2784$.

These values are effectively the same as those obtained by Goldstein and Atkinson for constant velocity injection into a straight pipe, any deviation being in the fourth significant figure.

$\varkappa$	A_1	A_2	A_3	A_4
0.0	3.442	-6.351	331.7	-9016
0.05	3.435	-6.319	333.1	-9128
0.1	3.414	-6.222	337.1	-9471
0.2	3.330	-5.831	353.9	-10931
0.4	2.992	-4.206	428.6	-18700
0.6	2.417	-1.178	595.5	-44805
0.8	1.573	4.702	1051	-206136

TABLE (4.1). The variation of the A_n with curvature ratio for the particular case of constant velocity injection.

It is now possible to write down the velocity distribution in dimensional form in terms of known quantities. Thus, from equations (3.19) and the expansion of f , the axial velocity component in the boundary layer is

$$w = \frac{1}{2} W_o \left[\frac{\partial f_1}{\partial \eta} + \frac{\partial f_2}{\partial \eta} \xi + \frac{\partial f_3}{\partial \eta} \xi^2 + \ldots\ldots \right]. \quad (4.2)$$

If g_3 is replaced by $Re^2 \beta_o h_o^2 G_3$ and g_4 by $Re^2 \beta_o h_o^2 G_4$ and so on, the tangential velocity distribution in the boundary layer can be written as

$$v = \frac{W_o}{2h_o Re \xi} Re^2 \beta_o h_o^2 \left[\frac{\partial G_3}{\partial \eta} \xi^3 + \frac{\partial G_4}{\partial \eta} \xi^4 + \ldots. \right],$$

$$\text{i.e. } v = \frac{W_o s}{R} \cos\psi \left[\frac{\partial G_3}{\partial \eta} + \frac{\partial G_4}{\partial \eta} \xi + \ldots.. \right] . \quad (4.3)$$

Similarly the radial component of velocity in the boundary layer becomes

$$u = \frac{a\varepsilon W_o \xi}{a h_o s} \left[(f_1 + 2f_2 \xi + \ldots) - \eta \left(\frac{\partial f_1}{\partial \eta} + \frac{\partial f_2}{\partial \eta} \xi + \ldots. \right) \right.$$

$$\left. + \frac{4s^2}{a^2} \left(\frac{1}{\varepsilon} \frac{\partial}{\partial \psi} - \frac{\eta}{\varepsilon^2} \frac{d\varepsilon}{d\psi} \frac{\partial}{\partial \eta} \right) \left(\varepsilon G_3 + \varepsilon G_4 \xi + \ldots \right) \right]. \quad (4.4)$$

Application to the skin friction and the limiting streamlines

These two applications are considered together because the expressions for the skin friction can be applied directly to obtain the limiting streamlines at the wall of the pipe.

There are two components of the skin friction and they will be defined as

$$\tau_{ws} = \mu\left(\frac{\partial w}{\partial r}\right)_{r=0} \quad \text{and} \quad \tau_{w\psi} = \mu\left(\frac{\partial v}{\partial r}\right)_{r=0} . \tag{4.5}$$

Transforming these using the relations of (3.17) and eliminating w and v using equations (3.19),

$$\tau_{ws} = \frac{-\mu W_o}{4\varepsilon a \xi^2} f_{\eta\eta}(o) , \tag{4.6}$$

$$\tau_{w\psi} = \frac{-\mu W_o}{4\varepsilon a \xi^2 h_o Re} \cdot g_{\eta\eta}(0) . \tag{4.7}$$

In order that these results may be compared with possible future experiments, the mean drag coefficient will be found as a function of distance down the pipe. If the mean drag coefficient is defined as

$$D(\ell) = \frac{-1}{\frac{1}{2}\rho W_o^2 \ell} \int_0^{\ell} \frac{1}{2\pi} \int_0^{2\pi} \tau_{ws} \, d\psi . ds$$

then

$$D(\xi_\ell) = \frac{a}{2\pi\ell} \int_0^{\left(\frac{2\ell}{aRe}\right)^{1/2}} \int_0^{2\pi} \frac{f_{\eta\eta}(o)}{\varepsilon \xi} \, d\psi \, d\xi \tag{4.8}$$

The results of the previous section for constant velocity injection were inserted in this integral and the integration was carried out numerically for various values of $\xi_\ell = \left(\frac{2\ell}{aRe}\right)^{1/2}$ and for various curvature ratios. The increase in resistance with curvature is exhibited by plotting $\frac{D_c}{D_s}$ against ξ_ℓ where D_s is the drag coefficient for a straight pipe and D_c is that for a curved pipe [see Fig. (4.1)].

The equation for the limiting streamlines at the wall can be written as

$$a\,\frac{d\psi}{ds} = \lim_{r\to a}\ \frac{v}{w}\ ,$$

and since w and v are zero at the wall,

$$a\,\frac{d\psi}{ds} = \lim_{r\to a}\ \frac{\frac{\partial v}{\partial r}}{\frac{\partial w}{\partial r}} = \frac{\tau_{w\psi}}{\tau_{ws}}\ . \qquad (4.9)$$

Transforming as before and using equations (4.6) and (4.7)

$$\frac{d\psi}{d\xi} = \frac{\xi\, g_{\eta\eta}(o)}{h\, f_{\eta\eta}(o)}\ . \qquad (4.10)$$

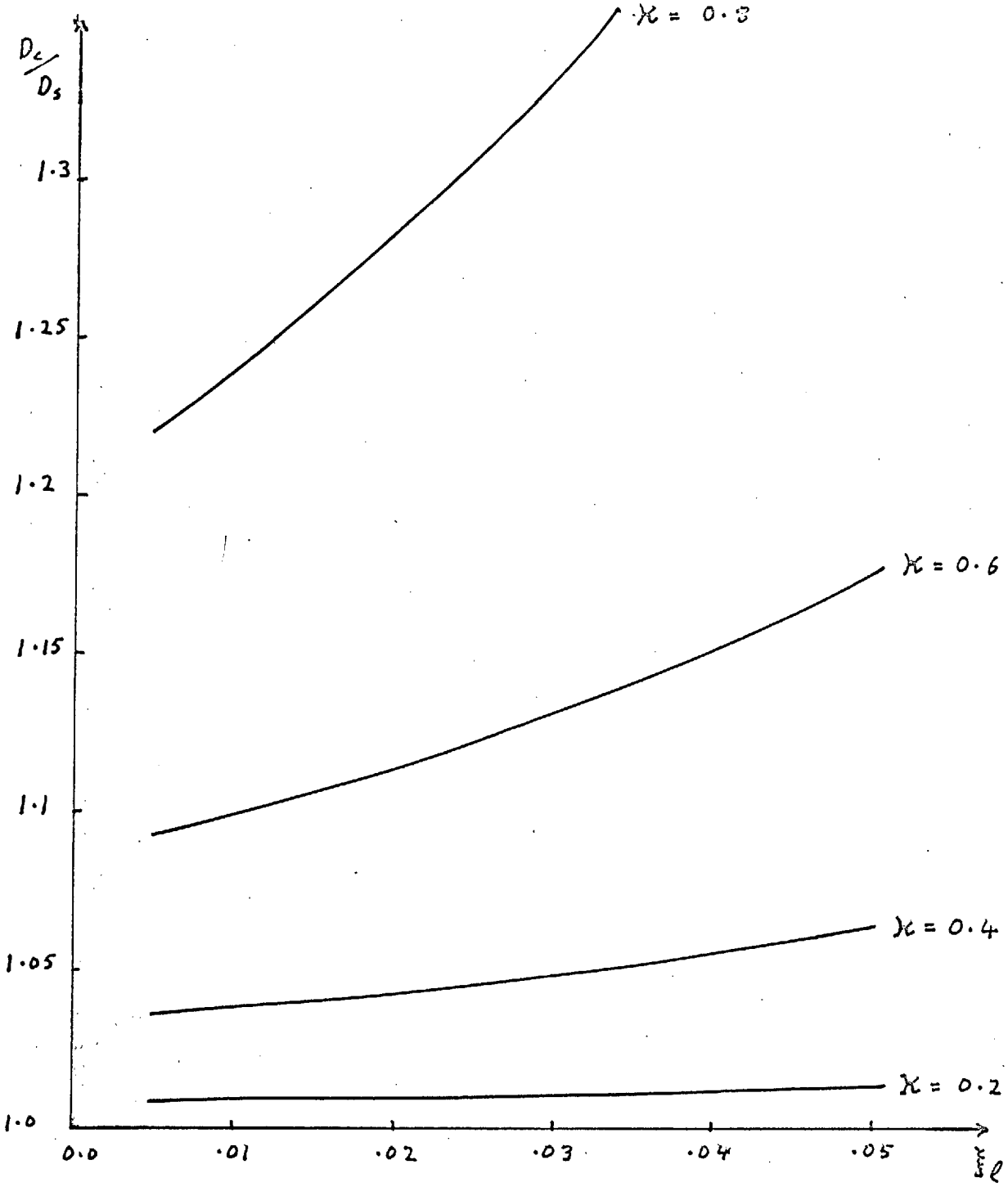

Fig (4.1). The increase in resistance due to curvature.

To obtain a first approximation to the streamlines, for constant velocity injection, $f_{\eta\eta}(o)$ and $g_{\eta\eta}(o)$ will be written as

$$f_{\eta\eta}(o) = 1.328\ \xi$$

$$g_{\eta\eta}(o) = -2.172\ Re^2 \beta_o h_o^2\ \xi^3 \ .$$

Equation (4.10) then becomes

$$\frac{d\Psi}{d\xi} = -1.64\ Re^2\ \kappa \cos\Psi . \xi^3 \ ,$$

the solution of which can be written as

$$\Psi - \Psi_o = 2 \tan^{-1}\left[\exp\left\{-0.41\ Re^2 \kappa\ \xi^4\right\}\right] - \pi/2 \qquad (4.11)$$

where Ψ_o is the initial value of Ψ at $\xi = 0$.

Equation (4.10) was solved numerically, again for constant velocity injection, taking the first four terms in the expansion of $f_{\eta\eta}(o)$ and the first two terms in the expansion of $g_{\eta\eta}(o)$. The results were found to be dependent on κ and $Re^2\kappa$ and the limiting streamlines for $Re\ \kappa^{1/2} = 2000$ and $\kappa = .05$ are illustrated in Fig. (4.2).

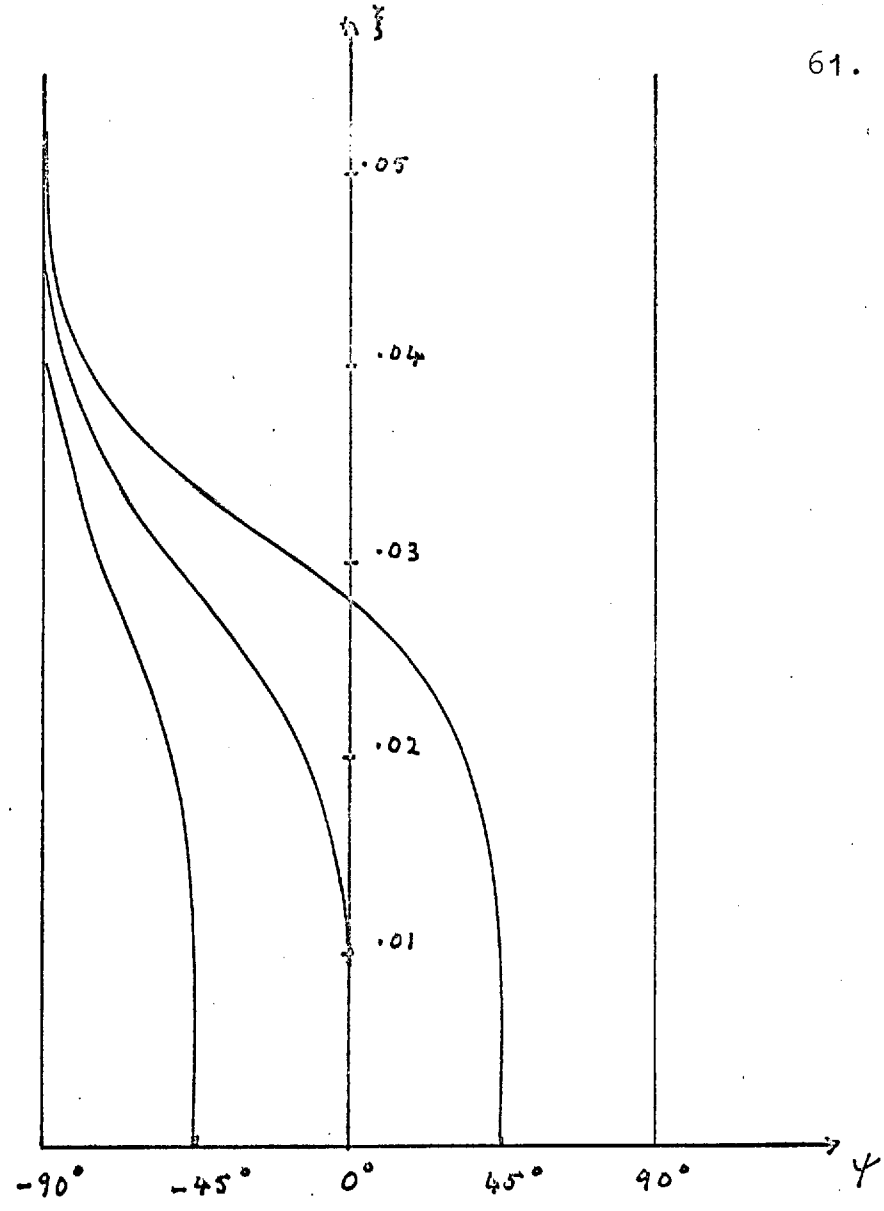

Fig. (4.2). The limiting streamlines in the top half of the pipe for the particular case of Re $\kappa^{1/2}$ = 2000 and κ = .05 . (The limiting streamlines in the bottom half of the pipe are identical due to the symmetry about the $\psi = 90^{\circ}$, $\psi = -90^{\circ}$ line).

Conclusions

The object of this investigation was to find the effect of viscous forces in the inlet region of a curved pipe. The types of injection velocity were restricted to those that were nowhere zero at the wall, those that had no initial secondary flow and those that generated little secondary vorticity apart from that produced by the viscous forces. In this way, an attempt was made to isolate the effects of viscosity.

It was shown that a necessary condition for there to be no generation of vorticity is that $w_c = w_c(r_1, \theta)$ which is equivalent to $w_c = w_c(h,s)$. It was noted, however, that secondary vorticity has to be generated to preserve continuity if w_c varies with θ. The analysis was then continued on the assumption that the secondary flow produced was sufficiently small so that the equations of (3.8) represented reasonably well the pressure distribution in the core. This additional restriction on the injection velocity is now considered and it will be seen that the particular case of constant velocity injection, which was used to obtain the numerical results of this chapter, is a satisfactory example within certain limitations.

Since the flux across any cross section is constant and the boundary layer thickness is increasing, the core is accelerated and so there must be a variation in axial velocity with axial distance. This is, however, an effect of the growing boundary layer and the amount of vorticity generated by this means will increase from zero as the boundary layer thickness increases. It is therefore reasonable to assume that the equations of (3.8) become invalid because of this effect some way down the pipe, which may well be beyond the point where the boundary layer approximation breaks down. If it is nearer the entrance of the bend than this point, it merely restricts the validity of the theory to a smaller region at the entrance.

In a similar way, since there is no initial secondary flow, any other means of generating secondary vorticity will only effect the validity of the equations of (3.8) when a certain amount of secondary flow has been produced. Again this will occur a little way from the entrance depending on how quickly the secondary vorticity is generated. This may be kept to a minimum by letting the core be represented by the inviscid irrotational flow through a curved pipe.

If ω_n , ω_b and ω_s are zero, the following equations may be obtained from (3.10), (3.11) and (3.14).

$$\frac{\partial v_1}{\partial \theta} - r_1 \frac{\partial w_1}{\partial z} = 0 \ , \tag{4.12}$$

$$\frac{\partial u_1}{\partial z} - \frac{\partial v_1}{\partial r_1} = 0 \ , \tag{4.13}$$

$$\frac{\partial}{\partial r_1} (r_1 . w_1) - r_1 \frac{\partial u_1}{\partial \theta} = 0 \ . \tag{4.14}$$

A solution of these equations which also satisfies the continuity equation of (3.16) is

$$\left.\begin{aligned} u_1 = v_1 = 0 \qquad &, \\ w_1 = \frac{A'}{r_1} = \frac{A}{h} \qquad &, \end{aligned}\right\} \tag{4.15}$$

where A is a constant. Thus, with an injection velocity given by (4.15), secondary vorticity is generated only by the growing boundary layer. This particular injection velocity is of practical interest since it can be obtained by having the dynamic pressure constant across the cross

section at the entrance to the bend. This may be the case if a curved pipe takes fluid from a reservoir at constant pressure. The proof is as follows: if the dynamic pressure is constant at the entrance to the pipe

$$\frac{P}{\rho} = \text{const} - \frac{1}{2} w_1^2(s=0) \ ,$$

$$= \text{const} - \frac{1}{2} W_o^2 K_o^2(h) \ , \qquad (4.16)$$

where W_o is the mean axial velocity and is constant. From the equations of motion in (r_1, θ, z) coordinates

$$\frac{1}{\rho} \frac{\partial P}{\partial r_1} = \frac{w_1^2}{r_1} = \frac{W_o^2 K_o^2(h)}{r_1} \qquad (4.17)$$

Eliminating the pressure from (4.16) and (4.17) yields the injection velocity

$$w_1(s=0) = \frac{W_o}{h} \ . \qquad (4.18)$$

If $\varkappa \ll 1$, $h \doteq 1$ and this injection velocity is a good approximation to constant velocity injection. If $\varkappa$ is of order one, the constant injection velocity case is still valid but in a smaller region near the

entrance to the bend.

In the historical survey of Chapter one, it was seen that most research work on the inlet region considered injection velocities which were modified by the centrifugal force. The past two chapters have considered injection velocities which were modified by viscous forces. In practical cases, it is often a combination of these factors which modifies the injection velocity. The consideration of this problem is, however, formidable, since the equations of (3.8) will be far more complicated and the F_n's from the boundary layer would probably have to be matched to the core velocity.

PART II

FLOW IN THE FULLY DEVELOPED REGION

CHAPTER 5

Introduction

In Chapter one, the fully developed region was defined as that region, sufficiently far from the entrance to the bend, where the flow is similar at every cross section. The equations of motion depicting flow in this region contain only two independent variables instead of three and, as a consequence, most theoretical investigations concentrated on this region.

In practice, fully developed flow is obtained by passing fluid through a pipe which is coiled about a cylindrical former. When comparing theoretical results with experimental results, it is assumed that the torsion introduced in such a coil is negligible. For pipes with very small curvature ratio, such an assumption is justified. If, however, this curvature ratio is increased, the amount of torsion in the pipe is also increased.

The results obtained in previous theories assumed that the curvature ratio was very much less than one and were not concerned with the effects of torsion. Results derived in this thesis are, however, extended to large values of the curvature ratio and a comparison with

possible future experiments is practical only if the effects of torsion are understood. To this end, a suitable orthogonal coordinate system including curvature and torsion will be derived and the corresponding equations of motion investigated.

Effects of torsion

If a point in a curved pipe with torsion is defined by (x,y,s), where s is the distance measured along the axis of the pipe and x and y define a point in the cross section relative to a set of axes $(\underline{l},\underline{m})$ at right angles to and capable of rotating about the axis of the pipe. If the unit vectors $\underline{t}$, $\underline{n}$, $\underline{b}$ are the conventional unit vectors of differential geometry [see fig. 5.1], the ~~metric~~ position vector can be written as

$$\underline{r} = \underline{r}_o + \underline{l}x + \underline{m}y \,, \tag{5.1}$$

where

$$\begin{aligned} \underline{l} &= \sin\phi\, \underline{n} + \cos\phi\, \underline{b} \,, \\ \underline{m} &= -\cos\phi\, \underline{n} + \sin\phi\, \underline{b} \,. \end{aligned} \tag{5.2}$$

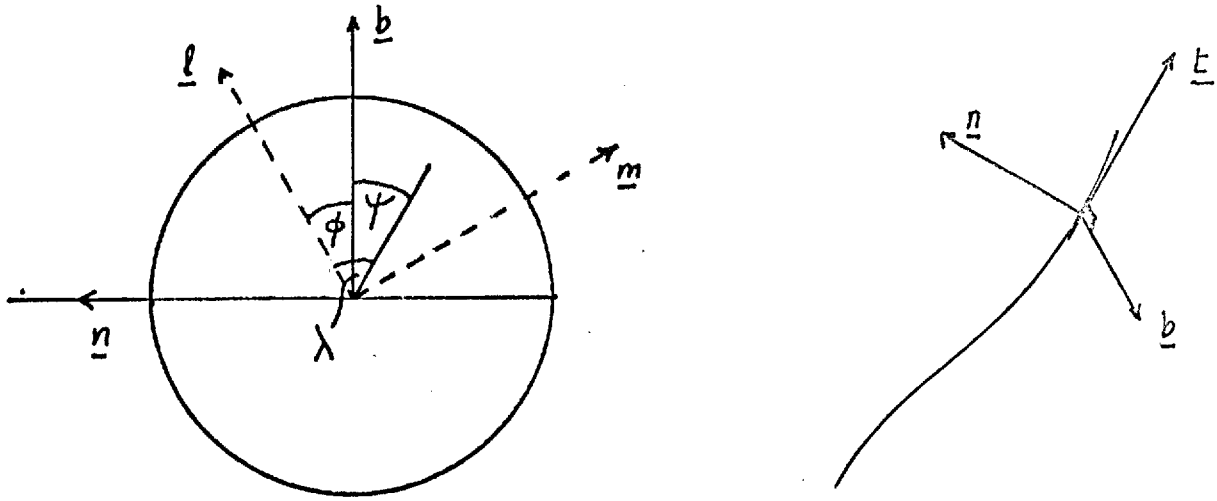

Fig. (5.1). The coordinate system for investigating the effects of torsion.

Using the Frenet formulae,

$$d\underline{n} = (-\frac{1}{c}\,\underline{t} + \frac{1}{\tau}\,\underline{b})\,ds\ ,$$

$$d\underline{b} = -\frac{1}{\tau}\,\underline{n}\,ds\ , \qquad (5.3)$$

$$d\underline{r}_o = \underline{t}\,ds\ ,$$

where $\frac{1}{c}$ is the curvature and $\frac{1}{\tau}$ is the torsion, equation (5.1) can be differentiated yielding

$$d\underline{r} = \left[1 - \frac{1}{\sigma}(x \sin\phi - y \cos\phi)\right] ds\, \underline{t}$$

$$+ \left[\sin\phi\, dx - \cos\phi\, dy + \left\{ - \frac{1}{\tau}(x \cos\phi + y \sin\phi) \right.\right.$$

$$\left.\left. + x \frac{d}{ds} \sin\phi - y \frac{d}{ds} \cos\phi \right\} ds\right]\underline{n} + \left[\cos\phi\, dx + \sin\phi\, dy\right.$$

$$\left. + \left\{ \frac{1}{\tau}(x \sin\phi - y \cos\phi) + x \frac{d}{ds} \cos\phi + y \frac{d}{ds} \sin\phi \right\} ds\right] \underline{b} \,. \tag{5.4}$$

For orthogonality, the coefficients of $dx.dy$, $dy.ds$ and $dx.ds$, obtained from $(dr)^2$ must be zero. This condition is found to be satisfied if

$$\frac{1}{\tau} + \sin\phi \frac{d}{ds} \cos\phi - \cos\phi \frac{d}{ds} \sin\phi = 0 \,,$$

whereupon

$$\frac{1}{\tau} = \frac{d\phi}{ds} \,,$$

$$\text{or} \quad \phi = \int \frac{ds}{\tau} \,. \tag{5.5}$$

In this case

$$(d\underline{r})^2 = \left[1 + \frac{1}{\sigma}(y \cos\phi - x \sin\phi)\right]^2 ds^2 + dx^2 + dy^2 \,.$$

If (x,y) is transformed to (r,λ) using $x = r\cos\lambda$ and $y = r\sin\lambda$,

$$(d\underline{r})^2 = \left[1 + \frac{1}{c} r \sin(\lambda-\phi)\right]^2 ds^2 + r^2 d\lambda^2 + dr^2 . \quad (5.6)$$

The scale factors for the new coordinate system thus become $h_1 = 1$, $h_2 = r$ and $h_3 = 1 + \frac{1}{c} r \sin(\lambda-\phi)$.

The equations of motion are the same as those given by (2.5) - (2.9) except that h , a function of r and ψ , is replaced by h_3 , a function of r , λ and s . It is immediately evident that if $1/\tau$ is non zero, the flow cannot become fully developed in the sense described earlier.

Before proceeding to an approximate solution of these equations for a particular type of flow, it will be constructive to consider a pipe of radius 'a' coiled about a former of radius $(R-a)$ so that the torsion introduced is kept to a minimum. This would be the case in an experiment designed to investigate flow in the fully developed region. In such a coil, the centre of the pipe forms a helix defined by the equations

$$x = R\cos\Theta \qquad y = R\sin\Theta \qquad \text{and} \qquad z = R\Theta\tan\gamma ,$$

where (x,y,z) now represents the cartesian coordinate system and where γ is the helix angle. Since this angle is to take its minimum practical value, z must increase by $2a$ for each complete revolution about the former. Thus

$$2a = 2\pi R \tan\gamma$$

$$\text{or} \quad \gamma = \tan^{-1}\frac{a}{\pi R} = \tan^{-1}\frac{\varkappa}{\pi} \quad , \tag{5.7}$$

if $\varkappa$ is defined, as is usual, by $\varkappa = a/R$.

The curvature and torsion can then be written as

$$\frac{1}{\sigma} = \frac{\cos^2\gamma}{R} = \frac{1}{R\left[1 + \left(\frac{\varkappa}{\pi}\right)^2\right]} \quad ,$$

$$\frac{1}{\tau} = \frac{\sin\gamma\,\cos\gamma}{R} = \frac{\varkappa}{\pi R\left[1 + \left(\frac{\varkappa}{\pi}\right)^2\right]} \quad . \tag{5.8}$$

If s and r are replaced by as' and ar' , then, since the torsion is constant,

$$h_3 = 1 + \frac{\varkappa r'}{1 + \left(\frac{\varkappa}{\pi}\right)^2} \sin\left[\lambda - \frac{\varkappa^2 s'}{\pi\left\{1 + \left(\frac{\varkappa}{\pi}\right)^2\right\}}\right] \quad . \tag{5.9}$$

If it is assumed that the torsional effects are very small,

$$h_3 = 1 + \frac{\kappa r'}{1 + \left(\frac{\kappa}{\pi}\right)^2} \left[\sin \lambda - \frac{\kappa^2 s'}{\pi \left\{ 1 + \left(\frac{\kappa}{\pi}\right)^2 \right\}} \cos \lambda \right] .$$

Thus, if they are to be neglected, it is necessary that

$$\kappa^2 s' \ll 1 . \qquad (5.10)$$

Physically, this restriction implies that two reference points on the coiled pipe yield effectively the same results so long as the distance between them is much less than $1/\kappa^2$. This fact must be taken into account if the results derived later are compared with experiment. In addition, it should be noted that (5.10) is a necessary condition; a sufficient condition is derived only after consideration of the equations of motion.

Returning to the equations of motion, it can be seen that for the case of constant torsion, they can be transformed from the (r,λ,s) coordinate system to the (r,ψ,s) coordinate system using the transform

$$\begin{aligned} \psi &= \lambda - \phi , \\ &= \lambda - s/\tau . \end{aligned} \qquad (5.11)$$

It can then be seen that a solution exists such that the velocity distribution is a function of r and ψ alone and the pressure takes the form $p = -Gs + p'(r,\psi)$, where G is a constant. In this case, the equations of motion become

$$u\frac{\partial u}{\partial r} + \frac{v}{r}\frac{\partial u}{\partial \psi} - \frac{w}{\tau h}\frac{\partial u}{\partial \psi} - \frac{v^2}{r} - \alpha w^2 = -\frac{\partial p'}{\partial r} - \frac{\nu}{rh}\Bigg[\frac{\partial}{\partial \psi}\left\{\frac{h}{r}\left(\frac{\partial}{\partial r}(rv) - \frac{\partial u}{\partial \psi}\right)\right\} - \frac{1}{\tau}\frac{\partial}{\partial \psi}\left\{\frac{r}{h}\left(\frac{1}{\tau}\frac{\partial u}{\partial \psi} + \frac{\partial}{\partial r}(hw)\right)\right\}\Bigg], \quad (5.12)$$

$$u\frac{\partial v}{\partial r} + \frac{v}{r}\frac{\partial v}{\partial \psi} - \frac{w}{\tau h}\frac{\partial v}{\partial \psi} - \frac{\beta w^2}{r} + \frac{uv}{r} = -\frac{1}{\rho r}\frac{\partial p'}{\partial \psi} - \frac{\nu}{h}\Bigg[\frac{1}{\tau}\frac{\partial}{\partial \psi}\left\{\frac{1}{rh}\left(\frac{\partial}{\partial \psi}(hw) - \frac{\partial}{\partial \psi}(rv)\right)\right\} - \frac{\partial}{\partial r}\left\{\frac{h}{r}\left(\frac{\partial}{\partial r}(rv) - \frac{\partial u}{\partial \psi}\right)\right\}\Bigg], \quad (5.13)$$

$$u\frac{\partial w}{\partial r} + \frac{v}{r}\frac{\partial w}{\partial \psi} - \frac{w}{\tau h}\frac{\partial w}{\partial \psi} + \alpha uw + \frac{\beta vw}{r} = \frac{G}{h} - \frac{1}{\tau h}\frac{\partial p'}{\partial \psi} + \frac{\nu}{r}\Bigg[\frac{\partial}{\partial r}\left\{\frac{r}{h}\left(\frac{\partial}{\partial r}(hw) - \frac{1}{\tau}\frac{\partial u}{\partial \psi}\right)\right\} + \frac{\partial}{\partial \psi}\left\{\frac{1}{rh}\left(\frac{\partial}{\partial \psi}(hw) - \frac{\partial}{\partial r}(rv)\right)\right\}\Bigg], \quad (5.14)$$

$$\frac{\partial}{\partial r}(rhu) + \frac{\partial}{\partial \psi}(hv) - \frac{1}{\tau}\frac{\partial}{\partial \psi}(rw) = 0, \quad (5.15)$$

where $h = 1 + \frac{r}{\sigma} \sin \psi$.

If a solution is obtained from these equations subject to the usual boundary conditions, it is probably valid some way from the entrance of the bend and fully developed flow can be said to exist in a curved pipe with constant torsion if it has a velocity distribution of the above form.

Solution for flow at low Reynolds number in a pipe of small curvature ratio.

If a fluid is flowing through a curved pipe with constant torsion in the fully developed region as defined in the last section and if it is assumed that the curvature ratio of the pipe is sufficiently small, so that terms of order κ can be rejected relative to terms of order one, the flow is represented by the equations

$$u\frac{\partial u}{\partial r} + \frac{v}{r}\frac{\partial u}{\partial \psi} - \frac{w}{\tau}\frac{\partial u}{\partial \psi} - \frac{v^2}{r} - \alpha w^2 = -\frac{\partial p'}{\partial r} + \nu\left[\nabla^2 u - \frac{u}{r^2} - \frac{2}{r^2}\frac{\partial v}{\partial \psi}\right], \tag{5.16}$$

$$u\frac{\partial v}{\partial r} + \frac{v}{r}\frac{\partial v}{\partial \psi} - \frac{w}{\tau}\frac{\partial v}{\partial \psi} - \frac{\beta w^2}{r} + \frac{uv}{r} = -\frac{1}{\rho r}\frac{\partial p'}{\partial \psi} + \nu\left[\nabla^2 v + \frac{2}{r^2}\frac{\partial u}{\partial \psi} - \frac{v}{r^2}\right], \tag{5.17}$$

$$u\frac{\partial w}{\partial r} + \frac{v}{r}\frac{\partial w}{\partial \psi} - \frac{w}{\tau}\frac{\partial w}{\partial \psi} + \alpha uw + \beta\frac{vw}{r} = G - \frac{1}{\tau}\frac{\partial p'}{\partial \psi} + \nu \nabla^2 w \ , \quad (5.18)$$

and

$$\frac{\partial}{\partial r}(ru) + \frac{\partial v}{\partial \psi} - \frac{1}{\tau}\frac{\partial}{\partial \psi}(rw) = 0 \ , \quad (5.19)$$

where

$$\nabla^2 = \frac{\partial^2}{\partial r^2} + \frac{1}{r}\frac{\partial}{\partial r} + \frac{1}{r^2}\frac{\partial^2}{\partial \psi^2}$$

and

$$\alpha = \frac{\sin\psi}{\sigma} \qquad \text{and} \qquad \beta = \frac{\cos\psi}{\sigma} \ .$$

In deriving these equations, all curvature effects were rejected in the viscous terms and they were only retained elsewhere when directly coupled with the axial velocity w . The fact that $1/\tau$ is of the same order as $1/\sigma$ was also used.

If equations (5.16) - (5.19) are made non-dimensional replacing v by $\frac{v\nu}{a}$, u by $\frac{u\nu}{a}$, w by $W_o w$, r by ar , s by as and p' by $W_o^2 p$, where W_o is the mean axial velocity,

$$u\frac{\partial u}{\partial r} + \frac{v}{r}\frac{\partial u}{\partial \psi} - \frac{aRe}{\tau}\, w\frac{\partial u}{\partial \psi} - \frac{v^2}{r} - \frac{aRe^2}{\sigma}\sin\psi . w^2 = -Re^2\frac{\partial p}{\partial r}$$

$$+ \nabla^2 u - \frac{u}{r^2} - \frac{2}{r^2}\frac{\partial v}{\partial \psi} \ , \quad (5.20)$$

$$u\frac{\partial v}{\partial r} + \frac{v}{r}\frac{\partial v}{\partial \psi} - \frac{aRe}{\tau} w\frac{\partial v}{\partial \psi} + \frac{uv}{r} - \frac{aRe^2}{\sigma}\cos\psi . w^2 =$$

$$- \frac{Re^2}{r}\frac{\partial p}{\partial \psi} + \nabla^2 v + \frac{2}{r^2}\frac{\partial u}{\partial \psi} - \frac{v}{r^2} \quad , \qquad (5.21)$$

$$u\frac{\partial w}{\partial r} + \frac{v}{r}\frac{\partial w}{\partial \psi} - \frac{aRe}{\tau} w\frac{\partial w}{\partial \psi} = \frac{aG}{\rho\nu W_o} + \frac{aRe}{\tau}\frac{\partial p}{\partial \psi} + \nabla^2 w \quad , \qquad (5.22)$$

and $$\frac{\partial}{\partial r}(ru) + \frac{\partial v}{\partial \psi} - \frac{aRe}{\tau}\frac{\partial}{\partial \psi}(rw) = 0 \quad . \qquad (5.23)$$

Since $\frac{a}{R} << 1$, $\frac{a}{\sigma} \doteq \varkappa$ and $\frac{a}{\tau} \doteq 1/2\,\varkappa \sin 2\gamma$.
A solution for low Reynolds number can now be obtained by considering an expansion solution of the form

$$\left.\begin{aligned} w &= w_o + \varkappa w_1 + \ldots \quad , \\ u &= u_1 \varkappa + \ldots \quad , \\ v &= v_1 \varkappa + \ldots \quad , \\ p &= \varkappa p_1 + \ldots \quad , \end{aligned}\right\} \qquad (5.24)$$

Inserting (5.24) into (5.20) - (5.23) and equating coefficients of like powers of $\varkappa$

$$\nabla^2 w_o + C = 0 \quad . \qquad (5.25)$$

where $C = \frac{aG}{\mu w_o}$ and $w_o = w_o(r)$ only.

$$\text{Also} - Re^2 w_o^2 \frac{\sin\psi}{\cos^2\gamma} = -\frac{\partial p_1}{\partial r} + \nabla^2 u_1 - \frac{u_1}{r^2} - \frac{2}{r^2}\frac{\partial v_1}{\partial \psi}, \quad (5.26)$$

$$- Re^2 w_o^2 \frac{\cos\psi}{\cos^2\gamma} = -\frac{1}{r}\frac{\partial p_1}{\partial \psi} + \nabla^2 v_1 + \frac{2}{r^2}\frac{\partial u_1}{\partial \psi} - \frac{v_1}{r^2}, \quad (5.27)$$

$$u_1 \frac{\partial w_o}{\partial r} = \nabla^2 w_1, \quad (5.28)$$

and

$$\frac{\partial}{\partial r}(r u_1) + \frac{\partial v_1}{\partial \psi} = 0 . \quad (5.29)$$

The boundary conditions for these equations are

$$w_o = w_1 = u_1 = v_1 = 0 \quad \text{at} \quad r = 1 .$$

This set of equations (5.25 - 5.29) are almost identical to those obtained by Dean in his first analysis and the boundary conditions are the same. It is thus possible to write down the solution immediately in dimensional form. To a first approximation

$$u = \frac{\kappa \nu}{288a}(1 - r^2/a^2)^2(4 - r^2/a^2)\frac{\sin\psi}{\cos^2\gamma}, \quad (5.30)$$

$$v = \frac{\kappa\nu}{288a}(1 - r^2/a^2)(4 - 23r^2/a^2 + 7r^4/a^4)\frac{\cos\psi}{\cos^2\gamma}, \qquad (5.31)$$

$$w = 2W_o(1 - r^2/a^2)\left[1 + \frac{Re^2\kappa\, r\sin\psi}{23{,}040\cos^2\gamma}\left\{19 - 21\frac{r^2}{a^2} + \frac{9r^4}{a^4} - \frac{r^6}{a^6}\right\}\right]; \qquad (5.32)$$

where $Re = \frac{2aW_o}{\nu}$.

If the helix angle γ is zero, these results reduce to those of flow in a curved pipe without torsion. The upper limit of γ is seen from (5.8) to be restricted by the condition $\kappa \ll \cos^2\gamma$ and so $\cos^2\gamma$ must be of order one. It can also be seen from (5.1) that ψ is measured from the binormal; thus the velocity distribution is determined.

From equation (5.23), it can be seen that this expansion solution breaks down when $Re = O(\tau/a)$. In such a case and for higher Reynolds numbers, the problem becomes difficult to solve owing to the dependence on two non-dimensional parameters $Re^2\kappa$ and $Re\,\kappa$ and the fact that the equation of continuity contains u , v and w . For the remainder of part II, it will be assumed that torsional effects are negligible and the original definition of the fully developed flow region will be applied.

Equations of motion for the fully developed region.

In the fully developed region it is assumed that the components of velocity are independent of s and that the motion is steady. The Navier-Stokes equations and the equation of continuity are

$$\underline{v} \wedge \underline{\omega} = \underline{\text{grad}} \left(\frac{p}{\rho} + {}^1/_2 \underline{v}^2 \right) + \nu \, \underline{\text{curl}} \; \underline{\omega} \quad , \tag{5.33}$$

$$\text{div } \underline{v} = 0 \quad , \tag{5.34}$$

where ν is the Kinematic coefficient of viscosity, ρ is the density, p is the pressure and, in the (r,ψ,s) coordinate system

$$\underline{v} = (u,v,w) \quad ,$$

$$\text{div } \underline{v} = \frac{1}{rh} \left\{ \frac{\partial}{\partial r}(rhu) + \frac{\partial}{\partial \psi}(hv) \right\} \quad , \tag{5.35}$$

$$\underline{\omega} = \text{curl } \underline{v} = \frac{1}{rh} \begin{vmatrix} \hat{\underline{r}} & r\hat{\underline{\psi}} & h\hat{\underline{s}} \\ {}^\partial/_{\partial r} & {}^\partial/_{\partial \psi} & 0 \\ u & rv & hw \end{vmatrix} \tag{5.36}$$

and $$h = 1 + \frac{r \sin \psi}{R} \quad . \tag{5.37}$$

Since u, v and w are independent of s, $\frac{\partial p}{\partial s} = \text{const} = -G$ say. The pressure then takes the form

$$p = -Gs + p'(r,\psi) \quad . \tag{5.38}$$

$p'(r,\psi)$ can be eliminated by considering the axial component of the curl of equation (5.33).

$$\left\{ \text{curl } (\underline{v} \wedge \underline{\omega}) \right\}_s = \nu \left\{ \text{curl } (\text{curl } \underline{\omega}) \right\}_s \quad . \tag{5.39}$$

From equation (4.35), a stream function f can be introduced so that

$$u = \frac{-1}{rh} \frac{\partial f}{\partial \psi} \quad \text{and} \quad v = \frac{1}{h} \frac{\partial f}{\partial r} \quad . \tag{5.40}$$

If these are substituted into (5.39) and the axial component of (5.33), and if the equations are made non-dimensional by replacing r by ar, w by $W_o w$ and putting $f = \nu \phi$, the equations of motion can be written in the form

$$\frac{1}{h^7}\left[\left(\frac{\partial\phi}{\partial\psi}\frac{\partial}{\partial r}-\frac{\partial\phi}{\partial r}\frac{\partial}{\partial\psi}\right)\nabla^2\phi-2\left(\alpha\frac{\partial\phi}{\partial\psi}-\beta\frac{\partial\phi}{\partial r}\right)\nabla^2\phi\right.$$

$$-\alpha\left(\frac{\partial}{\partial r}\left\{\frac{\partial\phi}{\partial\psi}\frac{\partial\phi}{\partial r}\right\}-\frac{\partial}{\partial\psi}\left\{\frac{\partial\phi}{\partial r}\right\}^2\right)+\beta\left(\frac{\partial}{\partial r}\left\{\frac{1}{r}\frac{\partial\phi}{\partial\psi}\right\}^2\right.$$

$$\left.\left.-\frac{\partial}{\partial\psi}\left\{\frac{1}{r^2}\frac{\partial\phi}{\partial\psi}\frac{\partial\phi}{\partial r}\right\}\right)\right]-\frac{\partial\phi}{\partial\psi}\frac{\partial\phi}{\partial r}\frac{\partial}{\partial r}\left(\frac{\alpha}{h^2}\right)-\left(\frac{1}{r}\frac{\partial\phi}{\partial\psi}\right)^2\frac{\partial}{\partial r}\left(\frac{\beta}{h^2}\right)$$

$$+\left(\frac{\partial\phi}{\partial r}\right)^2\frac{\partial}{\partial\psi}\left(\frac{\alpha}{h^2}\right)+\frac{1}{r^2}\frac{\partial\phi}{\partial r}\frac{\partial\phi}{\partial\psi}\frac{\partial}{\partial\psi}\left(\frac{\beta}{h^2}\right)+K^2w\left(r\cos\psi.\frac{\partial w}{\partial r}\right.$$

$$\left.-\sin\psi.\frac{\partial w}{\partial\psi}\right)=-\frac{r}{h}[\nabla^2-D][\nabla^2-D]\phi\quad,\qquad(5.41)$$

and

$$\frac{1}{r}\left(\frac{\partial\phi}{\partial r}\frac{\partial w}{\partial\psi}-\frac{\partial\phi}{\partial\psi}\frac{\partial w}{\partial r}\right)-\frac{\alpha w}{r}\frac{\partial\phi}{\partial\psi}+\frac{\beta w}{r}\frac{\partial\phi}{\partial r}=C$$

$$+h\left[\nabla^2w+\alpha\frac{\partial w}{\partial r}+\frac{\beta}{r^2}\frac{\partial w}{\partial\psi}-\left(\alpha^2+\frac{\beta^2}{r^2}\right)w\right]\quad,\qquad(5.42)$$

where

$$h=1+\kappa\, r\sin\psi\quad,\quad\alpha=\frac{1}{h}\frac{\partial h}{\partial r}\quad,\quad\beta=\frac{1}{h}\frac{\partial h}{\partial\psi}\quad,\qquad(5.43)$$

$$\nabla^2 = \frac{\partial^2}{\partial r^2} + \frac{1}{r}\frac{\partial}{\partial r} + \frac{1}{r^2}\frac{\partial^2}{\partial \psi^2} ,$$

$$D = \alpha \frac{\partial}{\partial r} + \frac{\beta}{r^2}\frac{\partial}{\partial \psi} , \qquad (5.44)$$

$$K^2 = \frac{2W_o^2 a^3}{\nu^2 R} ,$$

$$C = \frac{Ga^2}{\mu W_o} ,$$

and W_o is the mean axial velocity.

Since, without any loss in generality, the pipe is taken to be of radius one, the boundary condition on equations (5.41) and (5.42) are

$$w = \frac{\partial \phi}{\partial \psi} = \frac{\partial \phi}{\partial r} = 0 \quad \text{at} \quad r = 1 . \qquad (5.45)$$

The flow is seen to depend only on the non-dimensional parameter K since the value of C can theoretically be found as a function of K by applying the constant flux condition.

These equations represent a non linear sixth order system in two independent variables and a solution is required in a circular domain.

If $\varkappa$ is sufficiently small so that terms of order $\varkappa$ can be neglected relative to terms of order one, these equations reduce to those derived by Dean in his second paper. The parameter K in his theory, however, is different from that used here, since he takes the axial velocity at the centre of the pipe as his representative velocity. From here on, his parameter will be denoted by K_D and it is related to the Dean number of this theory, at least for low Dean number, by

$$K_D = 4K^2 \tag{5.46}$$

It should be noted that both these values differ from the Dean number chosen by most experimentalists. Since White was the first to use this parameter, it will be denoted by K_W ; it is related to K as follows:

$$K_W = \sqrt{2}K \quad . \tag{5.47}$$

Resistance Coefficient

If the resistance coefficient in a curved pipe is denoted by γ_c , then according to the usual definition

$$\gamma_c = \frac{-\frac{a}{2}}{\frac{1}{2}\rho W_o^2} \frac{\partial p}{\partial s} \quad .$$

Since $\quad -\frac{\partial p}{\partial s} = G \quad$ and $\quad G = \frac{\mu W_o C}{a^2}$

$$\gamma_c = \frac{2C}{Re} \quad . \tag{5.48}$$

Equations (5.41) and (5.42) are seen to depend on the parameters K, C and $\varkappa$ and it is clear to see that C is a function of K by considering the flux relation

$$\pi a^2 W_o = \int_0^{2\pi} \int_0^a r W_o \, w(K,C,\varkappa) \, dr \, d\psi \quad . \tag{5.49}$$

Thus if the mean axial velocity is known for the flow in a curved pipe, and a relation for w is obtained, the resistance coefficient can be found as a function of K which is also known.

In a straight pipe the resistance coefficient can be denoted by γ_s, where

$$\gamma_s = \frac{16}{Re} \quad . \tag{5.50}$$

The increase in resistance due to curvature is generally measured as the ratio $\frac{\gamma_c}{\gamma_s}$ for the same Reynolds numbers. Thus

$$\frac{\gamma_c}{\gamma_s} = \frac{\alpha}{\delta} \quad . \tag{5.51}$$

The experimental values of $\frac{\gamma_c}{\gamma_s}$ against K_W for $\varkappa \ll 1$ were collected by Goldstein and the results are shown graphically in Fig. (5.2)

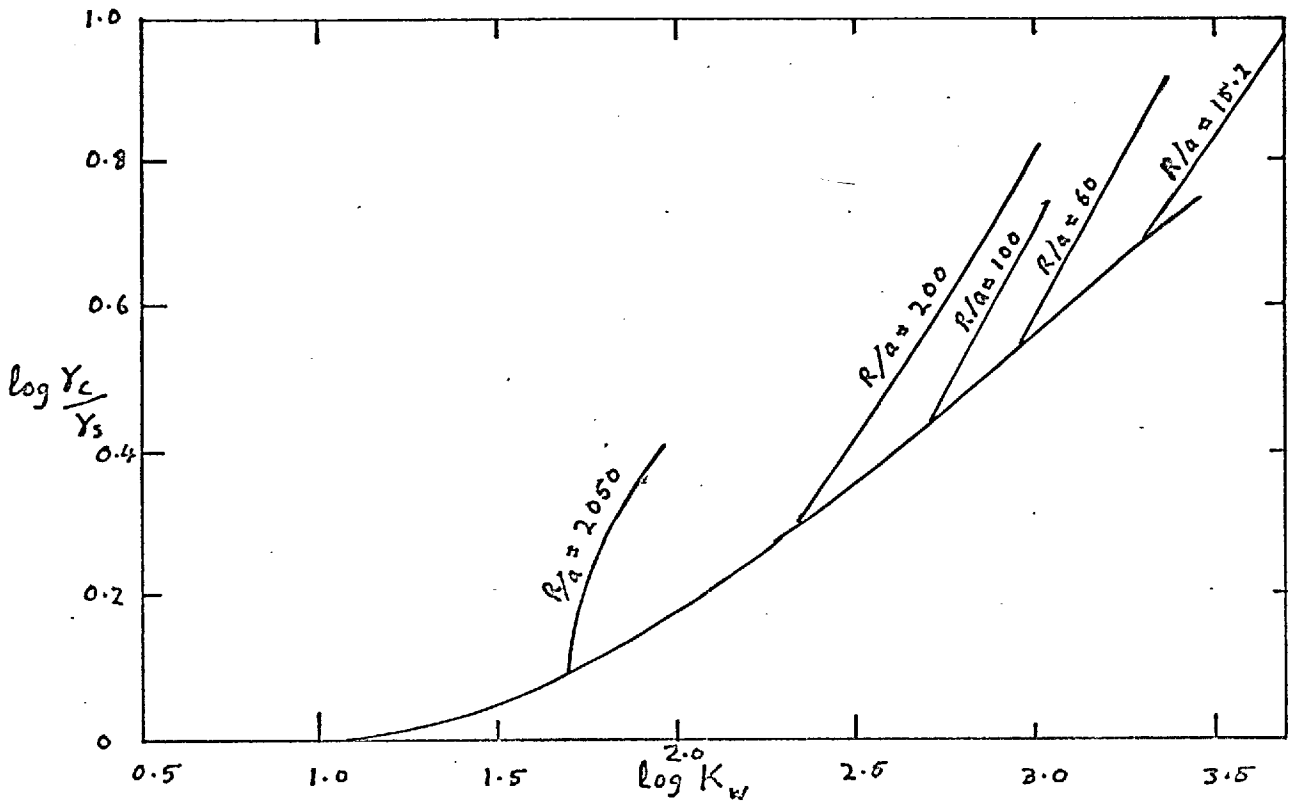

Fig. (5.2). The experimental observations of White and Adler for the increase in resistance due to curvature. The curve is the mean of the observed results which differ by no more than ± 2% (Farugia, M. Unpublished).

Solution for small K

The first approximation for low Dean number flow, namely that of investigating a small perturbation of order κ from the Poiseuille flow, has been considered earlier. The second paper produced by Dean extended this approximation by assuming series expansion solutions in powers of K_D. He inserted these expansions in the equivalent of equations (5.41) and (5.42) for small curvature and obtained solutions by comparing coefficients of like powers of K_D. An expression for the decrease in flux was then calculated to the fourth power of K_D as

$$\frac{F_c}{F_s} = 1 - \left(\frac{K_D}{576}\right)^2 (.03058) + \left(\frac{K_D}{576}\right)^4 (.01195) , \qquad (5.52)$$

where F_c and F_s represent the flux through a curved pipe and a straight pipe respectively. In both cases the flux was defined as the mean axial velocity multiplied by the cross sectional area.

In this analysis, however, it was assumed that C was a constant equal to that for a straight pipe. Since the resistance coefficient must increase with K, it can be seen from (5.51) that C is a function of K

and should contribute terms when coefficients of like powers of K are equated. Also, the decrease in flux was obtained assuming that the central velocities in the curved and straight pipes were equal. This makes the result extremely difficult to compare with experiments, which generally measure the increase in resistance for equal flux. A modification of Dean's theory will now be considered which does not include these restrictions.

If it is assumed that $\varkappa \ll 1$ and w is replaced by $C.w$, equations (5.41) and (5.42) reduce to

$$\left(\frac{\partial\phi}{\partial\psi}\frac{\partial}{\partial r} - \frac{\partial\phi}{\partial r}\frac{\partial}{\partial\psi}\right)\nabla^2\phi + Jw\left(r\cos\psi\frac{\partial w}{\partial r} - \sin\psi\frac{\partial w}{\partial\psi}\right) = -r\nabla^4\phi \ , \tag{5.53}$$

$$\frac{1}{r}\left(\frac{\partial\phi}{\partial r}\frac{\partial w}{\partial\psi} - \frac{\partial\phi}{\partial\psi}\frac{\partial w}{\partial r}\right) = 1 + \nabla^2 w \ , \tag{5.54}$$

where

$$J = C^2K = \frac{2G^2a^7}{\rho^2\nu^4R} \ . \tag{5.55}$$

If an expansion solution in J is now assumed and inserted in (5.53) and (5.54), comparison of coefficients of like powers of J will yield equations identical to those produced by Dean. The flux through a curved pipe

can thus be found as a modification of Dean's result.

$$F_c = \int_0^{2\pi} \int_0^1 W_o C \, wr \, dr \, d\psi ,$$

$$\text{i.e. } \pi W_o = \frac{W_o C \pi}{8} \left[1 - \left(\frac{J}{16 \times 576} \right)^2 (.03058) + \left(\frac{J}{16 \times 576} \right)^4 (.01195) \right] \tag{5.56}$$

If W_s and C_s are the mean axial velocity and the non-dimensional pressure gradient for a straight pipe,

$$F_s = \frac{W_s \, C_s \pi}{8} = \pi \, W_s \, . \tag{5.57}$$

To find the increase in resistance due to curvature, equation (5.56) can be solved for C in terms of K and this can be substituted into (5.51). To find the decrease in flux for equal pressure gradients $(G = G_s)$,

$$\frac{F_c}{F_s} = 1 - \left(\frac{G^2 a^7}{8 \times 576 . \rho^2 \nu^4 R} \right)^2 (.03058) + \left(\frac{G^2 a^7}{8 \times 576 \, \rho^2 \nu^4 R} \right)^4 (.01195) \tag{5.58}$$

If C is assumed to have a solution of form

$$C = C_o + C_1 K^2 + C_2 K^4 + \ldots\ldots,$$

the C_i can be obtained by inserting this solution in (5.56) and comparing coefficients of like powers of K. In this way, C becomes

$$C = 8 + .06116 \left(\frac{K^2}{72}\right)^2 - .00364 \left(\frac{K^2}{72}\right)^4 \cdots$$

and this can be compared with experiment by replacing K^2 by $1/2\ K_w^2$. The increase in resistance due to curvature is then

$$\frac{\gamma c}{\gamma s} = 1 + .1223 \left(\frac{K_w}{24}\right)^4 - .1165 \left(\frac{K_w}{24}\right)^8 . \qquad (5.59)$$

An upper bound of the region of validity of this formula can be obtained by noting that it has a maximum value when $K_w \doteq 20.4$ and that $\frac{\gamma c}{\gamma s}$ increases as K_w increases throughout the range of K_w and so this formula is certainly not valid for $K_w \geq 20.4$.

It has been assumed by Adler and Hawthorn that a relationship exists between $\frac{\gamma c}{\gamma s}$ and F_c/F_s of the form

$$\frac{\gamma c}{\gamma s} = \frac{F_s}{F_c} . \qquad (5.60)$$

This is not possible, however, since $\frac{\gamma_c}{\gamma_s}$ is defined assuming that the mean axial velocities in a straight and curved pipe are equal. Since the cross sectional areas of the straight and curved pipes are the same, this implies that $F_c = F_s$, implying from equation (5.60) that $\gamma_c = \gamma_s$. Since this is untrue, equation (5.60) is false.

CHAPTER 6

Introduction to method of solution for large Dean Number flow

The purpose of this chapter is to obtain a method for solving equations (5.41) and (5.42) for large values of the parameter K. The analysis of Adler, Barua and Mori and Nakayama will be considered in detail and the problems inherent in their approach to the problem will be discussed.

The major simplifying feature for flow at large Dean number is that the viscous forces are of the same order as the inertia forces only in a thin layer next to the wall of the pipe. This idea first appeared in Adler's paper, no doubt prompted by Prandtl whose supervision was acknowledged in that paper. A further assumption that the motion outside this layer is confined to planes parallel to the plane of symmetry of the pipe is also made.

The experimental evidence justifying these assumptions is very sparse. Barua outlines the experiments of Hawes (17), showing that there is approximately a linear rise in the axial velocity from the inner part of the wall to the outer part, and of Squire (18), who shows that the

lines of equal dynamic pressure appear vertical over most of the cross section. It appears, however, that Barua overlooked the fact that Squire's experiments were conducted in the turbulent regime. Despite this, it does seem highly likely that for large Dean number flow, the lines of equal dynamic pressure in the laminar regime are similar to those in the turbulent regime; but it would be more satisfying to the theory if the experiments of Squire were repeated for laminar flow.

In what follows, the thin layer next to the wall, where viscous forces are of the same order of magnitude as the inertia forces, will be called the boundary layer and the region where viscous forces can be neglected, that is the rest of the cross section, will be called the core. The surface separating these two regions will be called the interface.

The velocity distribution in the core

Assuming that the lines of equal dynamic pressure are vertical and that viscous forces are negligible, the equations of motion and continuity for the fully developed flow region can be written in the (r_1, θ, z) coordinate system as follows:

$$u_1 \frac{\partial u_1}{\partial r_1} + v_1 \frac{\partial u_1}{\partial z} - \frac{w_1^2}{r_1} = - \frac{1}{\rho} \frac{\partial p}{\partial r_1} \quad , \tag{6.1}$$

$$u_1 \frac{\partial w_1}{\partial r} + v_1 \frac{\partial w_1}{\partial z} + \frac{u_1 w_1}{r_1} = - \frac{1}{\rho r_1} \frac{\partial p}{\partial \theta} \quad , \tag{6.2}$$

$$u_1 \frac{\partial v_1}{\partial r_1} + v_1 \frac{\partial v_1}{\partial z} = 0 \quad , \tag{6.3}$$

$$\frac{\partial}{\partial r_1} (r_1 u) + r_1 \frac{\partial v_1}{\partial z} = 0 \quad . \tag{6.4}$$

Since the velocity distribution is assumed independent of θ , p must be of the form

$$p = -GR\theta + p'(r,\psi) \quad , \tag{6.5}$$

where G is a constant.

A solution of these equations is

$$v_1 = 0 \quad , \tag{6.6}$$

$$u_1 = \frac{A}{r_1} \quad , \tag{6.7}$$

$$w_1 = \frac{GR}{2A\rho}\left(r_1 + \frac{B}{r_1}\right) , \qquad (6.8)$$

$$p = -GR\theta - \frac{A^2\rho}{2r_1^2} + \rho\left(\frac{GR}{2A\rho}\right)^2\left[r_1^2+2B\log r_1 - \frac{B}{2r_1^2}\right], \qquad (6.9)$$

where A and B are constants. Although A and B could be functions of z , the complications introduced into the analysis by such a step makes this prohibitive.

The velocities can be non-dimensionalised by replacing u_1 by $\frac{\nu u_1}{a}$, v_1 by $\frac{\nu v_1}{a}$, w_1 by $w_1 W_o$, A by $\frac{RU\nu}{a}$ and B by BR^2 , where U is a constant and W_o is the mean axial velocity. Then

$$u_1 = \frac{U}{h} , \qquad (6.10)$$

$$w_1 = \frac{GRa}{2W_o\rho U\nu}\left(h + \frac{B}{h}\right) , \qquad (6.11)$$

$$p = -GR\theta - \frac{U^2\nu^2\rho}{2a^2h^2} + \rho\left(\frac{GRa}{2\rho U\nu}\right)^2\left[h^2+2B\log Rh - \frac{B^2}{2h^2}\right], \qquad (6.12)$$

where $h = 1 + \frac{\kappa r}{a}\sin\psi = \frac{r_1}{R}$.

Introducing a stream function in the (r,ψ,s) coordinate system and replacing r by ar , the

corresponding non-dimensional velocities can be written as

$$u = -\frac{1}{rh}\frac{\partial \phi}{\partial \psi}, \quad v = \frac{1}{h}\frac{\partial \phi}{\partial r} \tag{6.13}$$

$$\phi = Ur\cos\psi, \quad w = \frac{C}{2\kappa U}\left(h + \frac{B}{h}\right), \tag{6.14}$$

where $C = \frac{Ga^2}{\rho W_o}$ and $h = 1 + \kappa r \sin\psi$.

The non-dimensional pressure P defined by $P = \frac{2p}{\rho W_o^2}$ becomes

$$P = -\frac{2C\ s}{Re\ a} - \frac{U^2}{h^2 Re^2} + 2\left(\frac{C}{2\kappa U}\right)^2\left[h^2 + 2B\ \log Rh - \frac{B^2}{2h^2}\right] . \tag{6.15}$$

Equations (6.13) and (6.14) will be taken to represent the velocity distribution in the core. It can be seen that for any given curvature ratio, the velocity distribution can be found only when B , C and U are known. Ideally, these three constants should be determined from a consideration of the equations of motion in the boundary layer.

Equations of motion in the boundary layer

In earlier papers, there are discrepancies as to the correct form of the boundary layer equations. Barua rejected the axial pressure gradient term after an order of magnitude analysis, whereas Mori and Nakayama retained it. Since many of the approximations made by Barua depend on this order of magnitude analysis, equations valid in the boundary layer will be deduced formally and the effects of rejecting this term will be considered.

In the last chapter, equations representing the flow were derived and it was seen that any solution of these is a function of the non-dimensional parameter K. In a conventional boundary layer analysis, the boundary layer thickness is assumed to be of order $Re^{-1/2}$. It will, however, be assumed in this analysis, that the boundary layer thickness is of order $K^{-1/2}$.

From the definition of ϕ (i.e. $f = \nu\phi$) and K, it is clear that ϕ and therefore U are of order $K^{1/2}$. To obtain the orders of magnitude of w and C, the relations obtained from the constancy of axial momentum and mass flux will be considered.

Integrating the non-dimensional axial momentum equation (5.42) across the cross section of the pipe

having divided through by h ,

$$\int_0^{2\pi}\int_0^1 \left\{\frac{1}{rh}\left(\frac{\partial\phi}{\partial r}\frac{\partial w}{\partial\psi}-\frac{\partial\phi}{\partial\psi}\frac{\partial w}{\partial r}\right)-\frac{w}{rh^2}\frac{\partial h}{\partial r}\frac{\partial\phi}{\partial\psi}+\frac{w}{rh^2}\frac{\partial h}{\partial\psi}\frac{\partial\phi}{\partial r}\right\} r\,dr\,d\psi=$$

$$\int_0^{2\pi}\int_0^1 \frac{Cr}{h}\,dr\,d\psi+\int_0^{2\pi}\int_0^1 \left\{\frac{\partial^2 w}{\partial r^2}+\frac{1}{r}\frac{\partial w}{\partial r}+\frac{1}{r^2}\frac{\partial^2 w}{\partial\psi^2}+\right.$$

$$\left.\frac{1}{h}\left(\frac{\partial h}{\partial r}\frac{\partial w}{\partial r}+\frac{1}{r^2}\frac{\partial h}{\partial\psi}\frac{\partial w}{\partial\psi}\right)-\frac{w}{h^2}\left(\left[\frac{\partial h}{\partial r}\right]^2+\frac{1}{r^2}\left[\frac{\partial h}{\partial\psi}\right]^2\right)\right\} r\,dr\,d\psi\,. \qquad (6.16)$$

Using the boundary conditions of (5.45) and integrating by parts,

$$2\int_0^{2\pi}\int_0^1 \frac{w}{h^2}\left\{\frac{\partial h}{\partial\psi}\frac{\partial\phi}{\partial r}-\frac{\partial h}{\partial r}\frac{\partial\phi}{\partial\psi}\right\} dr\,d\psi = C\int_0^{2\pi}\int_0^1 \frac{r\,dr\,d\psi}{h}+$$

$$\int_0^{2\pi}\left(\frac{\partial w}{\partial r}\right)_{r=1} d\psi. \qquad (6.17)$$

For constant mass flux

$$\pi a^2 W_o = \int_0^{2\pi}\int_0^a r\,w\,dr\,d\psi\,.$$

Considering the non dimensional form of this equation

$$\pi = \int_0^{2\pi} \int_0^1 rw \, dr \, d\psi \quad . \tag{6.18}$$

From equation (6.18), w is seen to be of order one. In the boundary layer, $\frac{\partial w}{\partial r}$ is of order $K^{1/2}$ and so it follows from equation (6.17) that C is of order $K^{1/2}$.

If equations (5.41) and (5.42) are transformed using

$$\left.\begin{aligned} r &= 1 - \eta K^{-1/2} \quad , \\ \phi &= \phi_1 K^{1/2} \quad , \\ U &= U_1 K^{1/2} \quad , \\ C &= C_1 K^{1/2} \quad , \end{aligned}\right\} \tag{6.19}$$

and only the coefficients of the dominant powers of K are equated,

$$\frac{\partial}{\partial \eta}\left(\frac{\partial \phi_1}{\partial \psi}\frac{\partial^2 \phi_1}{\partial \eta^2}\right) - \beta_o \frac{\partial}{\partial \eta}\left(\frac{\partial \phi_1}{\partial \eta}\right)^2 - \tfrac{1}{2}h_o^2 \cos\psi \frac{\partial}{\partial \eta} w^2 + h_o \frac{\partial^4 \phi_1}{\partial \eta^4} = 0 \quad , \tag{6.20}$$

$$\frac{\partial \phi_1}{\partial \psi}\frac{\partial w}{\partial \eta} - \frac{\partial \phi_1}{\partial \eta}\frac{\partial w}{\partial \psi} - \beta_o w \frac{\partial \phi_1}{\partial \eta} - h_o \frac{\partial^2 w}{\partial \eta^2} = 0 \quad , \tag{6.21}$$

where $h_o = 1 + \varkappa \sin \psi$ and $\beta_o = \frac{1}{h_o} \frac{\partial h_o}{\partial \psi}$. (6.22)

The essential boundary conditions on these equations are

$$w = \frac{\partial \phi_1}{\partial \psi} = \frac{\partial \phi_1}{\partial r} = 0 \quad \text{at} \quad \eta = 0 \, . \tag{6.23}$$

It is also required that w and ϕ_1 and as many derivatives with respect to ψ and η as is practical are continuous across the interface. If, from the relations for the velocity distribution in the core,

$$\phi_c = U_1 r \cos \psi \quad \text{and} \quad w_c = \frac{C_1}{2\varkappa U_1} \left(h + \frac{B}{h} \right) ,$$

$$\phi_1 = \phi_c \quad , \quad w = w_c \quad , \tag{6.24}$$

$$-K^{1/2} \frac{\partial \phi_1}{\partial \eta} = \frac{\partial \phi_c}{\partial r} \quad , \quad -K^{1/2} \frac{\partial w}{\partial \eta} = \frac{\partial w_c}{\partial r} \, , \quad ,$$

$$K \frac{\partial^2 \phi_1}{\partial \eta^2} = \frac{\partial^2 \phi_c}{\partial r^2} \quad , \quad K \frac{\partial^2 w}{\partial \eta^2} = \frac{\partial^2 w_c}{\partial r^2} \quad , \text{ etc.} \tag{6.25}$$

It is seen from these relations that, for asymptotically large K ,

$$\left.\begin{aligned} \frac{\partial \phi_1}{\partial \eta} = \frac{\partial^2 \phi_1}{\partial \eta^2} = \ldots\ldots = 0 \ , \\ \frac{\partial w}{\partial \eta} = \frac{\partial^2 w}{\partial \eta^2} = \ldots\ldots = 0 \ , \end{aligned}\right\} \text{ at the interface . } \quad (6.26)$$

If it is assumed that at least $\frac{\partial \phi_1}{\partial \eta}$, $\frac{\partial^2 \phi_1}{\partial \eta^2}$ and $\frac{\partial^3 \phi_1}{\partial \eta^3}$ are zero at the interface, equation (6.20) can be integrated readily with respect to η yielding

$$\frac{\partial \phi_1}{\partial \psi} \frac{\partial^2 \phi_1}{\partial \eta^2} - \beta_o \left(\frac{\partial \phi_1}{\partial \eta}\right)^2 + \tfrac{1}{2} h_o^2 \cos\psi . (w_{c1}^2 - w^2) + h_o \frac{\partial^3 \phi_1}{\partial \eta^3} = 0 \ , \quad (6.27)$$

where w_{c1} is the velocity in the core as given by equation (6.14) when $r = 1$.

Equations (6.21) and (6.27) are identical, save for a different notation, to those deduced by Barua after a conventional boundary layer approximation and an order of magnitude analysis. The axial pressure gradient term is not evident in the asymptotic form of the equations, it being of order $K^{-1/2}$ compared with those terms retained in equation (6.21). The effect of retaining this term by Mori and Nakayama is not critical but superfluous and in fact rejection of this term would have made their analysis simpler. The fact that equation

(6.20) is directly integrable is expected since this is recognition that the pressure does not vary appreciably across the boundary layer.

A complete solution of equations (6.21) and (6.27) subject to the boundary conditions of (6.23), (6.24) and (6.26) is extremely improbable and approximate methods have to be applied. Adler, Barua and Mori and Nakayama employed the Polhausen approximate method (8), but because of the widely different techniques of application, it will be constructive to pause in the development of yet another Polhausen approximation and consider the differences and assumptions, together with their consequences, of these three theories.

Analysis of the theories of Adler, Barua and Mori and Nakayama

Since the equations (6.21) and (6.27) are effectively the same as those obtained by Barua, the theory of Barua and its differences with the theory of Mori and Nakayama will be considered first and then the theory of Adler, though first to be published, will be considered last.

Integrating the boundary layer equations across the boundary layer with respect to the non-dimensional radial

component η , Barua inserts profiles of the form

$$v = v_o(\eta - 2\eta^2 + \eta^3) ,$$

$$w = w_o(2\eta - \eta^2) ,$$

where w_o is the axial velocity in the core, $\eta = \frac{a-r}{\delta}$ and δ is the boundary layer thickness. The boundary conditions satisfied are

$$v = w = 0 \quad \text{at} \quad r = a ,$$

$$w = w_o , \; v = \frac{\partial v}{\partial r} = \frac{\partial w}{\partial r} = 0 \quad \text{at} \quad r = a-\delta .$$

The two momentum integrals then reduce to two first order non linear differential equations in $\delta(\Psi)$ and $v_o(\Psi)$.

Mori and Nakayama likewise integrated the boundary layer equations across the boundary layer and inserted the profiles

$$v = -D\sin\Psi \left[\left(-\frac{12}{\delta} + 6\right)\frac{\xi}{\delta} + \left(\frac{24}{\delta} - 9\right)\frac{\xi^2}{\delta^2} + \left(-\frac{12}{\delta} + 4\right)\frac{\xi^3}{\delta^3} \right] ,$$

$$w = w_{1\delta}\left(\frac{2\xi}{\delta} - \frac{\xi^2}{\delta^2}\right) + \frac{\delta C}{D}\cos\psi\left(\frac{\xi}{\delta} - \frac{\xi^2}{\delta^2}\right),$$

where $w_{1\delta}$ is the axial velocity in the core at the interface, $\xi = 1 - r/a$ and δ is again the boundary layer thickness; v and w satisfy the boundary conditions

$$v = w = 0 \quad \text{at} \quad \xi = 0 ,$$

$$v = v_1 \cdot \frac{\partial v}{\partial \xi} = 0 , \quad w = w_{1\delta} , \quad \frac{\partial w}{\partial \xi} = \left(\frac{\partial w_1}{\partial \xi}\right)_\delta \quad \text{at} \quad \xi = \delta .$$

The constants D and C can best be seen by their connection with the velocity distribution in the core, namely:

$$u = D \sin\psi ,$$

$$v = D \cos\psi ,$$

$$w = A + \frac{C}{D}\frac{r}{a}\sin\psi ,$$

which is the same as the core velocity distribution represented in the present analysis by (6.13) and (6.14) for the limiting case when $\varkappa$ tends to zero. Barua's

analysis in the core is essentially that deduced in the present analysis.

Inserting these profiles, the momentum integrals reduce to two ordinary equations with ψ as parameter. The reason for this is that the profiles are specified as to their variance with ψ as well as with ξ. Also, the variation of δ with ψ is neglected in the derivation of these equations although it is considered later. In contrast, Barua does not specify the variance of the tangential velocity v with ψ, though he does so with the axial velocity w; the variation of δ with ψ is also taken into account.

Mori and Nakayama combine the average value of the axial momentum equation in the form $E + F \cos \psi$, with the relation obtained between the axial pressure gradient and the velocity gradient at the wall to form an expression between D and δ_m, where δ_m is the mean value of δ through out the interval $(-\pi/2, \pi/2)$. the relation used is the limiting form as $\varkappa \longrightarrow 0$ of equation (6.17). Another relation between D and δ_m is obtained from the tangential momentum equation by equating only the constant terms and assuming that variations in δ with ψ, neglected in the past, account for the variable terms; averaging this last

equation would have led to discrepancies when compared with experiment.

Expanding D and δ_m as a power series in $K_w^{1/2}$ of the form

$$D = D_1 K_w^{1/2} + D_2 + \ldots\ldots ,$$

$$\delta_m = \delta_{m1} K_w^{-1/2} + \delta_{m2} K_w^{-1} + \ldots\ldots ,$$

first and second approximations were found to the resistance coefficient by comparing coefficients of like powers of K_w together with the constant flux condition. Good agreement with the experimental results of Ito (19) was obtained for values of $K_w > 250$, the increase in resistance due to curvature being calculated to a second approximation as

$$\frac{\gamma_c}{\gamma_s} = \frac{0.108\ K_w^{1/2}}{1 - 3.253\ K_w^{-1/2}} \quad . \tag{6.28}$$

Barua derives two first order differential equations in v_o and δ without assuming small curvature ratio, but in the determination of the relevant constants which arise from the core flow analysis, an assumption that v_o has a stationary point at $\psi = 0^\circ$ is made and the variation

in the boundary layer thickness δ is assumed very small. The advantage gained by assuming that $v = 0$ at the interface is readily seen since the equation of continuity is of such a form that substitution in the axial momentum equation determines the ψ variation in v_o .

Assuming that $\delta = \delta(\pi/2)$ throughout the range $(\pi/2, -\pi/2)$ and that $\kappa \ll 1$, Barua obtains an expression for the increase in resistance due to curvature in the form

$$\frac{\gamma_c}{\gamma_s} = .09185\ K_w^{1/2} + 0.5093 + \ldots, \qquad (6.29)$$

which again agrees well with the experimental observations for $K_w > 250$. The variation of v_o and δ were then calculated numerically and the most prominent feature was found to be that for small curvature ratio, the transverse velocity reverses its direction of flow at about $\psi = -63^o$ This appears to indicate a condition of separation, together with a break down in the boundary layer approximation. Thus the motion cannot be specified from $\psi = -63^o$ to $\psi = -\pi/2$. Evidence of this separation was said by Barua to be apparent in Squire's experiments, but, as was pointed out earlier, these applied to the turbulent regime.

The assumption that a stationary value of v_o exists at $\psi = 0^\circ$ is probably good for small curvature ratio, but may deteriorate as the curvature ratio is increased. A criticism of the theory is that the tangential momentum equation is only satisfied at one point (i.e. at $\psi = 0^\circ$). Although Mori and Nakayama maintain that, among others, Barua did not consider a momentum balance analysis and that discontinuities at the interface led to the unreasonable result of a finite tangential velocity at $\psi = -\pi/2$, it should be stated here that Barua did not have a finite tangential velocity at $\psi = -\pi/2$ and even if this were the case, this would have been as a result of the break down in the boundary layer approximation after separation. The discontinuities at the interface are consistent with the order of magnitude analysis used by Barua and if a momentum analysis is applied to his results, it is satisfied to an error of $\pm 2\%$; a value well within the boundary layer approximations.

The review of Adler's paper is considered last since much of his work was definitely improved by the methods of Barua and Mori and Nakayama. There are, however, certain fundamental differences to those of the previous two which deserve mention.

Adler inserted velocity profiles into the momentum integrals to obtain two first order non linear differential equations in δ , the boundary layer thickness and D , a variable introduced in the tangential velocity profile. The solution of these equations was sought as a power series in ψ about the point $\psi = \pi/2$. As in succeeding theories, the equations were dependent on three constants. Adler gave numerical values obtained from experiments for two of these constants and successive approximations to δ and D were obtained by considering solutions in the form

$$\frac{\delta}{\delta_o} = 1 + \frac{\delta_2}{\delta_o} (\pi/2-\psi)^2 + \frac{\delta_4}{\delta_o} (\pi/2-\psi)^4 + \ldots ,$$

$$\frac{D}{D_1} = (\pi/2-\psi) + \frac{D_3}{D_1} (\pi/2-\psi)^3 + \frac{D_5}{D_1} (\pi/2-\psi)^5 + \ldots .$$

It was found that for values of ψ in the range $(\pi/2, -\pi/6)$, δ was sufficiently well represented by four terms of the series. The series for D , however, was more erratic up to four terms in the series though it did converge in the region $(\pi/2,0)$. Adding successive terms made the value of D alternately positive and negative at $\psi = -\pi/2$, which, in the light of Barua's theory predicting back flow in this variable, is not

really surprising. It is, if anything, justification that there is a breakdown in the equations representing this flow after a certain value of ψ ; too much should not, however, be read into this since only four terms were considered.

Summary of Problem

The problem is that of solving the two differential equations

$$\frac{\partial \phi_1}{\partial \psi}\frac{\partial w}{\partial \eta} - \frac{\partial \phi_1}{\partial \eta}\frac{\partial w}{\partial \psi} - \beta_o w \frac{\partial \phi_1}{\partial \eta} - h_o \frac{\partial^2 w}{\partial \eta^2} = 0 , \qquad (6.30)$$

$$\frac{\partial \phi_1}{\partial \psi}\frac{\partial^2 \phi_1}{\partial \eta^2} - \beta_o\left(\frac{\partial \phi_1}{\partial \eta}\right)^2 + \tfrac{1}{2}h_o^2\cos\psi.(w_{c1}^2 - w^2) + h_o\frac{\partial^3 \phi_1}{\partial \eta^3} = 0 , \qquad (6.31)$$

for ϕ_1 and w , subject to the boundary conditions

$$\left.\begin{aligned} &w = \frac{\partial \phi_1}{\partial \psi} = \frac{\partial \phi_1}{\partial \eta} = 0 \quad \text{at} \quad \eta = 0 , \\ &\phi_1 = \phi_c \quad , \quad w = w_c \quad \text{at} \quad \eta = \delta , \end{aligned}\right\} \qquad (6.32)$$

and as many as is practical of the following:

$$\left.\begin{aligned} &\frac{\partial \phi_1}{\partial \eta} = \frac{\partial^2 \phi_1}{\partial \eta^2} = \frac{\partial^3 \phi_1}{\partial \eta^3} = \ldots\ldots = 0 \ , \\ &\frac{\partial w}{\partial \eta} = \frac{\partial^2 w}{\partial \eta^2} = \ldots\ldots = 0 \ , \end{aligned}\right\} \text{at } \eta = \delta \ , \qquad (6.32) \text{ contd.}$$

where $\delta = \delta(\Psi)$ represents the unknown boundary layer thickness and ϕ_c and w_c are representative of the velocity distribution in the core given by

$$\phi_c = U_1 \, r \cos \Psi \ , \qquad (6.33)$$

$$w_c = \frac{C_1}{2\kappa U_1} \left(h + \frac{B}{h} \right) , \qquad (6.34)$$

$$h = 1 + \kappa r \sin \Psi \ .$$

Two of the three constants in (6.33) and (6.34) can theoretically be found from the constant axial mass and momentum flux conditions of (6.17) and (6.18), which can be written as

$$\pi = 2 \int_{-\pi/2}^{\pi/2} \int_{0}^{1} r \, w \, dr \, d\Psi \ , \qquad (6.35)$$

$$2\int_{-\pi/2}^{\pi/2}\int_{0}^{1} \frac{w}{h^2}\left(\frac{\partial h}{\partial \Psi}\frac{\partial \phi}{\partial r} - \frac{\partial h}{\partial r}\frac{\partial \phi}{\partial \Psi}\right) dr\, d\Psi = C_1\int_{-\pi/2}^{\pi/2}\int_{0}^{1} \frac{r\, dr\, d\Psi}{h} +$$

$$\int_{-\pi/2}^{\pi/2} \left(\frac{\partial w}{\partial r}\right)_{r=1} d\Psi \,, \qquad (6.36)$$

since the flow is symmetrical about the $\Psi = \pi/2$, $\Psi = -\pi/2$ line.

This problem is not well posed since there are six unknowns namely: $\phi_1(\Psi)$, $w(\Psi)$, $\delta(\Psi)$, C_1 , B and U_1 and only four equations, namely: (6.30), (6.31), (6.35) and (6.36). It is possible to make the problem well posed, however, if either an additional physical condition is imposed or an experimental value is given to one of the constants and if the three unknown variables are written in terms of two unknown variables. The differences in the theories described in the last section are due to various ways of making the problem well posed.

Barua expressed the velocity distribution in terms of $\delta(\Psi)$ and $v_o(\Psi)$ and assumed that the tangential velocity had a stationary point at $\Psi = 0^o$; this reduced the unknown variables from three to two and

determined one of the constants. The other two constants were derived by satisfying the constant axial mass flux condition and by satisfying the tangential momentum equation specifically at the point $\psi = 0^{o}$. It was found necessary to assume that δ was approximately constant to evaluate these constants and this restricted the validity of his theory to small curvature ratios. Had Barua tried to find one of the constants using the constant axial momentum flux condition, thus enabling him to satisfy both momentum equations up to the point of separation, the analysis and computation would have been greatly complicated. The reason for this is that the equivalent of equations (6.35) and (6.36) would have to be solved and the complete solution is not possible if the flow separates since the velocity distribution in the boundary layer is not known about a point of separation.

Mori and Nakayama expressed the velocity distribution in terms of $\delta(\psi)$ and reduced the number of unknowns to four of which only one, $\delta(\psi)$, was variable. They were thus able to find values for these in the way described in the last section. This method produced results which were in good agreement with the experimental observations for the increase in resistance due to curvature.

but it gave no real indication as to the behaviour of the skin friction and the possibility of separation.

As a result of these investigations, the present analysis will continue in two stages. Firstly, a theory will be devised to determine the relevant physical constants which can be compared with experiment. The velocity distribution will be expressed in terms of two unknowns, one of which will be the boundary layer thickness δ and an additional physical restriction will be imposed. Secondly, a theory will be presented which makes use of experimental results and those obtained in the first part to determine the behaviour of the skin friction and to investigate the possibility of separation.

CHAPTER 7

The momentum integral

It was seen in the last chapter that an approximate solution to the problem is possible if the velocity distribution is expressed in terms of the boundary layer thickness and another variable and if an extra physical restraint is imposed. It was also seen that complications arise in determining the other constants if the flow separates. As a consequence, any theory devised to obtain values for the constants introduced from the core velocity profile, must introduce simplifying assumptions.

The dominant simplifying feature concerns the tangential momentum equation (6.31). Apart from Adler's theory, previous theories satisfied the tangential momentum integral at one point only. In the theory that follows, the contribution made by this equation will be restricted to that of it being satisfied at the wall of the pipe only. Thus

$$\frac{\partial^3 \phi_1}{\partial \eta^3}(0) = -\,{}^1/_2\, h_o\, w_{c1}^2 \cos\psi \,. \qquad (7.1)$$

Imposing this condition on the flow instead of evaluating the tangential momentum integral is perhaps extreme, but it is no more extreme than evaluating the momentum integral and satisfying it at one point as in the theory of Barua: it has the advantage that ϕ_1 can be specified as a function of Ψ at all points on the wall and will avoid the complications of separation.

Integrating equation (6.30) across the boundary layer yields

$$\int_0^{\delta} \left\{ \frac{\partial \phi_1}{\partial \Psi} \frac{\partial w}{\partial \eta} - \frac{\partial \phi_1}{\partial \eta} \frac{\partial w}{\partial \Psi} - \beta_o w \frac{\partial \phi_1}{\partial \eta} \right\} d\eta = -h_o \frac{\partial w(0)}{\partial \eta} , \qquad (7.2)$$

so long as $\frac{\partial w(\delta)}{\partial \eta}$ is considered zero.

Transforming equations (7.1) and (7.2) using

$$\eta = \delta(\Psi)x \qquad (7.3)$$

and denoting partial differentiation with respect to x by primes,

$$\phi_1'''(0) = -\tfrac{1}{2} h_o \delta^3 w_{c1}^2 \cos\Psi , \qquad (7.4)$$

$$\frac{-h_o w'(0)}{\delta} = \int_0^1 \left\{ \frac{\partial \phi_1}{\partial \psi} w' - \phi_1' \left(\frac{\partial w}{\partial \psi} + \beta_o w \right) \right\} dx +$$

$$\int_0^1 \frac{1}{\delta} \frac{\partial \delta}{\partial \psi} \left\{ \frac{x \phi_1' w'}{\delta} - \frac{x w' \phi_1'}{\delta} \right\} dx ,$$

i.e.

$$\frac{-h_o w'(0)}{\delta} = \int_0^1 \left\{ \frac{\partial \phi_1}{\partial \psi} w' - \phi_1' \left(\frac{\partial w}{\partial \psi} + \beta_o w \right) \right\} dx . \quad (7.5)$$

The velocity profiles

Following a conventional Polhausen approximate method of solution, the simplest boundary conditions that the velocity profiles must satisfy, that are consistent with the derivation of equations (7.4) and (7.5) are:

$$\left.\begin{aligned} & w = \frac{\partial \phi_1}{\partial \psi} = \frac{\partial \phi_1}{\partial x} = 0 \quad \text{at} \quad x = 0 , \\ & w = w_{c1} , \quad \frac{\partial w}{\partial x} = 0 \quad \text{at} \quad x = 1 , \\ & \phi_1 = \phi_{c1} , \quad \frac{\partial \phi_1}{\partial x} = \frac{\partial^2 \phi_1}{\partial x^2} = \frac{\partial^3 \phi_1}{\partial x^3} = 0 \quad \text{at} \quad x = 1 , \end{aligned}\right\} \quad (7.6)$$

where w_{c1} and ϕ_{c1} represent the velocity distribution in the core when r is put equal to one. Thus

$$\phi_{c1} = U_1 \cos \psi \ , \tag{7.7}$$

$$w_{c1} = \frac{C_1}{2\pi U_1} \left(h_o + \frac{B}{h_o} \right) \ . \tag{7.8}$$

These conditions are the necessary and sufficient conditions that the velocity, the gradient of velocity and the pressure are continuous at the interface within the errors of the approximation used.

The velocity profiles chosen, consistent with (7.6) are

$$\phi_1 = [\phi_{c1} + F(x)H(\psi)]g(x) \ , \tag{7.9}$$

$$w = w_{c1} f(x) \ , \tag{7.10}$$

where $f(x)$, $g(x)$ and $F(x)$ satisfy the conditions

$$f(0) = 0 \ , \quad f(1) = 1 \ , \quad f'(1) = 0 \ ,$$

$$g(0) = g'(0) = 0 \ , \quad g(1) = 1 \ , \quad g'(1) = g''(1) = g'''(1) = 0 \ ,$$

$$\text{and} \quad F(1) = F'(1) = F''(1) = F'''(1) = 0 \ . \tag{7.11}$$

These profiles are expressed in terms of two variables of which one is the boundary layer thickness and therefore comply with the necessary conditions for a solution. They differ in form from those considered in previous theories, in as much as the variable $H(\Psi)$ has been introduced together with a multiplier $F(x)$; these allow for any deviation from the standard form of velocity profile which in this case would be of the form $\phi_{c1} g(x)$.

Inserting these profiles in equations (7.4) and (7.5)

$$\phi_{c1} g'''(0) + H[F(0)g'''(0)+F'(0)g''(0)] = - {}^{1}/_{2} h_o \delta^3 w_{c1}^2 \cos\Psi , \quad (7.12)$$

$$\frac{h_o f'(0)}{\delta} + (1-P) \frac{\partial \phi_{c1}}{\partial \Psi} - \frac{\partial}{\partial \Psi}(QH) - \left\{ \frac{\partial}{\partial \Psi}(\log w_{c1}) + \beta \right\} \times (P\phi_{c1} + QH) = 0 , \quad (7.13)$$

where $$P = \int_0^1 f \frac{dg(x)}{dx} dx \quad \text{and} \quad Q = \int_0^1 f \frac{d}{dx}(Fg) dx . \quad (7.14)$$

The boundary condition on $H(\Psi)$ is obtained from the fact that ϕ_1 must be zero at $\Psi = \pm {}^{\pi}/_{2}$. Equation (7.13) is, however, only a first order differential equation and (7.12) is an ordinary equation relating

δ , H and Ψ and so only one of these conditions can be satisfied. Any solution obtained from a boundary layer analysis for the point $\Psi = -\pi/2$ is doubtful, due to the fact that the flow must detatch itself from the wall of the pipe about this point. It will, therefore, be assumed that ϕ_1 is only necessarily zero at $\Psi = \pi/2$. The boundary condition on $H(\Psi)$ thus becomes

$$H(\pi/2) = 0 \ . \tag{7.15}$$

Substituting for ϕ_{c1} and w_{c1} from (7.7) and (7.8) and replacing $QH(\Psi)$ by $y(\Psi)$,

$$\frac{d}{d\Psi}\left\{ (h_o^2+B)y \right\} = \frac{h_o f'(0)}{\delta}(h_o^2+B) - (1-P)U_1 \sin\Psi\,(h_o^2+B) - PU_1 \cos\Psi \frac{dh_o^2}{d\Psi} \ , \tag{7.16}$$

subject to the initial condition that $y(\pi/2) = 0$.

Equation (7.12) can be rewritten as

$$g'''(0)U_1 \cos\Psi + Ly = \frac{-h_o \delta^3 C_1^2}{8\kappa^2 U_1^2}\left(h_o + \frac{B}{h_o} \right)^2 \cos\Psi \tag{7.17}$$

where $L = \dfrac{F(0)g'''(0) + F'(0)g''(0)}{Q}$.

Having reduced the momentum equations to this form, it is necessary to obtain relations for the constants C_1 , U_1 and B .

Determination of the constants C_1 , U_1 and B

It was seen in the last chapter that two of the three constants can theoretically be found from equations (6.35) and (6.36). Inserting the values of w as given by (6.34) for the core and (7.10) for the boundary layer, equation (6.35) becomes

$$\pi = 2\int_{-\pi/2}^{\pi/2}\left\{\int_0^{1-\delta K^{-1/2}} r\, w_c\, dr + \int_{1-\delta K^{-1/2}}^{1} r\, w\, dr\right\} d\psi ,$$

$$= 2\int_{-\pi/2}^{\pi/2}\left\{\int_0^{1} r\, w_c\, dr - K^{-1/2}\int_0^{1}\delta(w_{c1}-w)dx\right\} d\psi ,$$

$$= \frac{C_1}{2\kappa U_1}\cdot 2\int_{-\pi/2}^{\pi/2}\left\{\int_0^{1}\left(h+\frac{B}{h}\right) r\, dr - K^{-1/2}\delta\left(h_o+\frac{B}{h_o}\right)\int_0^{1}(1-f(x))dx\right\} d$$

$$\text{i.e.}\quad \frac{2\kappa U_1 \pi}{C_1} = \pi\left[1 + \frac{2B}{\kappa^2}\left\{1-(1-\kappa^2)^{1/2}\right\}\right] - 2K^{-1/2} \times$$

$$\int_0^1 \left\{1-f(x)\right\} dx \cdot \int_{-\pi/2}^{\pi/2} \delta\left(h_o + \frac{B}{h_o}\right) d\Psi \,. \qquad (7.18)$$

Similarly, equation (6.36) can be written as

$$\int_0^{2\pi}\int_0^1 C_1\left(\frac{1}{h} + \frac{B}{h^3}\right) r\, dr\, d\Psi = C_1 \int_0^{2\pi}\int_0^1 \frac{r\, dr\, d\Psi}{h} - \frac{C_1}{2\kappa U_1} \times$$

$$\int_0^{2\pi}\left(h_o + \frac{B}{h_o}\right) \frac{f'(0)}{\delta}\, d\Psi + O(K^{-1/2}) \,,$$

whereupon

$$B = \frac{-\int_0^{2\pi} \frac{h_o f'(0) d\Psi}{\delta}}{2\kappa U_1 S + \int_0^{2\pi} \frac{f'(0)}{h_o \delta} d\Psi} + O(K^{-1/2}) \,, \qquad (7.19)$$

where

$$S = \int_0^{2\pi}\int_0^1 \frac{r\, dr\, d\Psi}{(1+\kappa r \sin\Psi)^2} \,,$$

$$= \frac{5\pi}{3\kappa^2}\left[\frac{1}{(1-\kappa^2)^{3/2}} - 1\right] - \frac{3\pi}{2(1+\kappa^2)} - \frac{\pi}{\kappa^2}\left[2 + \frac{(3\kappa^2-2)}{(1-\kappa^2)^{3/2}}\right] . \qquad (7.20)$$

The term of order $K^{-1/2}$ is retained in equation (7.18) so that a second approximation to the increase in resistance due to curvature can be obtained. It is not the complete second approximation, however, since it can be seen from (7.19) that there is a contribution from B of order $K^{-1/2}$, which can only be calculated by considering a second approximation of the momentum equations. Nevertheless, it is constructive to calculate the contribution indicated in equation (7.18) not only because it represents the physical situation, but also because it affords a comparison with similar results obtained by Barua and Mori and Nakayama; they also neglected second order effects from the momentum equations.

As was seen in the last chapter, the third constant can only be obtained without recourse to experiment, if an additional physical restraint is imposed on the flow. It is required of this restraint, that, unlike the restraint imposed by Barua, it be valid for a large range of curvature ratios. Since it seems likely that the curvature will have least effect at the point where the fluid from the core attaches itself to the wall of the pipe, it was assumed that the deviation from the standard velocity profile in the boundary layer would be a minimum at this point. Thus

$$\frac{dH(\pi/2)}{d\psi} = 0 \ . \qquad (7.21)$$

Since $H(\pi/2)$ is also zero, this assumption is tantamount to assuming that near $\psi = \pi/2$, which is defined as the attachment point, the stream function effectively behaves like $\phi_{c1}\, g(x) = U_1 \cos\psi . g(x)$. It cannot be stated a priori that this assumption is valid for a large range of curvature ratios. The justification can only be obtained by comparing the results of the theory for various curvature ratios with experiment.

Equation (7.21) implies that $\frac{dy}{d\psi} = 0$ at $\psi = \pi/2$ and thus, from equation (7.16)

$$[h_o^2(\pi/2)+B]\,\frac{dy}{d\psi}(\pi/2) = \frac{h_o(\pi/2)f'(0)}{\delta(\pi/2)}\,[h_o^2(\pi/2)+B] - (1-P)U_1[h_o^2(\pi/2)+B] = 0 \ ,$$

$$\therefore\ U_1 = \frac{(1+\kappa)f'(0)}{(1-P)\delta(\pi/2)} \ . \qquad (7.22)$$

A value of $\delta(\pi/2)$ can be obtained from equation (7.17) and the fact that $y(\pi/2) = 0$. Thus

$$\delta(\pi/2) = \left[\frac{-8\kappa^2 U_1^3 g'''(0)}{c_1^2 h_o(\pi/2)}\left(\frac{h_o(\pi/2)}{h_o^2(\pi/2)+B}\right)^2\right]^{1/3} . \qquad (7.23)$$

The values of C_1 and B , however, depend on a knowledge of δ for all $\psi \in [\pi/2 , -\pi/2]$ and it is found that a particularly simple expression can be derived if it is assumed that $F(0) = F'(0) = 0$. This assumption makes L zero and the following expression for δ can be obtained from equations (7.17) and (7.8):

$$\delta = \left[\frac{-2g'''(0)U_1}{h_o \, w_{c1}^2} \right]^{1/3} . \qquad (7.24)$$

The justification for this step is that in any Polhausen approximate method of solution, there is considerable licence in the choice of velocity profiles. It does not seem unreasonable, therefore, that the profiles affording the simplest solution should be considered first. The physical significance of the assumption is that near the walls of the pipe, the deviation from the standard velocity profile is small and the stream function again varies like $\phi_{c1} \, g(x)$.

The constants C_1 , U_1 and B can now be obtained for a given curvature ratio and thus the increase in resistance due to curvature can be found from equations (5.51) and (6.19) as a function of Dean number and curvature ratio. Thus

$$\frac{\gamma_c}{\gamma_s} = \frac{C_1 K^{1/2}}{8} \quad . \tag{7.25}$$

Special Case when $\varkappa \ll 1$

The simplest polynomial forms for $f(x)$, $g(x)$ and $F(x)$, consistent with (7.11) and $F(0) = F'(0) = 0$, are

$$f(x) = 2x - x^2 \quad ,$$

$$g(x) = 10x^2 - 20x^3 + 15x^4 - 4x^5 \quad , \tag{7.26}$$

$$F(x) = x^2(1-x)^4 \quad .$$

If the curvature ratio is sufficiently small so that the variation of $\delta(\psi)$ can be assumed negligible in the integrals of (7.18) and (7.19), $\delta(\psi)$ will be replaced by $\delta(\pi/2)$ and since for $\varkappa \ll 1$, $S \doteq \pi$ [see equation (7.20)],

$$B = \frac{-1}{1 + 1/2 \delta_o \varkappa U_1} \doteq -1 + 1/2 \, \delta_o \varkappa U_1 \quad , \tag{7.27}$$

$$C_1 = \frac{1}{1/4 \, \delta_o - 1/6 \delta_o^2 K^{-1/2}} \quad , \tag{7.28}$$

where $\delta_o = \delta(\pi/2)$.

From (7.14) and the profiles (7.26), $P = {}^{11}/_{21}$, $g'''(0) = -120$ and $f'(0) = 2$. Substituting these values in (7.22) and (7.23) and neglecting higher order terms in κ ,

$$U_1 = \frac{21}{5\delta_o} \quad , \tag{7.29}$$

and

$$\delta_o^3 = 960 \frac{U_1^3 \kappa^2}{C_1^2} \frac{1}{\left\{1+2\kappa-1+{}^{1}/_{2\delta_o U_1 \kappa}\right\}^2} \quad ,$$

whereupon, eliminating U_1 and C_1 using the first approximation to C_1

$$\delta_o = 4.04 \quad . \tag{7.30}$$

Thus from (7.28) and (7.29)

$$C_1 = \frac{1}{1.01 - 2.72\ K^{-1/2}} \quad , \tag{7.31}$$

and $U_1 = 1.04$. (7.32)

Finally, the increase in resistance due to curvature can be obtained from (7.25) and (7.31) as

$$\frac{\gamma_c}{\gamma_s} = \frac{K^{1/2}}{8.08 - 21.76\ K^{-1/2}} \quad . \tag{7.33}$$

In order that this may be compared with the experimental results of Adler and White, K must again be replaced by $K_w/.472$. Thus

$$\frac{\gamma_c}{\gamma_s} = \frac{.104\ K_w^{1/2}}{1 - 3.2\ K_w^{-1/2}} \quad . \tag{7.34}$$

This result bears strong resemblance to that of Mori and Nakayama (Equation 6.28) and it can be seen from Figure (7.1) that it agrees with the experimental observations of Adler and White extremely well for values of K_w greater than 100. There are, however, certain reservations as to the validity of the second approximation in (7.34) represented by the term $3.2\ K_w^{-1/2}$, which also apply to the results obtained by Barua and Mori and Nakayama. All these results were obtained from momentum equations that neglect higher orders in Dean number or Reynolds number and yet, in all cases, these

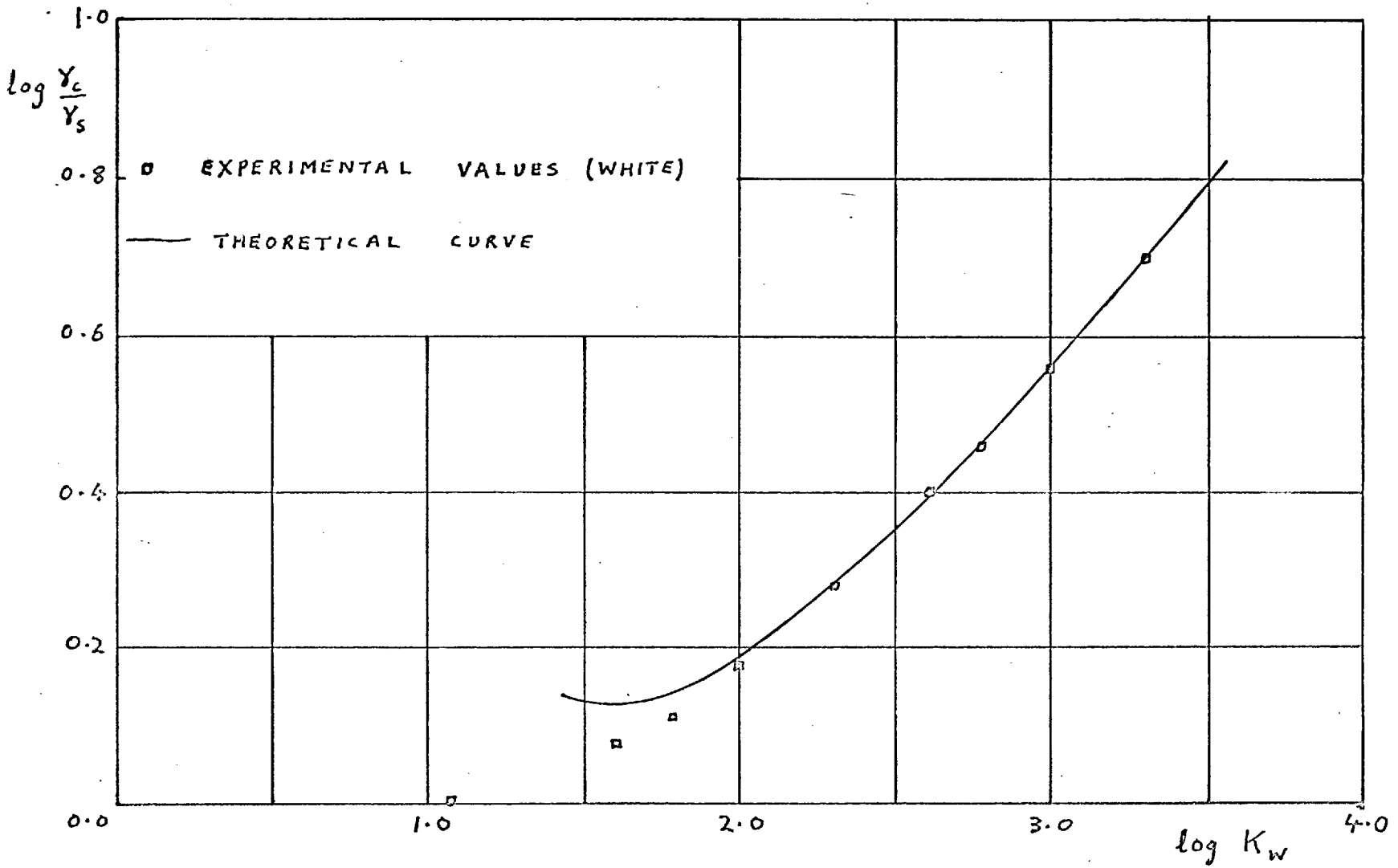

Fig. (7.1). Comparison of the theoretical resistance coefficient for $\chi \ll 1$ with the experimental observations of White which also represent the results of Adler (see Fig. 5.2).

would have contributed to the second approximation to the increase in resistance due to curvature. The inclusion of higher order effects severely complicates the problem and it is therefore assumed that the terms omitted have very little effect on the results.

The physical significance of this assumption can be seen by considering the fact that second order effects were included in the constant mass flux condition and omitted in the constant momentum flux condition. It is therefore assumed that the defect in mass flux in the boundary layer has more effect on the flow than the defect in momentum flux in the boundary layer.

Numerical Solution for various curvature ratios

The polynomial forms for $f(x)$ and $g(x)$ from (7.26) were inserted in equations (7.22) and (7.23) and values of U_1 and $\delta(\pi/2)$ were obtained. A value of δ was then obtained for various Ψ from (7.24) and these values were inserted into equations (7.18) and (7.19) for various curvature ratios and Dean Number. Integrating the various integrals using Simpson's formula with an interval length of $\pi/180$, values of B, C_1 and U_1 were obtained for various curvature ratios and

Dean number.

From the values of C_1 and equation (7.25), the increase in resistance due to curvature was plotted against Dean number for various curvature ratios and the results are exhibited in Fig. (7.2). It is seen that for small λ, the curve lies near to that obtained from experiment and that as the curvature ratio increases, the resistance increases. The accuracy of these results for large curvature ratios cannot be given until the experiments of Adler and White are repeated for this range of curvature ratios. It should be remembered from Chapter 5, however, that for large curvature ratios, torsional effects become important; it seems reasonable to add, therefore, that results for pipes of curvature ratio greater than about 0.4 are of academic interest.

The theory devised in this chapter is for asymptotically large K and it has been seen that any second approximations are not strictly valid. The results for asymptotically large K of the various constants are tabulated as functions of K_w for various curvature ratios in Table (7.1).

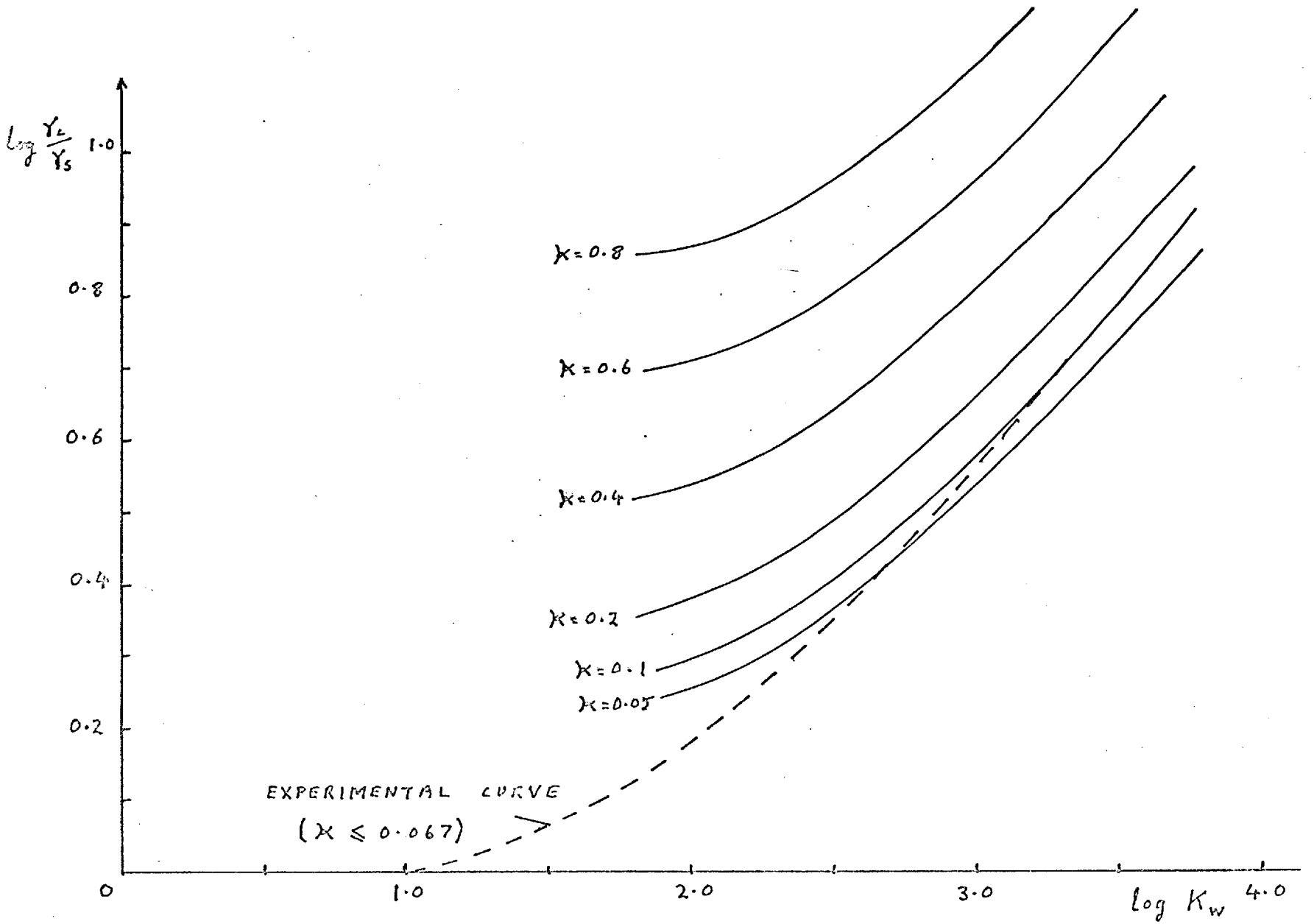

Fig. (7.2). The increase in resistance due to curvature for various curvature ratios.

$\varkappa$	$C/K_w^{1/2}$	$U/K_w^{1/2}$	B	$\frac{\gamma_c}{\gamma_s}/K_w^{1/2}$
.05	.776	.90	-0.876	0.097
.1	.856	.94	-0.765	0.107
.2	1.01	1.01	-0.567	0.127
.3	1.19	1.09	-0.40	0.149
.4	1.42	1.18	-0.276	0.178
.6	2.02	1.38	-0.117	0.252
.8	2.90	1.6	-0.039	0.363
.95	3.64	1.77	-0.006	0.455

TABLE (7.1). Asymptotic values for the constants for various curvature ratios.

It will be noticed that for $\varkappa = .05$, the dominant term for the increase in resistance is $.097\ K_w^{1/2}$. This value agrees well with the dominant term obtained by Hasson from White's experimental values for small curvature ratios. Hasson found that in the range $30 < K_w < 2000$, the relation

$$\frac{\gamma_c}{\gamma_s} = .0969\ K_w^{1/2} + 0.556 \qquad (7.35)$$

gives a good representation of the observed results.

The object of this chapter was to find numerical values for the constants which emerge from this type of analysis. These values have been obtained and they have shown reasonable agreement with experimental values for small curvature ratios. In the next chapter, the values of these constants for all curvature ratios will be used to investigate the skin friction and the possibility of separation.

CHAPTER 8

The momentum Integrals

In the previous chapter, assumptions were made which not only simplified the analysis, but also predetermined to a large extent the nature of the flow in the boundary layer. In a Polhausen approximate method type solution, profiles varying with the non-dimensional radial component and the boundary layer thickness have to be imposed; but in the previous theory, further restrictions were imposed on the profiles by assuming that separation did not exist. This facilitated a ready solution of the integrals involved in equations (6.35) and (6.36), since this assumption implies that the profiles are valid throughout the range $-\pi/2 \leq \psi \leq \pi/2$. If, however, separation does exist, at a point $\psi = \psi_1$, say, the boundary layer approximation breaks down about this point and the velocity distribution cannot be determined near the inner wall.

The present chapter will be concerned with finding a better representation of the velocity distribution in the boundary layer and in particular, to find whether, and at what point, separation exists.

In order that more accurate results may be obtained, both momentum equations (6.30) and (6.31) are integrated across the boundary layer.

$$\int_0^{\delta(\Psi)} \left\{ \frac{\partial \phi_1}{\partial \Psi} \frac{\partial w}{\partial \eta} - \frac{\partial \phi_1}{\partial \eta} \frac{\partial w}{\partial \Psi} - \beta_o w \frac{\partial \phi_1}{\partial \eta} \right\} d\eta = h_o \left[\frac{\partial w}{\partial \eta} \right]_o^{\delta(\Psi)} , \qquad (8.1)$$

$$\int_0^{\delta(\Psi)} \left\{ \frac{\partial \phi_1}{\partial \Psi} \frac{\partial^2 \phi_1}{\partial \eta^2} - \beta_o \left(\frac{\partial \phi_1}{\partial \eta} \right)^2 + \frac{1}{2} h_o^2 \cos \Psi . (w_{c1}^2 - w^2) \right\} d\eta$$

$$= -h_o \left[\frac{\partial^2 \phi_1}{\partial \eta^2} \right]_0^{\delta(\Psi)} \qquad (8.2)$$

Putting $\eta = \delta(\Psi)x$ and henceforward denoting partial differentiation with respect to x by primes,

$$\int_0^1 \frac{\partial \phi_1}{\partial \Psi} w' \, dx - \int_0^1 \phi_1' \left(\frac{\partial w}{\partial \Psi} + \beta_o w \right) dx = \frac{h_o}{\delta} [w']_0^1 , \qquad (8.3)$$

$$\frac{1}{\delta^2} \left(\frac{\partial}{\partial \Psi} - \beta_o - \frac{1}{\delta} \frac{d\delta}{d\Psi} \right) \int_0^1 \phi_1'^2 \, dx + \frac{1}{2} h_o^2 \cos \Psi \int_0^1 (w_{c1}^2 - w^2) dx$$

$$= -\frac{h_o}{\delta^3} [\phi_1'']_0^1 . \qquad (8.4)$$

The velocity profiles

The velocity profiles introduced in this section will be more complete than those of the previous theory in that both restrictions imposed by the momentum equations at the wall will be satisfied. The boundary conditions at the wall are

$$w = \frac{\partial \phi_1}{\partial \psi} = \phi_1' = 0 \quad \text{at} \quad x = 0 : \tag{8.5}$$

in addition, it can be seen from (6.30) and (6.31) that, at the wall,

$$\phi_1'''(0) = -\frac{1}{2} h_o \delta^3 w_{c1}^2 \cos \psi , \tag{8.6}$$

$$w''(0) = 0 . \tag{8.7}$$

At the interface, the following conditions will be satisfied:

$$w(1) = w_{c1} , \qquad w'(1) = w''(1) = 0 , \tag{8.8}$$

$$\phi_1(1) = \phi_{c1} , \qquad \phi_1'(1) = \phi_1''(1) = \phi_1'''(1) = 0 , \tag{8.9}$$

where ϕ_{c1} and w_{c1} are given by (7.7) and (7.8).

It can be seen from the conditions (8.5) to (8.9), that all the restrictions on ϕ_1 at the wall and at the interface are satisfied for all derivatives, save for $\phi''(0)$, up to the third. Similarly, the restrictions on w are satisfied for all derivatives up to the second, except for $w'(0)$. The values of $w'(0)$ and $\phi''(0)$ are determined from the momentum integrals and these are the values that determine the skin friction and indicate any separation.

The velocity profiles chosen, consistent with the conditions of (8.5), (8.7), (8.8) and (8.9) are

$$\phi_1 = \left\{ \phi_{c1} + g_1(x)\ \lambda(\Psi) \right\} g_0(x) \ , \tag{8.10}$$

$$w = \left\{ w_{c1} + f_1(x) \Omega(\Psi) \right\} f_0(x) \ , \tag{8.11}$$

where g_0, g_1, f_0 and f_1 satisfy the conditions

$$\begin{aligned}
&g_0(0) = g_0'(0) = 0 \ , \quad g_0(1) = 1 \ , \quad g_0'(1) = g_0''(1) = g_0'''(1) = 0 \ , \\
&g_1(1) = g_1'(1) = g_1''(1) = g_1'''(1) = 0 \ , \\
&f_0(o) = f_0''(0) = 0 \ , \quad f_0(1) = 1 \ , \quad f_0' = f_0''(1) = 0 \ , \\
&f_1(1) = f_1'(1) = f_1''(1) = 0 \ .
\end{aligned} \tag{8.12}$$

With these profiles, $\lambda(\Psi)$ and $\Omega(\Psi)$, together with their multipliers $g_1(x)$ and $f_1(x)$, represent the unknown deviation from $\phi = \phi_{c1} g_o(x)$ and $w = w_{c1} f_o(x)$ in the boundary layer.

Substituting them into equations (8.3) and (8.4),

$$\left(a_1 w_{c1}+a_2\Omega\right)\frac{d\phi_{c1}}{d\Psi} + \left(a_3 w_{c1}+a_4\Omega\right)\frac{d\lambda}{d\Psi} - \left\{\frac{dw_{c1}}{d\Psi} + \beta_o w_{c1}\right\}\left[(1-a_1)\phi_{c1}-a_2\right]$$

$$+ \left\{\frac{d\Omega}{d\Psi} + \beta_o \Omega\right\}(a_2\phi_{c1}+a_4\lambda) + \frac{h_o f_o'(0)}{\delta}\cdot\left(w_{c1}+f_1(0)\Omega\right) = 0 \quad , \qquad (8.13)$$

$$\frac{1}{\delta^2}\left\{\frac{d}{d\Psi} - \beta_o - \frac{1}{\delta}\frac{d\delta}{d\Psi}\right\}(a_5\phi_{c1}^2+a_6\phi_{c1}\lambda+a_7\lambda^2) +$$

$$\frac{1}{2}h_o^2\cos\Psi\,(a_8 w_{c1}^2+a_9\Omega w_{c1}+a_{10}\Omega^2) - \frac{h_o}{\delta^3}\left\{\phi_{c1}+g_1(0)\lambda\right\} g_o''(0) = 0 \quad ,$$

(8.14)

where

$$a_1 = \int_0^1 g_o f_o' dx \quad , \quad a_2 = \int_0^1 g_o \frac{d}{dx}(f_o f_1)dx \quad , \quad a_3 = \int_0^1 g_o g_1 f_o' dx$$

$$a_4 = \int_0^1 g_1 g_o \frac{d}{dx}(f_1 f_o)dx \quad , \quad a_5 = \int_0^1 g_o'^2 dx \quad , \quad a_6 = \int_0^1 2g_o' \frac{d}{dx}(g_o g_1)dx$$

(8.15)

$$a_7 = \int_0^1 \left\{ \frac{d}{dx}(g_o g_1) \right\}^2 , \quad a_8 = \int_0^1 (1 - f_o^2) dx , \quad a_9 = \int_0^1 2 f_1 f_o^2 dx$$

$$a_{10} = \int_0^1 f_o^2 f_1^2 \, dx . \qquad (8.15) \text{ contd.}$$

Finally, if the condition (8.6) is to be satisfied

$$\left\{ \phi_{c1} + g_1(0)\lambda \right\} g_o'''(0) + 3 g_1'(0) g_o''(0) \lambda = - \frac{1}{2} h_o \, \delta^3 w_{c1}^2 \cos\Psi ,$$

using the fact that $g_o(0) = g_o'(0) = 0$. From (7.7), this can be expressed as

$$\lambda = - \left[\frac{U_1 g_o'''(0) + \frac{1}{2} h_o \, \delta^3 \, w_{c1}^2}{g_1(0) g_o'''(0) + 3 g_1'(0) g_o''(0)} \right] \cos\Psi . \qquad (8.16)$$

Eliminating λ from (8.13), (8.14) and (8.16) , yields two first order, ordinary differential equations in $\delta(\Psi)$ and $\Omega(\Psi)$; they take the form

$$Q_1 \frac{d\Omega}{d\Psi} + Q_2 \frac{d\delta}{d\Psi} = \frac{Q_3}{\cos\Psi} + Q_4 , \qquad (8.17)$$

$$Q_5 \frac{d\delta}{d\Psi} = \frac{Q_6}{\cos\Psi} + Q_7 , \qquad (8.18)$$

where the Q_i's are functions of δ, Ω, Ψ, ε_1, B, U_1 and $\varkappa$ which are nowhere singular in the range $-\pi/2 \leq \Psi \leq \pi/2$. They can be defined in terms of the following functions:

$$\left.\begin{aligned} P_1 &= \frac{-\, g_o'''(0)\ .\ U_1}{g_1(0)g_o'''(0) + 3g_1'(0)g_o''(0)}\ , \\ P_2 &= \frac{\frac{1}{2}h_o\ w_{c1}^2}{g_1(0)g_o'''(0) + 3g_1'(0)g_o''(0)}\ , \\ P_3 &= -\ (P_1 + \delta^3\ P_2)\ , \\ P_4 &= h_o^2(a_8\ w_{c1}^2 + a_9\ w_{c1}\Omega + a_{10}\Omega^2) - \frac{20h_o}{\delta}\ (w_{c1} + \Omega)\ , \\ P_5 &= a_5\ U_1^2 - a_6\ U_1\ P_3 + a_7\ P_3^2\ , \end{aligned}\right\} \quad (8.19)$$

whereupon

$$\left.\begin{aligned} Q_1 &= a_2\ U_1 - a_4\ P_3\ , \\ Q_2 &= 3P_2\ \delta^2\ (a_3\ w_{c1} + a_4\Omega)\ , \end{aligned}\right\} \quad (8.20)$$

$$Q_3 = (a_1 w_{c1} + a_2 \Omega) U_1 \sin\Psi - (a_3 w_{c1} + a_4 \Omega) P_3 \sin\Psi - \frac{3h_o}{\delta}(w_{c1} + \Omega) ,$$

$$Q_4 = -(a_3 w_{c1} + a_4 \Omega)\delta^3 \frac{dP_2}{d\Psi} + \left[\frac{d}{d\Psi} w_{c1} + \beta_o w_{c1}\right] \times \left[(1-a_1)U_1 + a_3 P_3\right] - \beta_o Q_1 \Omega ,$$

$$Q_5 = \frac{P_5}{\delta^3} - 3a_6 U_1 P_2 + 6a_7 P_3 P_2 ,$$

$$Q_6 = -\frac{2P_5}{\delta^2} \sin\Psi + P_4 ,$$

$$Q_7 = -\frac{\kappa P_5 \cos\Psi}{\delta^2} .$$

The equations (8.17) and (8.18) have singularities at $\Psi = \pm \pi/2$ unless $Q_3(\pm\pi/2)$ and $Q_6(\pm\pi/2)$ are zero. Conditions cannot be imposed on the flow at $\Psi = -\pi/2$, because of the strong evidence predicting separation. In fact, the equations may well be singular at this point if, as is the case after separation, they do not truly represent the flow. If it is assumed that there cannot be singularities in the equations at $\Psi = \pi/2$, $Q_3(\pi/2) = Q_6(\pi/2) = 0$ and these two equations give the

initial conditions of δ and Λ.

It remains to obtain values for the constants C_1, B and U_1, whereupon equations (8.17) and (8.18) can be solved numerically.

Determination of the constants C_1, B and U_1

It was seen in chapter 6 that two of these constants can theoretically be found from the constant axial mass and momentum flux conditions given by (7.18) and (7.19). It was seen, however, in the development of the theory, that the integrals involved in these relations cannot be determined completely if the flow separates. It was also seen that a value for the third constant is obtained either by imposing an extra physical condition on the flow, or by giving to it a result obtained from experimental observations. Since the object of this present section, is to find a more accurate representation of the skin friction, the latter course of action will be adopted.

By far the most reliable experiments are those which measure the increase in resistance due to curvature as a function of Dean number. The experimental observations of White and Adler have been shown by Farugia (unpublished)

to be represented by White's empirical formula

$$\frac{\gamma_c}{\gamma_s} = \left[1 - \left\{ 1 - \left(\frac{11.6}{K_w^{1/2}} \right)^{0.45} \right\}^{2.22} \right]^{-1} , \qquad (8.21)$$

for $11.6 < K_w < 2000$, within an error of $\pm 2\%$. Unfortunately, these results only apply to small curvature ratios (i.e. $\kappa < .067$), whereas the present theory requires results for all curvature ratios. Since the theoretical results obtained in the last chapter agree reasonably well with the experimental results for small curvature ratios, the values of C_1 (from which the resistance is calculated) for the present theory, will be taken from table (7.1). This assumes that the values of C_1 for large curvature ratios are also accurate, but in the absence of experimental observations for pipes of large curvature ratio, these values will have to suffice.

Once a value for C_1 is obtained, B can be found as a function of U_1 from equation (7.18) by assuming that the $K^{-1/2}$ term is negligible. This is quite reasonable since the values shown in table (7.1) are only accurate to the first approximation and the $K^{-1/2}$ term was only retained in equation (7.18) so that a second approximation to the resistance could be obtained. Since

the remaining terms contain no integrals, they are unaffected by the possibility of separation and B can be expressed in terms of U_1 as follows:

$$B = \frac{\frac{1}{2}\kappa^2\left(\frac{2\kappa U_1}{3_1} - 1\right)}{1 - (1 - \kappa^2)^{1/2}}. \qquad (8.22)$$

If the flow does not separate, the remaining constant U_1 can be found by using the following iterative method: choose a value for U_1 ; take the particular value for C_1 from table (7.1) corresponding to the particular curvature ratio being considered and determine B from (8.22); insert these quantities into equations (8.17) and (8.18) and solve for $\delta(\psi)$ and $\Omega(\psi)$ in the range $-\pi/2 \leq \psi \leq \pi/2$. A different value of B can then be found from (7.19) and thus a different value of U_1 from (8.22). This process is then repeated until U_1 converges suitably.

If, however, the flow separates, or U_1 does not converge suitably, the above method will fail and an alternative approach has to be considered. In the next section, it will be seen that the flow does in fact separate. The values of U_1 for various curvature ratios were then assumed to be equal to those obtained

in the previous theory and exhibited in table (7.1).

Numerical solution for various curvature ratios

The simplest polynomial expressions for $f_o(x)$, $f_1(x)$, $g_o(x)$ and $g_1(x)$ satisfying the conditions of (8.12) are

$$\begin{aligned} f_o(x) &= 3x - 3x^2 + x^3 \ , \\ f_1(x) &= (1-x)^3 \ , \\ g_o(x) &= 10x^2 - 20x^3 + 15x^4 - 4x^5 \ , \\ g_1(x) &= (1-x)^4 \ . \end{aligned} \tag{8.23}$$

These profiles were substituted into the integrals of (8.15) to determine the a_i's which were in turn substituted into equations (8.13) and (8.14); subsequently, λ and the form of the Q_i's in equations (8.17) and (8.18) were found.

Equations (8.17) and (8.18) were solved on the computer at Imperial College for various values of curvature ratio and the corresponding value of C_1 and for various values of U_1 on and about the value given in

table (7.1). It was found in every case that separation as indicated by the fact that $\frac{\partial w}{\partial r}$ became positive was evident. As a result of the nature of this separation, values of B obtained from equation (7.19) were, in all cases, lower than those obtained from equation (8.22). It was decided, therefore, that the equations did not represent the flow about the region where $\frac{\partial w}{\partial r}$ is positive and that the value of U_1 for a particular curvature ratio should be taken as that given by table (7.1)

Equations (8.17) and (8.18) were solved numerically for the following values of κ : 0.05, 0.1, 0.2, 0.4, 0.6 and 0.8. Gill's process for the fourth order Runge-Kutta method was used with an interval length initially of $\frac{\pi}{4320}$ increasing to $\frac{\pi}{180}$ after 48 steps. This was necessary to avoid the inherent instability in the numerical process for the solution of these equations about the point $\psi = \pi/2$.

The values of ψ at which $\frac{\partial w}{\partial r}$ became positive were sought for each value of κ and it was found that values could be obtained only for $\kappa = 0.05$ up to $\kappa = 0.4$. For values of κ equal to 0.6 and 0.8, $\frac{\partial w}{\partial r}$ is at all points negative. The available points indicating separation are shown graphically in fig. (8.1). It is seen that the values shown can be connected with

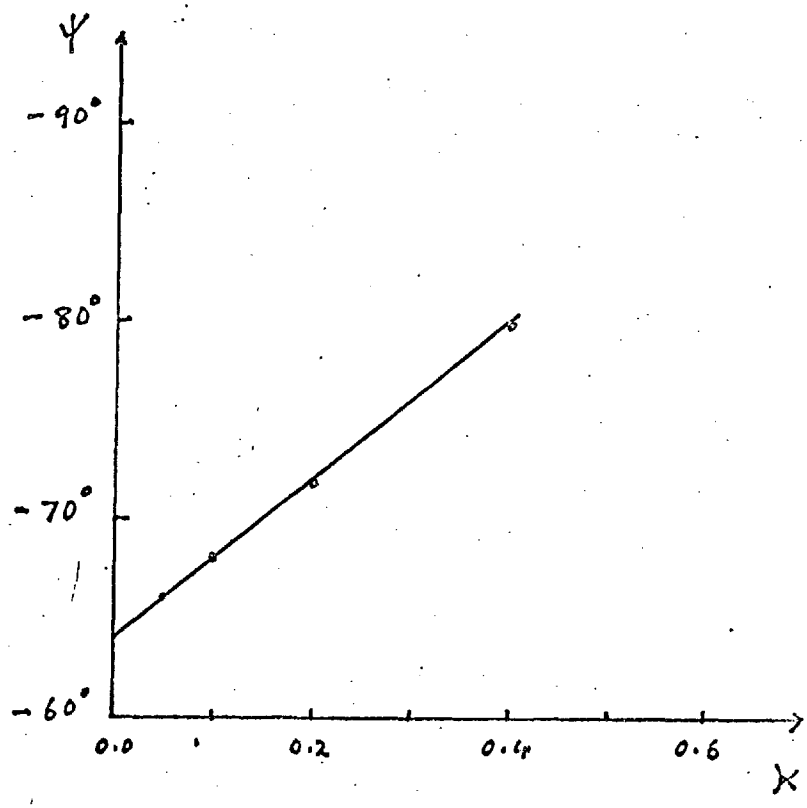

Fig. (8.1). Position of point of separation as a function of curvature ratio.

reasonable accuracy by a straight line recording a value of -64° for zero curvature ratio. This compares favourably with the calculated point of separation obtained by Barua. He found that the tangential velocity became positive in the boundary layer at $\Psi = -62^{\circ}\ 58'$ for very small curvature ratios.

The numerical results for $\delta(\Psi)$, $\Omega(\Psi)$ and $\lambda(\Psi)$ are shown in figure (8.2) to figure (8.4). A typical

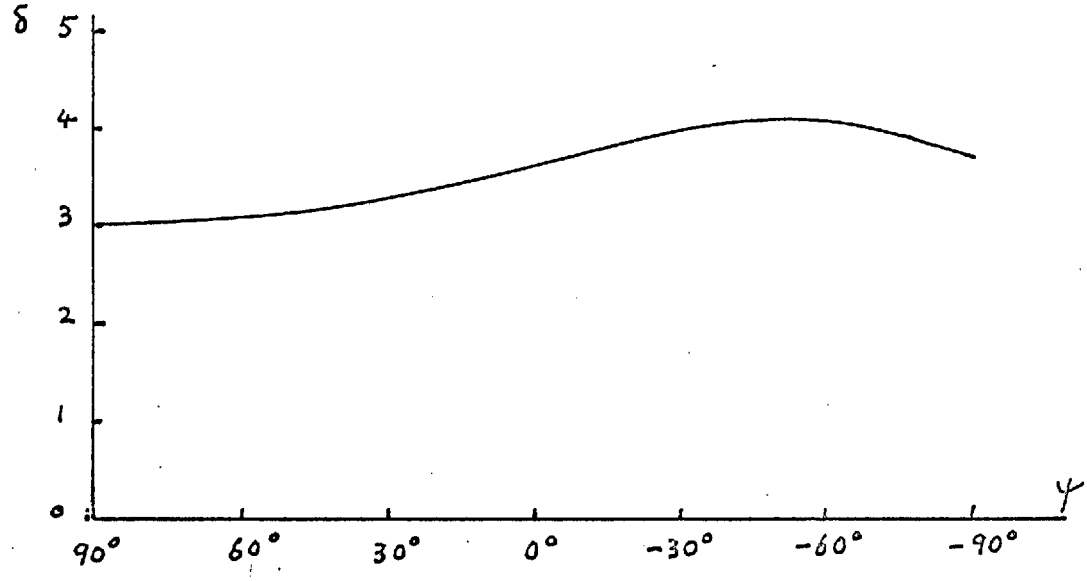

ψ \ κ	.05	.1	.2	.4	.6	.8
90°	3.01	3.02	3.05	3.04	2.99	2.86
60°	3.08	3.10	3.14	3.16	3.14	3.03
30°	3.28	3.31	3.38	3.48	3.55	3.53
0°	3.61	3.65	3.73	3.90	4.07	4.17
-30°	3.97	3.97	3.99	4.04	4.12	4.17
-60°	4.06	3.93	3.64	3.13	2.69	2.35
-89°	3.67	3.36	2.77	1.79	1.03	0.448

Fig. (8.2). The variation of δ with ψ for various curvature ratios.

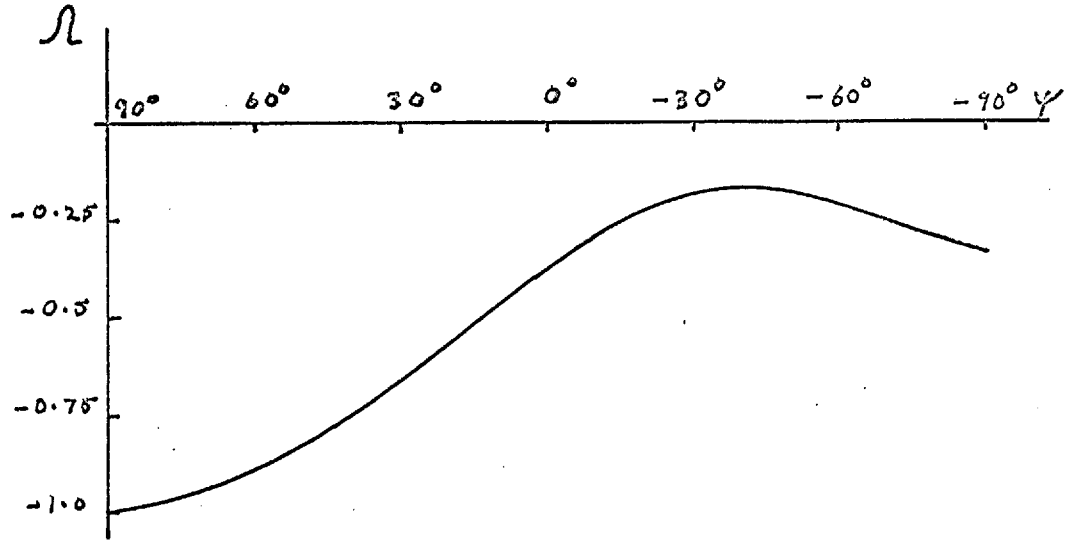

ψ \ κ	.05	.1	.2	.4	.6	.8
90°	-0.998	-0.987	-0.970	-0.976	-1.01	-1.10
60°	-0.896	-0.882	-0.852	-0.823	-0.810	-0.847
30°	-0.655	-0.621	-0.552	-0.413	-0.250	-0.80
0°	-0.368	-0.307	-0.184	0.145	0.615	1.26
-30°	-0.175	-0.098	0.061	0.600	1.55	3.15
-60°	-0.207	-0.153	-0.053	0.451	1.77	5.12
-89°	-0.328	-0.304	-0.289	-0.186	0.013	0.62

Fig. (8.3). The variation of Λ with ψ for various curvature ratios.

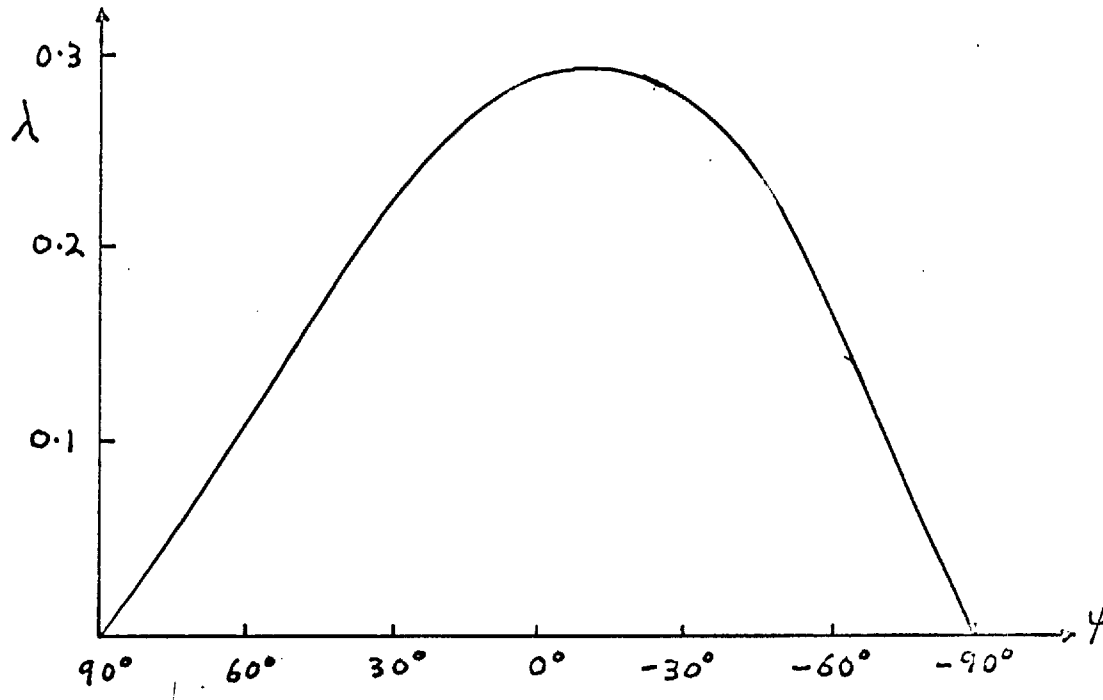

ψ \ κ	.05	.1	.2	.4	.6	.8
90°	0.0	0.0	0.0	0.0	0.0	0.0
60°	0.121	0.126	0.136	0.158	0.183	0.212
30°	0.226	0.235	0.253	0.291	0.337	0.389
0°	0.292	0.305	0.330	0.384	0.453	0.532
-30°	0.281	0.297	0.321	0.380	0.451	0.532
-60°	0.169	0.178	0.193	0.226	0.265	0.307
-89°	0.006	0.007	0.007	0.008	0.010	0.011

Fig. 8.4. The variation of λ with ψ for various curvature ratios.

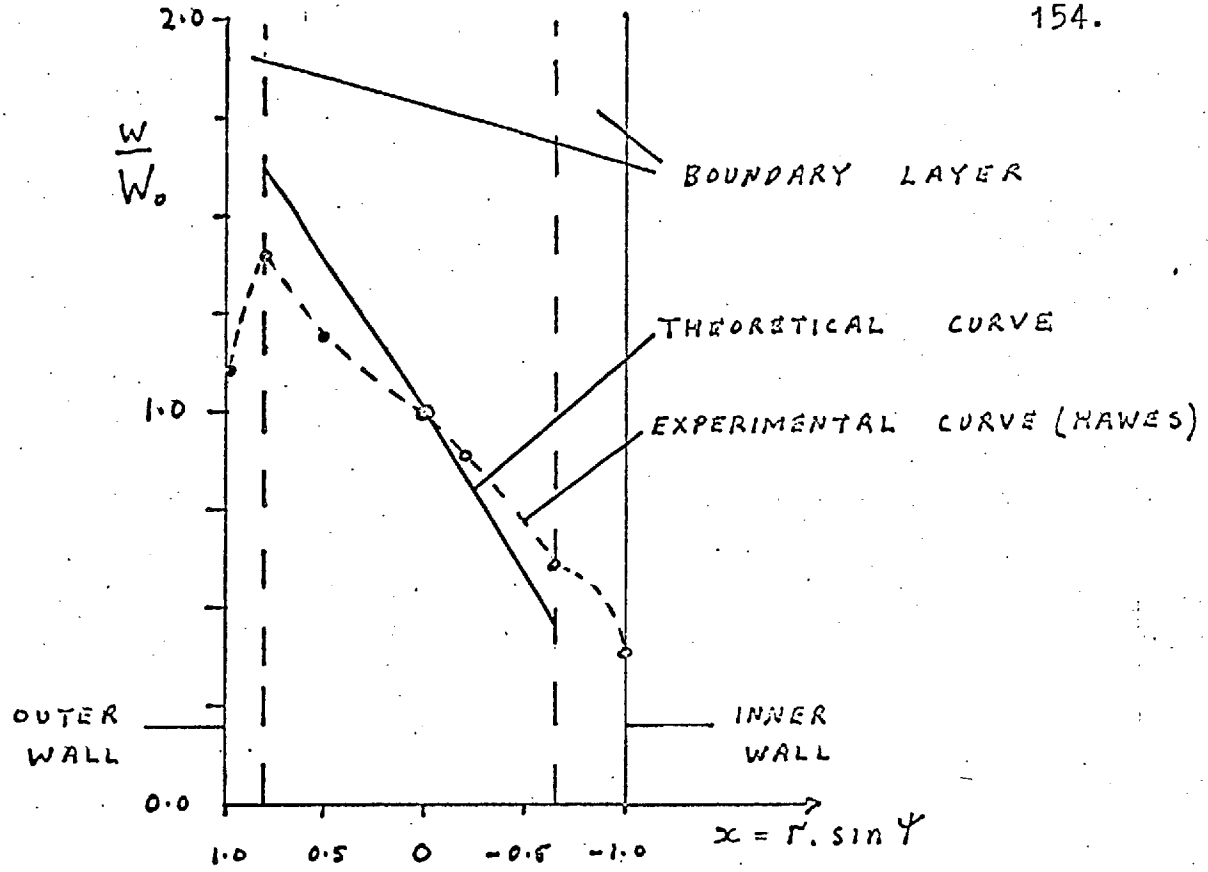

x \ κ	.05	0.1	0.2	0.4	0.6	0.8
1.0	1.80	1.79	1.76	1.76	1.83	1.98
0.5	1.69	1.68	1.66	1.66	1.72	1.85
0.0	1.00	1.00	1.00	1.01	1.01	1.01
-0.5	0.58	0.58	0.59	0.59	0.56	0.49
-1.0	0.17	0.16	0.15	0.10	-0.01	-0.31

Fig. (8.5). Experimental (Hawes) and theoretical velocity profiles in the plane of symmetry of a curved pipe.

graph for δ , Ω and λ is exhibited and an accompanying table gives details of the variations for different curvature ratios. In all cases the graphs were plotted for the particular curvature ratio of 0.05.

Finally since the values of C_1 , B and U_1 have been ascertained, it is possible to consider the asymptotic axial velocity profiles in the core for various curvature ratios. The velocity profile for κ = .05 is exhibited graphically together with the velocity profile obtained from experiment by Hawes for a pipe with κ = .05 and a Dean number K_W = 895. The deviations from the theoretical curve for various curvature ratios are shown in the accompanying table [see figure (8.5)].

Region of validity

The equations of motion for flow in a curved pipe [(5.41) and (5.42)] were solved for asymptotically large K and without the assumption that the curvature ratio was very much less than one. In addition to the restrictions imposed on the theory by the simplifying features introduced and discussed in the development of the theory, there are restrictions imposed by the physical nature of the problem. Examples of the former are

inherent in the assumptions. They include: assuming that viscous forces are only important in a thin layer next to the wall and that the constants derived in table (7.1), after imposing an intuitive physical restraint [see (7.21)], are valid for all curvature ratios. Examples of the latter arise from the fact that the flow becomes turbulent after a critical Reynolds number and the physical necessity of introducing large torsional effects as κ tends to one. It is difficult to obtain quantitative limitations to the present theory without a direct comparison with experimental observations, but it is possible, with the aid of fig. (8.6), to derive certain limitations imposed by the transition to turbulence.

It is known from the experiments of White and Adler that for given curvature ratios, there are critical Reynolds numbers and thus critical Dean Numbers, above which the flow is turbulent [see fig. (1.1)]. It is natural to ask whether the values of K, which are sufficiently large for an asymptotic solution, are greater than the critical Dean Number.

Ito derived an empirical formula from the results of White and Adler for the critical Reynolds number as a function of curvature ratio of the form

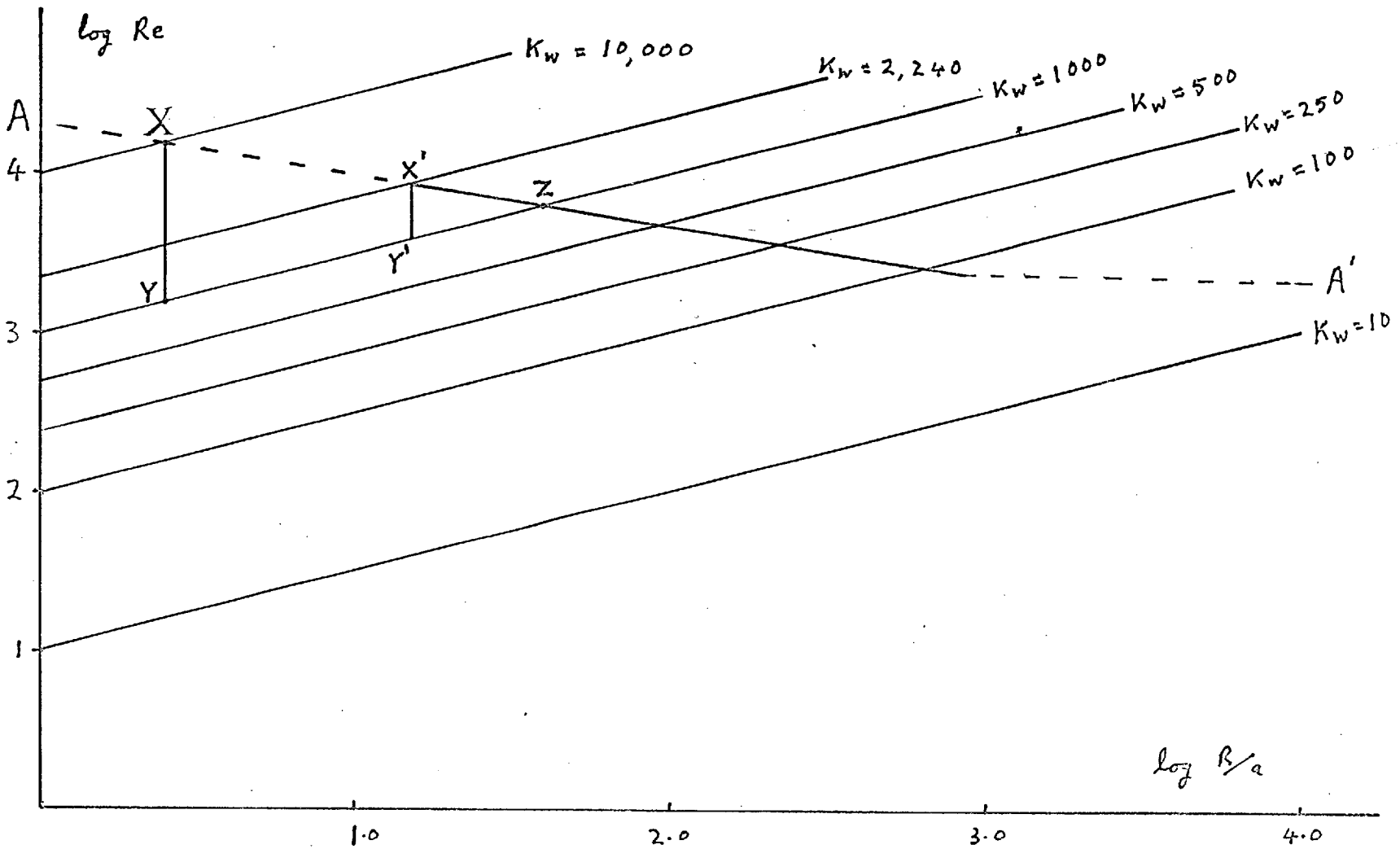

Fig. (8.6). The region of validity.

$$Re_c = 2 \times 10^4 \left(\frac{a}{R}\right)^{0.32} , \qquad (8.24)$$

valid for $15 < \frac{R}{a} < 860$. In fig. (8.6), this curve is plotted on a graph of log Re against log R/a and from the formula $K_w = Re\left(\frac{a}{R}\right)^{1/2}$, lines of constant K_w are drawn. The extension of Ito's curve is known for values of $R/a > 860$ since it is known that as $R/a \longrightarrow \infty$, the critical Reynolds number tends to that of a straight pipe which is approximately 2,300. The extension for values of $R/a < 15$ is not known and may be difficult to obtain even experimentally. The reason for this can be seen from fig. (5.2), where the deviation from the common curve for the increase in resistance due to curvature for various curvature ratios has been used to denote the onset of turbulence. As the curvature ratio κ increases, the line deviating from the common curve subtends a smaller angle with the common curve. Eventually it may not be possible to distinguish the two curves. Also, as κ increases, it is likely that this common curve will no longer be valid for the increase in resistance. In fact the results of chapter 7, illustrated in fig. (7.2), indicate that there will be a marked increase for these curvature ratios. In fig. (8.6),

Ito's curve is extended to values of $R/a < 15$ by a dashed line continuing the known curve. For values of Re above the curve AA' the flow is turbulent and below it, the flow is laminar. The theory developed in the last three chapters and those of Adler, Barua, and Mori and Nakayama are valid only below this line.

In order that an estimate of the value of K_w be obtained, above which the asymptotic solution is sufficiently accurate, it will be necessary to compare the theoretical results with those of available experiments and to remember the order of the terms neglected. Since K_w is of the same order as K and terms of order $K^{-1/2}$ have been neglected relative to terms of order one, it is essential that $K_w^{1/2} >> 1$. Although there is good agreement between the theoretical and experimental results for the increase in resistance due to very small curvature for values of K_w down to 250, the velocity profiles in the core (see fig. 8.5) are steeper than that observed by Hawes who obtained the profile for a pipe with $\delta = .05$ and at a Dean number of $K_w = 895$. Nothing is known as yet about the behaviour of the velocity profile with increasing K_w , but it may well steepen as K_w increases. If this is the case, K_w is not sufficiently large. This problem can only be resolved by repeating

the experiments of Hawes for several values of the Dean number approaching the critical Dean number.

The accuracy of the theoretical results for the resistance coefficient for such low Dean numbers is due largely to the second approximation. A comparison of the asymptotes of the theoretical results for $\varkappa \ll 1$ (i.e. $\gamma_c/\gamma_s = .104\ K_w^{1/2}$), for $\varkappa = .05$ (i.e. $\gamma_c/\gamma_s = .097\ K_w^{1/2}$) and for $\varkappa = 0.1$ (i.e. $\gamma_c/\gamma_s = .107\ K_w^{1/2}$), with the experimental observations of White is shown in table (8.1). It can be seen that although the accuracy increases as K_w increases, the results differ by as much as 15.2% for $K_w = 1000$ and 12% for $K_w = 2000$. Since the theory predicting the separation point depends on these asymptotic results, it is reasonable to restrict the validity to values of K_w greater than 1000.

Due to the effects of torsion discussed in chapter 5, there is a practical lower bound of R/a below which the theory presented here is invalid. Also, it is likely that the assumptions made in the development of the theory break down beyond a certain curvature ratio. An accurate value of this lower bound is possible only by comparing the theoretical results with possible future experiments designed to this end.

K_w	$\frac{\gamma_c}{\gamma_s}$ obtained from White's experiments	For $\varkappa \ll 1$ $\frac{\gamma_c}{\gamma_s} = .104K_w^{1/2}$	For $\varkappa = 0.5$ $\frac{\gamma_c}{\gamma_s} = .097K_w^{1/2}$	For $\varkappa = 0.1$ $\frac{\gamma_c}{\gamma_s} = .107K_w^{1/2}$
200	1.87	1.47	1.37	1.51
400	2.48	2.08	1.94	2.14
600	2.85	2.55	2.38	2.62
1000	3.61	3.29	3.06	3.39
2000	4.93	4.65	4.34	4.79

Table (8.1)

The region of validity of this theory can be obtained once lower bounds of R/a and K_w have been decided upon. It is represented in fig. (8.6) by the area bounded by the curves AA' , R/a = lower bound of R/a and K_w = lower bound of K_w . Thus if lower bounds of R/a and K_w are assumed to be 4 and 1000 respectively, the region of validity is represented by the area XYZ . It can be seen from this that an upper bound of R/a would be about 40. In previous theories, it is assumed that $\varkappa \ll 1$. If it is assumed that their theories are also valid for values of $K_w > 1000$ and that $R/a = 15$ is sufficiently large to make $\varkappa = a/R \ll 1$, it can be seen that the region of validity would be represented by the area X'Y'Z .

The separation condition

It was seen earlier that a condition conducive to separation was produced from the numerical solution of the differential equations (8.17) and (8.18). It was also seen that as $\kappa \longrightarrow 0$, the calculated value was effectively the same as that obtained by Barua whose theory is only valid for $\kappa << 1$. The difference between the determination of this value is that Barua's theory predicts separation in the tangential velocity component whereas the present theory predicts separation in the axial velocity component. The reasons for this are due to the different approaches to the problem and the fact that the boundary layer approximation breaks down near a point of separation. Thus it should only be deduced that separation occurs somewhere near the predicted values and that the type of separation is irrelevant since the equations are not valid about this point.

There may, however, be some significance in the fact that the separation point of the present theory recedes to $\psi = -90^{\circ}$ as κ increases [see fig. (8.1)]. Although it is quite likely that beyond a certain value of κ , the theory is not valid, there may be some correlation between this fact and the fact that the

flow in curved pipes becomes more stable as κ increases. This is not to say that separation causes instability in the flow, but it may well give rise to the effects which then produce instability and thus turbulence. This opinion is reinforced by the experimental observations of Taylor (6) which showed that the flow appeared to become turbulent initially in a layer next to the wall of the pipe.

Another facet to this problem is that although it is assumed that the flow is symmetrical about the $\psi = \pi/2$, $\psi = -\pi/2$ line and that if separation occurs at -64° then it also occurs at 244° , vortices may well be shed from these points alternately in the same way as flow over a cylinder. This, and the variation of separation point with curvature ratio, awaits experimental investigation.

REFERENCES

1. Dean, W.R. Phil.Mag. IV, p.208 (1927).
2. Dean, W.R. Phil.Mag. V, p.673 (1928).
3. White, C.M. Proc.Roy.Soc., 123A, p.645 (1929).
4. Goldstein, S. Modern Developments in Fluid Mechanics Vols. I and II, Oxford (1938).
5. Keulegan, E.H. and Beij, K.H. Journ.Res.Nat.Bur.Stand., 18, p.89 (1937).
6. Taylor, G.I. Proc.Roy.Soc., A124, p.243 (1929).
7. Adler, M. Zeitschr.f.angew.Math.u.Mech., 14, p.257 (1934).
8. Polhausen, K. Zeitschr.f.angew.Math.u.Mech., 1, p.257 (1921).
9. Barua, S.N. Quart.Journ.Mech.and Applied Math., 16, p.67, (1963).
10. Mori, Y. and Nakayama, W. Int.J.Heat Mass Transfer, 8, p.67, (1965).
11. Squire, H. B. and Winter, K.G. J.Aero.Sci., 18, p.271, (1951).
12. Hawthorne, W.R. Proc.Roy.Soc., A206, p.374 (1951)
13. Hawthorne, W.R. Proc. of the Seminar on Aero.Sci. (1961).

14. Goldstein, S. and Atkinson, . Modern Developments in Fluid Mechanics, Vol.I, p.304,

15. Nikuradse, . Modern Developments in Fluid Mechanics, Vol.I, p.304.

16. Scorer, R.S. and Wilson, S.D.R. Quart.J.R.Met.Soc., 89, p.532 (1963).

17. Hawes, W.B. Unpublished (1930),

18. Squire, H.D. Unpublished (1954).

19. Ito, H. Mem.Inst. High Speed Mech., Tohoku Univ., Japan, 14, p.137 (1959).

```
C
C       PROGRAM FOR SOLVING A SET OF SUCCESSIVELY DEPENDANT SIMULTANEOUS
C       DIFFERENTIAL EQUATIONS USING GILL'S PROCESS FOR THE FOURTH ORDER
C       RUNGE-KUTTA METHOD.
C
C
      REAL A(21),F(63),Y(63),Q(63),G(63)
      N=1
   57 N1=3*N-1
      N2=3*N-2
      N3=3*N
      XPRIN=0.2
      L=1
      A(N)=1.
      ALP=0.
      GO TO (23,52,23,52,23,52,23,52,23,52,23,52,23,52,23,52,23,52,23,
     152,23) ,N
   23 WRITE (6,20)
   20 FORMAT (1H1)
   52 X=0.
      H=0.02
   50 DO 56 I=1,N
      Y(3*I-1)=0.
      Y(3*I-2)=0.
   56 Y(3*I)=A(I)
      IF (L.EQ.1) GO TO 1
      WRITE (6,21)
   21 FORMAT (1H0)
      WRITE (6,22) X,Y(N2),Y(N1),Y(N3)
   22 FORMAT (1H0,F20.2,3F19.6)
C
C          THE INTEGRATION PROCESS.
C
      GO TO 1
  111 DO 59 I=1,N
      F(3*I-2)=H*Y(3*I-1)
   59 F(3*I-1)=H*Y(3*I)
      GO TO (61,62,63,64,65,66,67,68,69,70,71,72,73,74,75,76,77,78,79,80
     1,81),N
   81 F(63)=-H*(Y(1)*Y(63)-3.*Y(2)*Y(62))-2.*H*ALP*Y(44)*Y(1)
   80 F(60)=-H*(Y(1)*Y(60)-3.*Y(2)*Y(59))-2.*H*ALP*Y(44)*(Y(1)-X*Y(2))
   79 F(57)=-H*(Y(1)*Y(57)-3.*Y(2)*Y(56))-2.*H*ALP*Y(45)
   78 F(54)=-H*(Y(1)*Y(54)-3.*Y(2)*Y(53))+4.*H*ALP*X*(4.-Y(2)*Y(2))
   77 F(51)=-H*(Y(1)*Y(51)-3.*Y(2)*Y(50))+2.*H*ALP*(-Y(2)*Y(8)-Y(7)*Y(45
     1)+Y(8)*Y(44)+Y(1)*Y(44)+4.*Y(45))
   76 F(48)=-H*(Y(1)*Y(48)-3.*Y(2)*Y(47))+H*ALP*(8.-2.*(Y(2)*Y(5)+Y(4)*Y
     1(45)-Y(5)*Y(44)))
   75 F(45)=-H*(Y(1)*Y(45)-2.*Y(2)*Y(44))+H*ALP*(4.-Y(2)*Y(2))
   74 F(42)=-H*(Y(1)*Y(42)-3.*Y(2)*Y(41)+4.*Y(3)*Y(40))+H*ALP*(-2.*Y(21)
     1*Y(7)+3.*(Y(20)*Y(8)-Y(19)*Y(9))+4.*(Y(21)+X*F(21)/H))
   73 F(39)=-H*(Y(1)*Y(39)-3.*Y(2)*Y(38)+4.*Y(3)*Y(37))+H*ALP*(-2.*Y(7)*
     1Y(12)+3.*(Y(8)*Y(11)-Y(9)*Y(10))+4.*(Y(12)+X*F(12)/H))
   72 F(36)=-H*(Y(1)*Y(36)-3.*Y(2)*Y(35)+4.*Y(3)*Y(34))+H*ALP*(2.*(
     1-Y(7)*Y(18)-Y(4)*Y(21))+3.*(Y(17)*Y(8)-Y(16)*Y(9)+Y(20)*Y(5)-Y(6)*
     2Y(19))+4.*(Y(18)+X*F(18)/H))
```

```
   71 F(33)=-H*(Y(1)*Y(33)-3.*Y(2)*Y(32)+4.*Y(3)*Y(31))+H*ALP*(2.*(
     1-Y(4)*Y(18)-Y(7)*Y(15))+3.*(Y(17)*Y(5)-Y(16)*Y(6)+Y(14)*Y(8)-Y(13)
     1*Y(9))+4.*(Y(15)+X*F(15)/H))
   70 F(30)=-H*(Y(1)*Y(30)-3.*Y(2)*Y(29)+4.*Y(3)*Y(28))+H*ALP*(3.*(Y(14)
     1*Y(5)-Y(13)*Y(6))-2.*Y(4)*Y(15))
   69 F(27)=-H*(Y(1)*Y(27)-3.*Y(2)*Y(26)+4.*Y(3)*Y(25))+H*ALP*(3.*(Y(11)*
     1*Y(5)-Y(10)*Y(6))-2.*Y(4)*Y(12)-12.)
   68 F(24)=-H*(Y(1)*Y(24)-3.*Y(2)*Y(23)+4.*Y(3)*Y(22))-12.*H*ALP
   67 F(21)=-H*(Y(1)*Y(21)-2.*Y(2)*Y(20)+3.*Y(3)*Y(19))+H*ALP*(-2.*Y(9)*
     1Y(7)+Y(8)*Y(8)+4.*(Y(9)+X*F(9)/H))
   66 F(18)=-H*(Y(1)*Y(18)-2.*Y(2)*Y(17)+3.*Y(3)*Y(16))+2.*H*ALP*(
     1Y(5)*Y(8)-Y(4)*Y(9)-Y(7)*Y(6)+2.*(Y(6)+X*F(6)/H))
   65 F(15)=-H*(Y(1)*Y(15)-2.*Y(2)*Y(14)+3.*Y(3)*Y(13))+H*ALP*(-4.+Y(5)*
     1Y(5)-2.*Y(4)*Y(6))
   64 F(12)=-H*(Y(1)*Y(12)-2.*Y(2)*Y(11)+3.*Y(3)*Y(10))-8.*H*ALP
   63 F(9)=-H*(Y(1)*Y(9)-Y(2)*Y(8)+2.*Y(3)*Y(7))+4.*H*ALP*(Y(3)-X*Y(1)*Y
     1(3))
   62 F(6)=-H*(Y(1)*Y(6)-Y(2)*Y(5)+2.*Y(3)*Y(4))-4.*H*ALP
   61 F(3)=-H*Y(1)*Y(3)
      GO TO (100,101,102,103),M
    1 M=1
      GO TO111
  100 DO112I=1,N3
      G(I)=F(I)
      Q(I)=F(I)
  112 Y(I)=Y(I)+0.5*G(I)
      M=2
      X=X+0.5*H
      GO TO111
  101 DO113I=1,N3
      G(I)=F(I)
      Y(I)=Y(I)+.29289322*(G(I)-Q(I))
  113 Q(I)=.58578644*G(I)+.12132034*Q(I)
      M=3
      GO TO111
  102 DO114I=1,N3
      G(I)=F(I)
      Y(I)=Y(I)+1.7071068*(G(I)-Q(I))
  114 Q(I)=3.4142136*G(I)-4.1213203*Q(I)
      M=4
      X=X+0.5*H
      GO TO111
  103 DO115I=1,N3
      G(I)=F(I)
  115 Y(I)=Y(I)+0.16666667*(G(I)-2.*Q(I))
C
C     THE CONTROL OF STEP LENGTH AND OUTPUT.
C
      XP=10.*XPRIN+.02
      MN=XP
      VX=10.*X+.02
      ML=VX
      VXT=FLOAT (ML)/10.
      IF (L.EQ.1)  GO TO 6
```

```
      IF (ML.LT.MN) GO TO 6
      XPRIN=XPRIN+0.2
      WRITE (6,201) VXT,Y(N2),Y(N1),Y(N3)
  201 FORMAT (1H ,F20.2,3F19.6)
    6 IF (ML-4) 1,4,4
    4 H=0.05
      IF (ML-30) 1,5,5
    5 H=0.1
      IF (ML-50) 1,2,2
C
C     THE DETERMINATION OF THE THIRD INITIAL CONDITION  A(N).
C
    2 IF (L-1) 7,7,33
    7 IF (ALP.EQ.0.) GO TO 51
      GO TO 53
   51 V1=Y(N1)
      ALP=1.
      GO TO 52
   53 V2=Y(N1)
      A(N)=1.-V2/V1
      IF (N.EQ.1)  A(N)=(2./Y(N1))**1.5
      IF (N.EQ.2.OR.N.EQ.4.OR.N.EQ.8 )  A(N)=1.+(2.-V2)/V1
      L=L+1
      GO TO 52
   33 N=N+1
      IF (N-21) 57,57,34
   34 STOP
      END
```

η	$f_{10}(\eta)$	$f'_{10}(\eta)$	$f''_{10}(\eta)$
0.	0.	0.	1.328232
0.20	0.026560	0.265529	1.325882
0.40	0.106108	0.529419	1.309559
0.60	0.237949	0.787553	1.266359
0.80	0.420321	1.033515	1.186655
1.00	0.650025	1.259533	1.067007
1.20	0.922291	1.457966	0.912368
1.40	1.230979	1.623021	0.736027
1.60	1.569097	1.752164	0.556512
1.80	1.929527	1.846661	0.392345
2.00	2.305748	1.911038	0.256937
2.20	2.692363	1.951743	0.155891
2.40	3.085322	1.975580	0.087485
2.60	3.481869	1.988492	0.045367
2.80	3.880292	1.994956	0.021728
3.00	4.279622	1.997946	0.009608
3.20	4.679358	1.999224	0.003924
3.40	5.079261	1.999728	0.001480
3.60	5.479228	1.999912	0.000515
3.80	5.879217	1.999974	0.000166
4.00	6.279214	1.999993	0.000049
4.20	6.679213	1.999998	0.000014
4.40	7.079213	2.000000	0.000003
4.60	7.479212	2.000000	0.000001
4.80	7.879212	2.000000	0.000000
5.00	8.279212	2.000000	0.000000

η	$f_{20}(\eta)$	$f'_{20}(\eta)$	$f''_{20}(\eta)$
0.	0.	0.	5.418492
0.20	0.103018	1.003247	4.609621
0.40	0.390262	1.840691	3.754175
0.60	0.827433	2.500160	2.828604
0.80	1.377550	2.968223	1.845972
1.00	2.001503	3.238536	0.864535
1.20	2.660360	3.320502	-0.019541
1.40	3.319115	3.244292	-0.701137
1.60	3.950754	3.058539	-1.107617
1.80	4.539044	2.820307	-1.230489
2.00	5.078874	2.581476	-1.127669
2.20	5.574027	2.377847	-0.895639
2.40	6.033460	2.225379	-0.630124
2.60	6.467573	2.123524	-0.397376
2.80	6.885580	2.062253	-0.226271
3.00	7.294328	2.028868	-0.116904
3.20	7.698241	2.012325	-0.054994
3.40	8.099853	2.004847	-0.023618
3.60	8.500465	2.001756	-0.009278
3.80	8.900679	2.000586	-0.003339
4.00	9.300748	2.000180	-0.001102
4.20	9.700768	2.000050	-0.000334
4.40	10.100773	2.000012	-0.000093
4.60	10.500774	2.000002	-0.000024
4.80	10.900773	1.999999	-0.000006
5.00	11.300772	1.999998	-0.000002

η	$f_{21}(\eta)$	$f'_{21}(\eta)$	$f''_{21}(\eta)$
0.	0.	0.	-2.777293
0.20	-0.048456	-0.449067	-1.712617
0.40	-0.165439	-0.685571	-0.658047
0.60	-0.309002	-0.717512	0.316351
0.80	-0.440576	-0.572342	1.090681
1.00	-0.529627	-0.303265	1.536423
1.20	-0.558587	0.015030	1.577937
1.40	-0.525697	0.302707	1.245427
1.60	-0.443771	0.497635	0.681529
1.80	-0.334681	0.573351	0.087110
2.00	-0.221614	0.542211	-0.364617
2.20	-0.122367	0.442682	-0.592161
2.40	-0.046109	0.319222	-0.613532
2.60	0.006036	0.205858	-0.506159
2.80	0.038077	0.119629	-0.354688
3.00	0.055877	0.062967	-0.217227
3.20	0.064856	0.030125	-0.118050
3.40	0.068981	0.013139	-0.057495
3.60	0.070712	0.005235	-0.025254
3.80	0.071376	0.001909	-0.010048
4.00	0.071609	0.000639	-0.003634
4.20	0.071685	0.000197	-0.001197
4.40	0.071707	0.000057	-0.000360
4.60	0.071714	0.000016	-0.000099
4.80	0.071716	0.000005	-0.000025
5.00	0.071716	0.000003	-0.000005

η	$f_{30}(\eta)$	$f'_{30}(\eta)$	$f''_{30}(\eta)$
0.	0.	0.	8.164328
0.20	0.152620	1.472866	6.564352
0.40	0.567817	2.625820	4.965868
0.60	1.181689	3.460034	3.380632
0.80	1.930953	3.981455	1.847559
1.00	2.754549	4.207693	0.445223
1.20	3.596757	4.175628	-0.715825
1.40	4.411506	3.944774	-1.527406
1.60	5.166531	3.592020	-1.931577
1.80	5.845581	3.197813	-1.953418
2.00	6.447432	2.829360	-1.695885
2.20	6.981908	2.528697	-1.299206
2.40	7.464447	2.310372	-0.890413
2.60	7.911132	2.167829	-0.550335
2.80	8.335469	2.083613	-0.308368
3.00	8.747166	2.038392	-0.157222
3.20	9.152350	2.016255	-0.073136
3.40	9.554471	2.006353	-0.031105
3.60	9.955272	2.002298	-0.012111
3.80	10.355554	2.000776	-0.004319
4.00	10.755646	2.000253	-0.001407
4.20	11.155677	2.000090	-0.000414
4.40	11.555689	2.000044	-0.000104
4.60	11.955696	2.000034	-0.000015
4.80	12.355702	2.000034	0.000009
5.00	12.755708	2.000036	0.000015

η	$f_{31}(\eta)$	$f'_{31}(\eta)$	$f''_{31}(\eta)$
0.	0.	0.	-0.459910
0.20	-0.014528	-0.171868	-1.257071
0.40	-0.079218	-0.500339	-2.014610
0.60	-0.224031	-0.968429	-2.630804
0.80	-0.473076	-1.532634	-2.945938
1.00	-0.838367	-2.115060	-2.787401
1.20	-1.313228	-2.609266	-2.060018
1.40	-1.868822	-2.905955	-0.843144
1.60	-2.457423	-2.932290	0.583443
1.80	-3.023282	-2.684387	1.835459
2.00	-3.517391	-2.231213	2.598367
2.20	-3.909596	-1.685379	2.763983
2.40	-4.192885	-1.158355	2.442653
2.60	-4.379321	-0.725410	1.864476
2.80	-4.491270	-0.414523	1.253803
3.00	-4.552689	-0.216434	0.751615
3.20	-4.583514	-0.103378	0.404722
3.40	-4.597681	-0.045223	0.196824
3.60	-4.603651	-0.018135	0.086785
3.80	-4.605959	-0.006674	0.034795
4.00	-4.606778	-0.002256	0.012714
4.20	-4.607046	-0.000703	0.004241
4.40	-4.607126	-0.000203	0.001293
4.60	-4.607149	-0.000057	0.000360
4.80	-4.607155	-0.000017	0.000091
5.00	-4.607157	-0.000008	0.000020

η	$f_{32}(\eta)$	$f'_{32}(\eta)$	$f''_{32}(\eta)$
0.	0.	0.	-0.100634
0.20	0.024737	0.370208	3.582296
0.40	0.188022	1.337851	5.833205
0.60	0.579592	2.595502	6.394894
0.80	1.220365	3.764585	4.968364
1.00	2.053847	4.463267	1.770986
1.20	2.954996	4.410026	-2.357725
1.40	3.763412	3.550906	-6.042786
1.60	4.336326	2.114665	-7.954419
1.80	4.599283	0.530181	-7.519180
2.00	4.568013	-0.765162	-5.218922
2.20	4.330407	-1.510541	-2.232725
2.40	4.001859	-1.690970	0.277622
2.60	3.680669	-1.473549	1.704852
2.80	3.424011	-1.081162	2.073880
3.00	3.247986	-0.689492	1.774074
3.20	3.141534	-0.393531	1.226990
3.40	3.083887	-0.200264	0.735266
3.60	3.055919	-0.091630	0.384249
3.80	3.043680	-0.037896	0.177910
4.00	3.038827	-0.014218	0.073690
4.20	3.037078	-0.004848	0.027485
4.40	3.036505	-0.001500	0.009277
4.60	3.036336	-0.000415	0.002847
4.80	3.036291	-0.000094	0.000800
5.00	3.036283	-0.000007	0.000210

η	$f_{33}(\eta)$	$f'_{33}(\eta)$	$f''_{33}(\eta)$
0.	0.	0.	-2.661767
0.20	-0.065209	-0.697718	-4.030232
0.40	-0.285913	-1.498007	-3.693002
0.60	-0.649950	-2.079579	-1.857385
0.80	-1.085084	-2.177291	0.965575
1.00	-1.482042	-1.701643	3.675618
1.20	-1.736566	-0.796743	5.083572
1.40	-1.794746	0.195130	4.506437
1.60	-1.678553	0.891107	2.260745
1.80	-1.473613	1.066790	-0.467863
2.00	-1.284424	0.761717	-2.373039
2.20	-1.184908	0.219468	-2.813962
2.40	-1.193582	-0.279532	-2.040176
2.60	-1.282150	-0.564247	-0.801131
2.80	-1.403465	-0.614608	0.222997
3.00	-1.517623	-0.509982	0.737294
3.20	-1.604660	-0.358179	0.790734
3.40	-1.661322	-0.215121	0.629560
3.60	-1.693301	-0.113163	0.402974
3.80	-1.709230	-0.052833	0.219018
4.00	-1.716307	-0.022072	0.103724
4.20	-1.719129	-0.008291	0.043444
4.40	-1.720142	-0.002801	0.016252
4.60	-1.720469	-0.000840	0.005472
4.80	-1.720560	-0.000206	0.001675
5.00	-1.720578	-0.000019	0.000476

η	$f_{40}(\eta)$	$f'_{40}(\eta)$	$f''_{40}(\eta)$
0.	0.	0.	10.551405
0.20	0.195063	1.871131	8.168006
0.40	0.717134	3.272938	5.869462
0.60	1.474453	4.228272	3.711153
0.80	2.380851	4.770109	1.744395
1.00	3.357906	4.943679	0.043418
1.20	4.337916	4.811844	-1.292111
1.40	5.267781	4.457574	-2.168425
1.60	6.112582	3.977829	-2.547549
1.80	6.856978	3.468409	-2.481698
2.00	7.503148	3.005933	-2.105236
2.20	8.065574	2.635683	-1.587352
2.40	8.564476	2.370468	-1.075220
2.60	9.020041	2.199087	-0.658557
2.80	9.448840	2.098654	-0.366328
3.00	9.862612	2.045081	-0.185651
3.20	10.268688	2.019001	-0.085922
3.40	10.671162	2.007390	-0.036386
3.60	11.072092	2.002653	-0.014119
3.80	11.472415	2.000882	-0.005024
4.00	11.872519	2.000273	-0.001639
4.20	12.272550	2.000082	-0.000489
4.40	12.672559	2.000027	-0.000131
4.60	13.072562	2.000013	-0.000028
4.80	13.472564	2.000011	-0.000001
5.00	13.872566	2.000011	0.000006

η	$f_{41}(\eta)$	$f'_{41}(\eta)$	$f''_{41}(\eta)$
0.	0.	0.	-3.390438
0.20	-0.083700	-0.915353	-5.735332
0.40	-0.395664	-2.271091	-7.732922
0.60	-1.014485	-3.959322	-8.991395
0.80	-1.989107	-5.790639	-9.097034
1.00	-3.322629	-7.498806	-7.722163
1.20	-4.959885	-8.777001	-4.826271
1.40	-6.786486	-9.355753	-0.843467
1.60	-8.646156	-9.101165	3.332184
1.80	-10.375431	-8.080332	6.657173
2.00	-11.843819	-6.545544	8.395381
2.20	-12.982209	-4.837851	8.418489
2.40	-13.788166	-3.263996	7.162392
2.60	-14.309566	-2.011792	5.319323
2.80	-14.618057	-1.133882	3.502420
3.00	-14.785142	-0.584958	2.064303
3.20	-14.868057	-0.276463	1.096075
3.40	-14.905789	-0.119811	0.526755
3.60	-14.921547	-0.047646	0.229899
3.80	-14.927591	-0.017401	0.091353
4.00	-14.929722	-0.005844	0.033109
4.20	-14.930413	-0.001811	0.010954
4.40	-14.930621	-0.000527	0.003301
4.60	-14.930681	-0.000155	0.000892
4.80	-14.930700	-0.000061	0.000198
5.00	-14.930709	-0.000044	0.000012

η	$f_{42}(\eta)$	$f'_{42}(\eta)$	$f''_{42}(\eta)$
0.	0.	0.	5.578662
0.20	0.111586	1.116048	5.584895
0.40	0.446682	2.236219	5.624425
0.60	1.006914	3.368945	5.708934
0.80	1.795505	4.519673	5.787329
1.00	2.815002	5.671951	5.681238
1.20	4.060044	6.758016	5.061151
1.40	5.504576	7.637588	3.567038
1.60	7.088405	8.117741	1.084124
1.80	8.713455	8.028897	-2.018236
2.00	10.258346	7.321905	-4.947566
2.20	11.608733	6.117301	-6.880410
2.40	12.688718	4.665351	-7.399510
2.60	13.477013	3.242838	-6.651800
2.80	14.001702	2.053900	-5.166448
3.00	14.320201	1.185889	-3.529654
3.20	14.496631	0.624639	-2.144491
3.40	14.585879	0.300417	-1.167339
3.60	14.627143	0.132039	-0.572299
3.80	14.644594	0.053077	-0.253676
4.00	14.651350	0.019529	-0.101966
4.20	14.653746	0.006581	-0.037255
4.40	14.654525	0.002032	-0.012398
4.60	14.654756	0.000574	-0.003764
4.80	14.654819	0.000148	-0.001045
5.00	14.654834	0.000033	-0.000266

η	$f_{43}(\eta)$	$f'_{43}(\eta)$	$f''_{43}(\eta)$
0.	0.	0.	-9.600487
0.20	-0.196624	-2.000223	-10.620522
0.40	-0.822344	-4.333190	-12.899480
0.60	-1.966217	-7.207728	-15.918193
0.80	-3.744739	-10.658138	-18.307141
1.00	-6.245353	-14.327799	-17.676284
1.20	-9.434625	-17.365379	-11.701767
1.40	-13.072027	-18.617087	-0.021843
1.60	-16.700682	-17.187725	14.333172
1.80	-19.765555	-13.074771	25.857161
2.00	-21.822335	-7.361875	29.812458
2.20	-22.716153	-1.730777	25.273546
2.40	-22.617606	2.383405	15.400114
2.60	-21.904970	4.393603	4.990683
2.80	-20.982309	4.586509	-2.393098
3.00	-20.141400	3.713202	-5.705148
3.20	-19.514518	2.551303	-5.766614
3.40	-19.112274	1.519284	-4.448189
3.60	-18.886289	0.797948	-2.816059
3.80	-18.773607	0.373574	-1.527685
4.00	-18.723317	0.156942	-0.725860
4.20	-18.703124	0.059368	-0.306036
4.40	-18.695819	0.020172	-0.115550
4.60	-18.693459	0.006011	-0.039412
4.80	-18.692813	0.001363	-0.012330
5.00	-18.692710	-0.000058	-0.003709

η	$f_{44}(\eta)$	$f'_{44}(\eta)$	$f''_{44}(\eta)$
0.	0.	0.	9.716530
0.20	0.204336	2.140779	12.584850
0.40	0.924019	5.271822	18.985338
0.60	2.400355	9.680650	24.570709
0.80	4.838040	14.676205	23.939310
1.00	8.197337	18.549012	12.963478
1.20	12.041651	19.207033	-7.481625
1.40	15.580085	15.434661	-29.554943
1.60	17.969444	8.044378	-41.886335
1.80	18.741203	-0.176905	-37.464999
2.00	18.061667	-6.006901	-19.304568
2.20	16.619324	-7.708359	1.798479
2.40	15.221713	-5.815913	15.350597
2.60	14.398502	-2.343301	17.641340
2.80	14.253397	0.698239	11.931381
3.00	14.578935	2.294370	4.092964
3.20	15.082111	2.599849	-1.060253
3.40	15.561184	2.123996	-3.497921
3.60	15.913400	1.407721	-3.603023
3.80	16.129231	0.792466	-2.627232
4.00	16.243113	0.387982	-1.546823
4.20	16.295772	0.167300	-0.772861
4.40	16.317287	0.063724	-0.336247
4.60	16.325021	0.021026	-0.129634
4.80	16.327352	0.005298	-0.045166
5.00	16.327772	-0.000018	-0.014859

η	$f_{45}(\eta)$	$f'_{45}(\eta)$	$f''_{45}(\eta)$
0.	0.	0.	2.166224
0.20	0.082548	0.999736	7.391161
0.40	0.451670	2.775026	9.894820
0.60	1.208324	4.779909	9.610184
0.80	2.340059	6.433140	6.487937
1.00	3.724015	7.229844	1.207001
1.20	5.153646	6.863774	-4.852923
1.40	6.393126	5.366204	-9.786199
1.60	7.250854	3.139485	-11.945181
1.80	7.642291	0.813841	-10.810295
2.00	7.609769	-1.019284	-7.258735
2.20	7.289429	-2.040694	-2.986045
2.40	6.846790	-2.270480	0.462393
2.60	6.417238	-1.962385	2.352500
2.80	6.076771	-1.428112	2.796771
3.00	5.845107	-0.903657	2.360173
3.20	5.706043	-0.512211	1.615119
3.40	5.631241	-0.258946	0.959244
3.60	5.595179	-0.117764	0.497389
3.80	5.579487	-0.048440	0.228714
4.00	5.573297	-0.018089	0.094158
4.20	5.571076	-0.006147	0.034933
4.40	5.570350	-0.001901	0.011741
4.60	5.570134	-0.000529	0.003598
4.80	5.570078	-0.000123	0.001020
5.00	5.570067	-0.000010	0.000283

η	$f_{46}(\eta)$	$f'_{46}(\eta)$	$f''_{46}(\eta)$
0.	0.	0.	-6.922085
0.20	-0.157235	-1.682458	-10.157759
0.40	-0.718984	-4.027563	-12.870130
0.60	-1.783078	-6.564496	-11.479353
0.80	-3.284642	-8.194254	-3.831827
1.00	-4.924317	-7.803304	8.019942
1.20	-6.248899	-5.104588	18.037028
1.40	-6.881036	-1.164188	19.595626
1.60	-6.764704	2.036787	10.991390
1.80	-6.224966	2.913401	-2.248846
2.00	-5.761290	1.413030	-11.445848
2.20	-5.725064	-1.060424	-11.729866
2.40	-6.135528	-2.823286	-5.146250
2.60	-6.750371	-3.073558	2.384002
2.80	-7.283967	-2.133424	6.283142
3.00	-7.581900	-0.861839	5.847272
3.20	-7.654401	0.107980	3.563658
3.40	-7.577869	0.582245	1.016733
3.60	-7.452379	0.631877	-0.587736
3.80	-7.341347	0.473397	-1.075644
4.00	-7.266924	0.283974	-0.918211
4.20	-7.225766	0.143512	-0.580601
4.40	-7.206360	0.062236	-0.301129
4.60	-7.198514	0.022848	-0.133904
4.80	-7.195916	0.006257	-0.052693
5.00	-7.195420	-0.000040	-0.019234

η	$g_{30}(\eta)$	$g'_{30}(\eta)$	$g''_{30}(\eta)$
0.	0.	0.	-2.171943
0.20	-0.038137	-0.355158	-1.387120
0.40	-0.132037	-0.560397	-0.684639
0.60	-0.253794	-0.638401	-0.122005
0.80	-0.380998	-0.620515	0.271843
1.00	-0.497898	-0.541021	0.496151
1.20	-0.595442	-0.431843	0.574175
1.40	-0.670378	-0.318506	0.545034
1.60	-0.723720	-0.217995	0.453230
1.80	-0.759006	-0.138703	0.338706
2.00	-0.780722	-0.082082	0.230186
2.20	-0.793157	-0.045172	0.143125
2.40	-0.799780	-0.023108	0.081689
2.60	-0.803060	-0.010982	0.042879
2.80	-0.804569	-0.004846	0.020723
3.00	-0.805214	-0.001986	0.009227
3.20	-0.805470	-0.000756	0.003788
3.40	-0.805565	-0.000269	0.001433
3.60	-0.805597	-0.000090	0.000499
3.80	-0.805608	-0.000031	0.000159
4.00	-0.805612	-0.000012	0.000045
4.20	-0.805614	-0.000008	0.000010
4.40	-0.805615	-0.000007	-0.000000
4.60	-0.805617	-0.000007	-0.000003
4.80	-0.805618	-0.000008	-0.000004
5.00	-0.805620	-0.000009	-0.000004

η	$g_{40}(\eta)$	$g'_{40}(\eta)$	$g''_{40}(\eta)$
0.	0.	0.	-1.587091
0.20	-0.021231	-0.161266	-0.062344
0.40	-0.046270	-0.050986	1.078364
0.60	-0.030156	0.230677	1.634452
0.80	0.049326	0.562751	1.595208
1.00	0.191100	0.838535	1.105646
1.20	0.376381	0.990651	0.400843
1.40	0.577795	1.000757	-0.278142
1.60	0.768764	0.892879	-0.758596
1.80	0.930290	0.715229	-0.973779
2.00	1.053656	0.519126	-0.954475
2.20	1.139336	0.343287	-0.787623
2.40	1.193682	0.207538	-0.567884
2.60	1.225252	0.114969	-0.364330
2.80	1.242080	0.058449	-0.210137
3.00	1.250320	0.027299	-0.109667
3.20	1.254030	0.011722	-0.052011
3.40	1.255567	0.004628	-0.022489
3.60	1.256152	0.001678	-0.008887
3.80	1.256357	0.000555	-0.003217
4.00	1.256421	0.000162	-0.001070
4.20	1.256438	0.000036	-0.000329
4.40	1.256441	-0.000002	-0.000096
4.60	1.256439	-0.000013	-0.000028
4.80	1.256436	-0.000016	-0.000011
5.00	1.256433	-0.000018	-0.000006

η	$g_{41}(\eta)$	$g'_{41}(\eta)$	$g''_{41}(\eta)$
0.	0.	0.	3.076620
0.20	0.040595	0.312765	0.283132
0.40	0.097182	0.206161	-1.129352
0.60	0.112462	-0.061876	-1.392123
0.80	0.074444	-0.302980	-0.940188
1.00	-0.000377	-0.421712	-0.240759
1.20	-0.085234	-0.407180	0.346676
1.40	-0.157219	-0.302740	0.644802
1.60	-0.204399	-0.168852	0.652748
1.80	-0.226078	-0.053820	0.478667
2.00	-0.228772	0.019338	0.253948
2.20	-0.221157	0.050711	0.071420
2.40	-0.210420	0.053146	-0.034019
2.60	-0.200815	0.041681	-0.071359
2.80	-0.193927	0.027325	-0.067738
3.00	-0.189700	0.015601	-0.048516
3.20	-0.187413	0.007915	-0.029014
3.40	-0.186307	0.003613	-0.015062
3.60	-0.185823	0.001500	-0.006919
3.80	-0.185629	0.000575	-0.002842
4.00	-0.185556	0.000213	-0.001050
4.20	-0.185529	0.000084	-0.000348
4.40	-0.185517	0.000044	-0.000102
4.60	-0.185509	0.000033	-0.000025
4.80	-0.185503	0.000030	-0.000005
5.00	-0.185497	0.000030	-0.000001

η	$g_{42}(\eta)$	$g'_{42}(\eta)$	$g''_{42}(\eta)$
0.	0.	0.	-3.157047
0.20	-0.062134	-0.611575	-2.867489
0.40	-0.237486	-1.117419	-2.135227
0.60	-0.497508	-1.450856	-1.180523
0.80	-0.804723	-1.589008	-0.215115
1.00	-1.121085	-1.547701	0.590530
1.20	-1.414723	-1.370639	1.131086
1.40	-1.664114	-1.115119	1.376148
1.60	-1.859328	-0.837513	1.362687
1.80	-2.000627	-0.581894	1.171875
2.00	-2.095325	-0.374262	0.898020
2.20	-2.154108	-0.222838	0.620803
2.40	-2.187900	-0.122791	0.389738
2.60	-2.205883	-0.062598	0.223083
2.80	-2.214741	-0.029515	0.116720
3.00	-2.218777	-0.012871	0.055921
3.20	-2.220479	-0.005194	0.024564
3.40	-2.221144	-0.001945	0.009899
3.60	-2.221387	-0.000683	0.003656
3.80	-2.221470	-0.000235	0.001230
4.00	-2.221500	-0.000091	0.000366
4.20	-2.221513	-0.000051	0.000083
4.40	-2.221522	-0.000045	-0.000004
4.60	-2.221531	-0.000049	-0.000030
4.80	-2.221542	-0.000056	-0.000039
5.00	-2.221553	-0.000064	-0.000043

η	$g_{43}(\eta)$	$g'_{43}(\eta)$	$g''_{43}(\eta)$
0.	0.	0.	-0.854331
0.20	-0.011838	-0.094885	-0.149444
0.40	-0.030725	-0.081125	0.237333
0.60	-0.040994	-0.017433	0.362911
0.80	-0.037324	0.052502	0.315465
1.00	-0.021307	0.103313	0.185744
1.20	0.002113	0.126197	0.045982
1.40	0.027488	0.124001	-0.060310
1.60	0.050616	0.105373	-0.117786
1.80	0.069181	0.079832	-0.131403
2.00	0.082587	0.054743	-0.116069
2.20	0.091392	0.034253	-0.087859
2.40	0.096684	0.019643	-0.058801
2.60	0.099605	0.010350	-0.035326
2.80	0.101088	0.005016	-0.019210
3.00	0.101781	0.002237	-0.009504
3.20	0.102079	0.000916	-0.004294
3.40	0.102196	0.000341	-0.001779
3.60	0.102238	0.000111	-0.000680
3.80	0.102250	0.000026	-0.000244
4.00	0.102252	-0.000004	-0.000087
4.20	0.102250	-0.000016	-0.000037
4.40	0.102246	-0.000021	-0.000022
4.60	0.102241	-0.000026	-0.000020
4.80	0.102236	-0.000030	-0.000021
5.00	0.102229	-0.000034	-0.000022

η	$g_{44}(\eta)$	$g'_{44}(\eta)$	$g''_{44}(\eta)$
0.	0.	0.	0.130138
0.20	0.002604	0.026045	0.130306
0.40	0.010407	0.051857	0.126224
0.60	0.023208	0.075519	0.107122
0.80	0.040223	0.093317	0.067590
1.00	0.059893	0.101565	0.013513
1.20	0.080102	0.098708	-0.040759
1.40	0.098730	0.086254	-0.080395
1.60	0.114220	0.068079	-0.097435
1.80	0.125885	0.048713	-0.093198
2.00	0.133867	0.031704	-0.075438
2.20	0.138845	0.018824	-0.053294
2.40	0.141684	0.010225	-0.033431
2.60	0.143167	0.005094	-0.018828
2.80	0.143879	0.002333	-0.009592
3.00	0.144194	0.000984	-0.004445
3.20	0.144322	0.000384	-0.001882
3.40	0.144371	0.000139	-0.000729
3.60	0.144388	0.000048	-0.000260
3.80	0.144394	0.000016	-0.000085
4.00	0.144396	0.000006	-0.000026
4.20	0.144396	0.000003	-0.000008
4.40	0.144397	0.000002	-0.000003
4.60	0.144397	0.000002	-0.000002
4.80	0.144397	0.000001	-0.000002
5.00	0.144398	0.000001	-0.000003

η	$g_{45}(\eta)$	$g'_{45}(\eta)$	$g''_{45}(\eta)$
0.	0.	0.	-0.141168
0.20	-0.002824	-0.028256	-0.141433
0.40	-0.011295	-0.056346	-0.138006
0.60	-0.025238	-0.082500	-0.120390
0.80	-0.043928	-0.103132	-0.082603
1.00	-0.065867	-0.114459	-0.028883
1.20	-0.088949	-0.114450	0.028310
1.40	-0.110936	-0.103863	0.074757
1.60	-0.130001	-0.085917	0.100941
1.80	-0.145103	-0.064968	0.105143
2.00	-0.156057	-0.044995	0.092417
2.20	-0.163342	-0.028579	0.070986
2.40	-0.167791	-0.016665	0.048483
2.60	-0.170288	-0.008928	0.029738
2.80	-0.171577	-0.004398	0.016484
3.00	-0.172189	-0.001995	0.008293
3.20	-0.172457	-0.000835	0.003798
3.40	-0.172565	-0.000325	0.001587
3.60	-0.172607	-0.000119	0.000607
3.80	-0.172622	-0.000044	0.000213
4.00	-0.172627	-0.000018	0.000070
4.20	-0.172630	-0.000009	0.000024
4.40	-0.172631	-0.000006	0.000012
4.60	-0.172632	-0.000004	0.000011
4.80	-0.172633	-0.000001	0.000013
5.00	-0.172633	0.000002	0.000016